Materials Today Advances 12 (2021) 100169

Contents lists available at ScienceDirect

Materials Today Advances

journal homepage: www.journals.elsevier.com/materials-today-advances/

Preparation and application of 0D-2D nanomaterial hybrid heterostructures for energy applications

S. Sinha [a, b, c, **], H. Kim [d], A.W. Robertson [a, *]

[a] Department of Materials, University of Oxford, Parks Road, Oxford, OX1 3PH, United Kingdom
[b] Nanomaterials Research Institute, National Institute of Advanced Industrial Science and Technology, Tsukuba, 305-8565, Japan
[c] The Institute of Scientific and Industrial Research (ISIR-SANKEN), Osaka University, Osaka, 567-0047, Japan
[d] Energy Materials Laboratory, Korea Institute of Energy Research, 152 Gajeong-ro, Yuseong-gu, Daejeon 34129, South Korea

ARTICLE INFO

Article history:
Received 21 July 2021
Received in revised form
24 August 2021
Accepted 24 August 2021
Available online 20 September 2021

Keywords:
2D materials
Graphene
Fullerenes
0D-2D hybrid
2d heterostructure
Catalysts
Solar cells
Batteries

ABSTRACT

As research efforts into the two-dimensional (2D) materials continue to mature, finding applications in which they can be productively used has become of greater interest. Applications in the energy sector are of particular importance, with the pressing need to decarbonize our economy and to live more sustainably. For a material to be optimal for an application we typically tailor their specific properties and characteristics to best fit with the desired parameters. In the past, this has included the forging of metal alloys or the doping of semiconductors, allowing us to controllably adjust the material properties. For two-dimensional materials, one of the best routes for such controlled manipulation is via forming a heterostructure, or hybrid, with another nanomaterial. In this review, we will explore the emergence of 0D-2D hybrid materials, where a 2D layered material is combined with a zero-dimensional (0D) nanoparticle or fullerene to adjust and enhance overall performance. We will cover the basics of their structure and modes of interaction, the different synthetic methods used for their assembly and preparation and review several energy applications in which promising results have already been achieved.

1. Introduction

Since the discovery of graphene in 2004, the two-dimensional (2D) materials family has added many further members, ranging from layered metal dichalcogenides to 'MXenes', with a wide range of chemical, physical, and electronic properties [1]. As the field continues to grow and mature, a new frontier has opened in the integration of complementary 2D and non-2D materials [2–6]. Such combinations yield a much broader class of nano-heterostructures whose combinations can be adjusted for desired properties, and thus provide great opportunities for the design of hybrid materials tailored for specific applications.

The class of zero-dimensional materials (0D) primarily consist of fullerenes, organic molecules, quantum dots, and atomic clusters. Mixed dimensionality 0D-2D hybrids have been successfully demonstrated in a number of devices, and often show superior performance, stability, or chemistry. However, assembly of a mixed dimensional heterostructure requires precise control on the atomic level due to the difference in the crystal structure and thermal stabilities, and the necessity of forming a high-quality interface. Therefore, 0D-2D materials present unique challenges in the regard, along with opportunities in identifying novel methods for synthesis. In the past few years, such heterostructures have been synthesized by utilizing a few different methodologies, for instance, wet-chemistry, thermal deposition, chemical reaction pathways, and others, where the more stable 2D material is first synthesized, and then the 0D material is introduced. In addition to the general experimental parameters such as temperature, atmosphere, pressure, etc., the techniques used for interfacing 0D materials with other 2D systems also vary depending on the 0D material used as well as their desired concentration and required uniformity on the 2D host.

The present review highlights the different methods to produce these 0D-2D heterostructures and discusses their advantages as well as shortcomings. While we focus on the general synthetic approaches and the optimal experimental parameters used in different techniques, we also provide a general sense of which type

* Corresponding author.
** Corresponding author.
E-mail addresses: sapna.sinha@sanken.osaka-u.ac.jp (S. Sinha), alex.robertson@materials.ox.ac.uk (A.W. Robertson).

https://doi.org/10.1016/j.mtadv.2021.100169

of synthetic methodology is best suited for a specific 0D material. We have also dedicated sections on synthetic processes that do not require either complex mechanisms or high-cost materials. A further section has been added on green synthesis to recognize the efforts put in this direction to create high quality 0D/2D samples whilst using fewer resources. The latter half of this review explores the emerging energy applications of these 0D-2D heterostructures, in catalysis, energy storage, and solar cells, illustrating the challenges and opportunities these hybrids provide.

2. Types of morphologies and interactions between 0D particles and 2D materials

Realizing the potential of a 0D-2D composite requires engineering a system that promotes the respective advantages of each component. Ideally, it achieves a synergy or co-activity that is greater than the sum of its parts [7,8]. The morphology and mode of interaction of the composite will often be contingent on the synthesis process employed, which will be addressed in the subsequent section. There are four main schemes by which we can integrate 0D and 2D materials into a composite (Fig. 1a–d): Decorating the basal surface of the 2D material with the 0D component (Fig. 1a). Situating the 0D component along the 2D material edges (Fig. 1b). Encapsulation of the nanoparticle by a 2D material (Fig. 1c) [9,10]. And, in the case of the 0D component being single atoms, integrating the dopants into the 2D material (Fig. 1d).

In the case of a composite where the particle is situated on the basal plane (as per Fig. 1a), ensuring the nanoparticle or fullerene is well anchored to the 2D material host is essential; whether it is to facilitate catalytic activity, inhibit nanoparticle ripening, or simply to minimize the detachment of the 0D component while under application conditions. Understanding the interaction mechanisms available between the 0D and 2D components allows us to suitably design our materials, such as by appropriately capping the nanoparticle or by treating the 2D material host beforehand. Facilitating the adhesion of the 0D component can be achieved by engineering appropriate functional groups for it and/or the 2D material (Fig. 1e–h), leveraging one of four different modes of interaction: The van der Waals force (Fig. 1e). Electrostatic attractions, dipole-dipole, and hydrogen bonding (Fig. 1f). A π interaction with aromatic components (Fig. 1g). Or a covalent bond (Fig. 1h) [11,12]. We will explore the details of these in the following paragraphs.

The van der Waals interaction is often the target from ex-situ preparation pathways, i.e. where the nanoparticle and 2D material components are prepared separately, and then treated to form a composite [17]. The composite can then be prompted to self-assemble via solvent evaporation [18]. It is a weak interaction, and so not ideal for maintaining nanoparticle adhesion to the 2D host, which is a disadvantage for many applications that require the composite to be used in hostile conditions, such as an electrocatalyst in a proton electrolyte membrane fuel cell (PEMFC) or high temperature reaction processes [19,20]. However, a major advantage is that it does not require the host 2D material to present functional anchor groups to which nanoparticles can interact with, and so allows for pristine material to be used [21,22]. Such functional groups can limit the performance of a 2D material, reducing

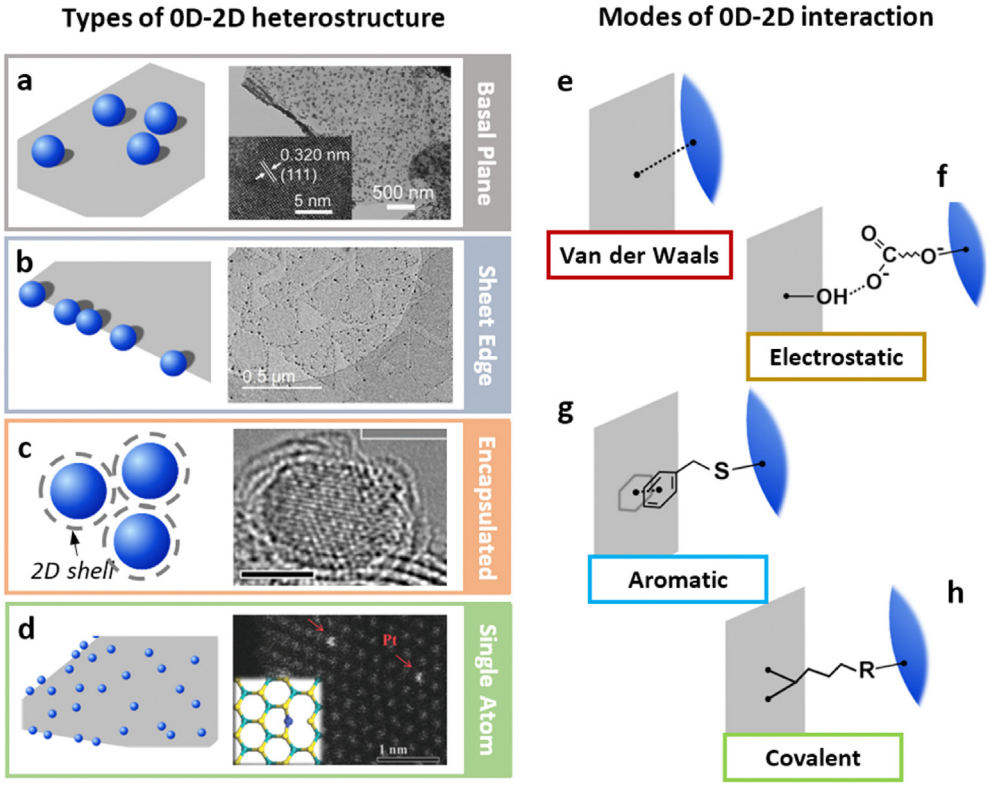

Fig. 1. The different morphologies and potential interaction mechanisms for 0D-2D hybrids. (a) Nanoparticles arranged on the basal plane. A TEM image of CoS_2 nanoparticles decorating a reduced graphene oxide (r-GO) nanosheet [13]. (b) Nanoparticles preferentially situated along the nanosheet edge. A TEM image of triangular MoS_2 flakes with Au nanoparticles along their edges [14]. (c) Nanoparticles encapsulated in 2D sheets. A TEM image of a Pt nanoparticle encapsulated in several graphene layers. Scale bar 2 nm [15]. (d) Single atom sites within, on top of, or along the edge of the nanosheet. High-angle annular dark-field (HAADF) scanning-mode transmission electron microscopy (STEM) image of Pt substitutions in MoS_2 [16]. (e) A van der Waals interaction, such as between graphene and a ligand-free nanoparticle. (f) Electrostatic dipole-dipole interaction, such as between a hydroxyl functional on GO and a citrate ligand on a nanoparticle. (g) An aromatic/π-π interaction, such as between graphene and a phenylethanethiol capped nanoparticle. (h) A covalent bond, typically formed between a functional group on GO and a ligand.

its electrical conductivity or durability, thus anchoring via van der Waals can be preferable for high performance electronics [23,24]. Aiming for a van der Waals interaction also allows for using a ligand-free nanoparticle component, which can be desirable for reducing cost [25,26] or ensuring optimal performance by keeping active sites free [27,28].

An electrostatic or covalent interaction between a 2D and partner 0D material can be obtained by appropriate functionalization of the 2D material [29,30], and coordinating the functional group anchor sites with corresponding capping ligands on the nanoparticle. These can yield a dipole-dipole interaction between the groups or can react and form a covalent bond. A common strategy is to self-assemble the nanoparticles on the 2D support, often relying on the polar oxygen and hydroxyl functional groups present on graphene oxide (GO) [31–34]. Such composites have the advantage of being straightforward to assemble with one or two steps, as the nanoparticle growth and adhesion can be done in-situ [35,36], and have a stronger interaction strength than with just relying on van der Waals, giving even dispersion and protection against ripening and/or detachment of the nanoparticle from the 2D host while under application conditions. Covalent bonding can be obtained by using appropriate functional groups [13,37], leading to an even stronger anchoring of the 0D component to the 2D host. In the case of 2D metal dichalcogenides, nanoparticles can covalently bond to defect sites on the basal plane [38–40], such as chalcogenide vacancies, or the defects can act as nucleation sites for subsequent nanoparticle growth [41,42]. Similarly, exploiting the dangling bonds along sheet edges is a way of preferentially decorating edges of monolayer transition metal dichalcogenides with nanoparticles [14,39,43].

However, functional groups or defects can impair the material performance. A major advantage of exploiting the π orbital attraction is that it allows us to keep a graphene 2D host pristine, with no functional groups degrading the sp^2 bonding network [44]. The π attraction occurs at electron-rich π orbitals of aromatic rings [45,46], generating an electrostatic force, although the details are somewhat more nuanced (see Ref. [47]). With a graphene host and an appropriately selected aromatic capping ligand for the nanoparticle, a π-stacking arrangement can be instigated between the 0D and 2D components [48]. The high electron density of the graphene π-orbitals can also be exploited via η^6 hapticity between the graphene ring and a transition metal-containing functional group [49]. This haptic approach preserves the high conductivity of graphene while still yielding well dispersed nanoparticles adhered to the graphene surface [50,51]. Beside attaching nanoparticles, fullerenes can also be adhered to a graphene host via π attraction, either by functionalization of the fullerene [52], or by simply mixing bare fullerenes together with graphene [53], where a combination of the π interaction and adhesion to amorphous carbon residue on the graphene maintains the fullerene-graphene composite [54].

The above 0D-2D composites have been discussed in the context of the 0D component decorating a 2D material. The inverse morphology, where the nanoparticle is wrapped in a 2D material, is also possible (Fig. 1c). The 2D material can act as a shield, enhancing the durability of nanoparticles while operating under severe conditions by militating against ripening, deactivation, or dissolution [15,55–57]. The 2D enclosing layers can have a stronger interaction with the host material system, such as a π - π interaction between a graphitic electrode and a graphene-shielded nanoparticle [58], helping to prevent nanoparticle detachment. With these morphologies, it is important to ensure that any activity of the 0D component is not passivated by the enwrapping 2D layer.

The ultimate 0D component is the single atom, and is of interest for controlling the electronic structure via doping, or for the emerging field of single-atom catalysts [60–62]. Fig. 2a outlines how single atoms can be bound in to a 2D host, with a metal dichalcogenide (e.g. molybdenum disulfide [MoS_2]) used as the example. The experimental prevalence of configurations shown will vary significantly, depending on the 2D host and the dopant atom. For transition metals doped to transition metal dichalcogenides (TMDCs), the typical preference is for situating at substitutions, top sites above the metal, or hollow sites [63]. Experimental examples illustrating this are captured in the high-angle annular dark-field scanning-mode transmission electron microscopy (HAADF-STEM) images shown in Fig. 2b, showing a cobalt [Co] substitution for a single sulfur [S] (top image, bright atomic site in the center of the image), and a Co atom interstitial located in the hollow site of the ring center (bottom image) [59]. The bridge site, where the dopant atom is situated above the bond between two of the sites in the 2D material, is generally unstable for 2D dichalcogenides [64,65], but is more viable for the case of graphene [66]. Several reviews have covered atomic doping of 2D materials recently [67–69], and so this review will discuss atomic doping of 2D materials in the context of providing a tailored 2D component for a composite, such as nitrogen doped graphene, along with larger 0D components, such as nanoparticles and fullerenes.

3. Synthesis methods

Several detailed studies have been carried out on understanding hybrid 0D-2D nanomaterials [70] often relying on sophisticated characterization methods like scanning tunneling microscopy (STM) and transmission electron microscopy (TEM) [71–74]. However, the preparation techniques employed for fabricating samples differ tremendously depending on the characterization tools used for that particular study. In addition, the sample preparation varies widely across the types of nanomaterials used to create the hybrid structure. For instance, some of the most commonly preferred techniques for fabricating a fullerene-2D hybrid material are the chemical addition reaction [75,76], thermal evaporation [77], and drop-casting (Fig. 3) [54]. In this section, we will focus on the different sample techniques used to prepare 0-D materials for 0D-2D hybrids. A special focus on sample preparation for high-resolution transmission electron microscopy (HRTEM) studies has been given in the section to reflect on the sophisticated sample synthesis required to carry out such studies. The section has been divided based on the type of methodology employed and subsequently divided into subsections based on the nanomaterials used. Table 1 at the end of this section summarizes a variety of techniques available for preparing the family of fullerene-2D heterostructures, and also contains separate columns to emphasize the TEM imaging conditions and sample annealing methods required to achieve high resolution imaging.

3.1. Thermal evaporation

One of the more popular methods for deposition of 0-D frameworks on 2D materials is thermal evaporation. Prior to thermal evaporation, annealing of the substrate containing the 2D materials beforehand is required, to minimize possible surface adsorbates. During the thermal deposition process the chamber is pumped to a high vacuum and the 2D material (the substrate) is kept heated at high temperature, usually in the range of 100–200 °C, during the deposition process. However, the ideal substrate temperature can vary significantly and should be determined by considering the type of 2D material and the type of 0D material being thermally evaporated so that it facilitates the deposition process. For instance, Kim et al. [82] studied the effect of

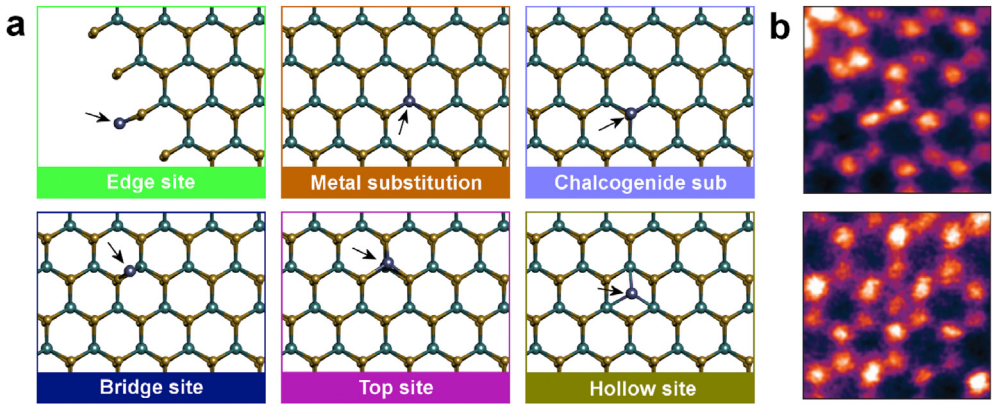

Fig. 2. Single atom catalyst sites on a monolayer transition metal dichalcogenide. (a) Slightly off-axis top-down atomic models, showing metal (cyan) and pairs of chalcogenide (yellow) atoms. An added single-atom (blue) can typically occupy one of the shown six sites. (b) HAADF-STEM images of a single Co atom occupying the S substitution and the hollow site in monolayer MoS_2 [59].

substrate temperature and uniformity and thickness of the deposited 0D material. C_{60} was thermally deposited on graphene substrate whose temperature was varied in the range of 20–120 °C. The authors showed that a substrate temperature of 120 °C resulted in 10 nm thickness of highly uniform morphology of C_{60} on graphene. The same group carried out another investigation on

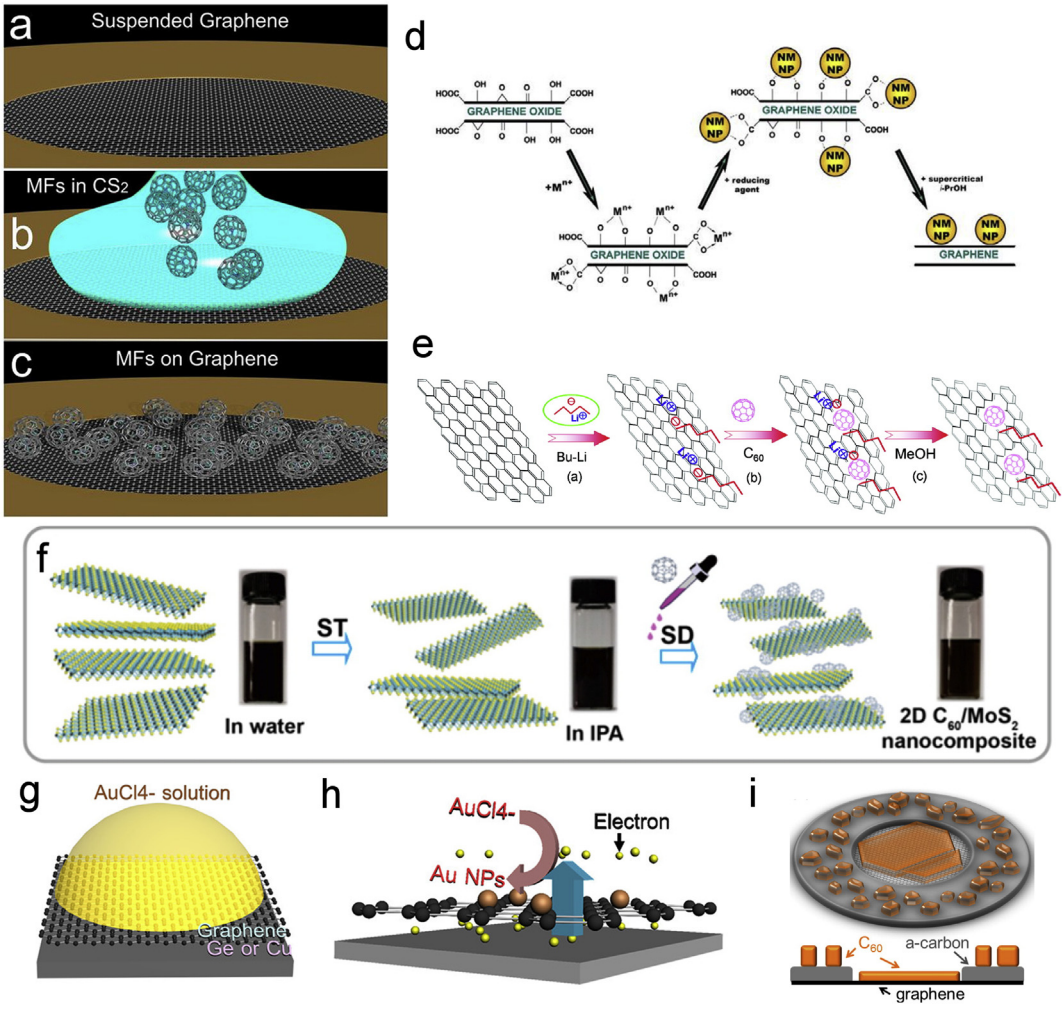

Fig. 3. Schematic representation of different methodologies for introducing different nanomaterials to graphene. (a–c) Drop-casting technique to introduce endohedral metallofullerenes (MFs) on suspended graphene [54]. (d) The chemical reduction process for formation of nanoparticles onto graphene via an intermediate nanocomposite made of metal particles and graphene oxide [78]. (e) Grafting of C_{60} onto graphene through a chemical addition reaction [79]. (f) Preparation of C_{60}–MoS_2 nanocomposite via solvent transfer and surface deposition (STSD) method by first solvent transferring MoS_2 from water to isopropanol (IPA) and then surface depositing the fullerenes [80]. ST refers to solvent transfer and SD refers to surface deposition in the figure. (g–h) Electrochemical method of formation of nanoparticle decorated graphene by introducing chloroauric acid anion ($AuCl_4^-$) solution in (h), that leads to spontaneous galvanic reaction on the surface through charge communication between the solution and graphene [81]. (i) Thermal deposition technique to introduce uniform fullerene crystals to graphene [82].

Table 1
Summary of preparation methods of fullerene-2D hybrid materials and their characterization by TEM imaging.

0D/2D hybrid	2D material annealing	Preparation method	Annealing of hybrid structure	TEM imaging conditions[a]	Ref
Gr-C_{60}	30 min, 400 °C, in air	Thermal evaporation (10^{-5} mbar; 1 Å/s; Graphene 100 °C)	N/A	STEM, 60 kV, 60–200 mrad	[77]
Gr-C_{70}	200 °C, 30 min, in air	Thermal evaporation (0.05 Å/s , 2×10^{-6} Torr, Graphene 110 °C)	N/A	TEM, 80 kV, electron dose ~ 2×10^4 e nm^{-2}/s.	[119]
Gr-C_{60}	Air annealing, 200 °C, 30 min	Thermal evaporation (3×10–6 Torr; 0.2 Å/s; Graphene 120 °C)	N/A	TEM, 80 kV	[82]
hBN-C_{60}	200 °C, 30 min, Air	Thermal evaporation 0.2 Å/s , h-BN 110 °C	N/A	TEM, 80 kV	[120]
FNG-Fullero-benzyne	Vacuum annealing	Chemical Addition	Vacuum annealing, 48 h	TEM, 200 kV	[75]
C_3N_4–C_{60}	Drying	Chemical Addition	80 °C vacuum 12 h	TEM, 200 kV	[86]
Gr-C_{60}	Reducing Graphene	Chemical Addition	Vacuum 60 °C, overnight	TEM, 200 kV	[79]
GrO-C_{60}	Chemical modification	Chemical Addition then drop-casting on TEM grid	Left in air to dry	TEM, 200 kV	[87]
Gd_3N@C_{80}-Gr	Ar/H_2; annealing	Drop-casting	60 °C, vacuum annealing	STEM, 60 kV, 72–271 mrad	[54]
MoS_2–C_{60}	N/A	Catalyzed Transport Method, 2 wt.-% C_{60} in MoS_2 powder @ 10^{-3} Pa, 1,030 K, 22 days	Thoroughly washed with toluene	TEM, 300 kV	[89]
MoS_2–C_{60}	N/A	Ultrasonication (C_{60} 2.9–5.6 wt% in Toluene with MoS_2 IPA solution)	N/A	TEM, 200 kV	[80]
MoS_2–C_{60}	N/A	Ball milling then mechanically exfoliated	60 °C, vacuum	TEM, 200 kV	[118]
Gr-C_{60} hybrid	N/A	Ball milling process		TEM, 200 kV	[121]

[a] Imaging conditions for TEM, including accelerating voltage, imaging mode (TEM vs. STEM), dose, and collection angle (for STEM, mrad).

thermally depositing pentacene molecules on graphene and found that the ideal substrate temperature was 60 °C.

Recently, Nguyen et al. [83] reported that the epitaxial growth of vacuum deposition of fullerenes on graphene can occur by the charge transfer occurring between the two materials. The authors were successful in carrying out layer-by-layer growth of highly ordered C_{60} in A-B-A stacking on top of graphene by in-situ electrical gating to finely tune the Fermi level (E_F) of graphene during the deposition process. The number of transferred electrons to graphene during the electrical gating not only determined the crystal structure and morphology of the C_{60} crystals, but also how they assembled into thin films on top of graphene. Controlling such growth dynamics of these organic frameworks is essential, as they are the key to the optoelectronic behavior of the resultant hybrid material. Studying such charge-transfer-induced interaction could help the development of a reliable procedure to optimize the deposition and growth procedure for obtaining organic-2D templates.

Organic molecular beam deposition (OMBD) is a variant of this process where organic films can be grown from a resistively heated Knudsen cell onto a substrate. Felix et al. [84] reported that epitaxial growth of perfluoropentacene on graphene substrate by the OMBD method, were found to be form well-ordered islands aligned to the zigzag direction of the substrate.

Pulsed laser deposition (PLD) of the 0D component can synthesize clusters of metal atoms on the surface of a 2D material. In this particular method, a high-power focused pulsed laser beam is used to target the material that is to be deposited on the 2D material. Dong et al. [85] realized deposited Pt clusters through a PLD chamber with an argon (Ar) pressure of 50 mTorr. These clusters were of nanoscale dimensions, allowing for e-beam irradiation from a TEM to instigate interesting dynamics of the nanoclusters on the suspended graphene. 2D materials are known to contain defects, which can effectively form trapping centers for metal atoms. Therefore, although PLD can be damaging to the 2D material support, the defects introduced in the sheet can act as effective anchoring sites for atom clusters. Thus, this variant of deposition method is an interesting pathway for potentially forming metal cluster composites embedded in a 2D material.

One of the advantages of thermal deposition is that the vacuum conditions required to carry out the process anneals the heterostructures and provides a clean interface to the heterostructure. The added benefit is that the sample can then directly be loaded into the microscope to carry out the study without the intermediate substrate annealing process as the synthesis process itself is carried out at high temperature under inert conditions. However, it should be noted that there are several variants of the thermal deposition method that are used for a particular type of nanomaterial, i.e. for organic frameworks, metal clusters, etc., and equally important is the vacuum, heating conditions and cooling duration used during such synthesis.

3.2. Chemical addition

The chemical modification and functionalization of 2D materials is another route to introduce 0D materials on to its surface. For instance, introduction of organolithium to the graphene surface can activate it for direct nucleophilic addition of C_{60} to the surface causing hybridization of these nanostructures [79]. The absence of surfactants involved in the chemical process yields clean interfaces of such hybrids, which is advantageous for device applications. Such modification of the surface of 2D materials for addition of 0D materials has been shown for various other organic systems such as graphene/fullerobenzyne [75], C_3N_4–C_{60} [86], and GrO-C_{60} [87] (GrO = graphene oxide) [88]. One aspect of such chemical additions can be the difficulty in precise determination of the chemical bonding between 0-D and 2-D material, especially if the 0-D material is a big molecule rather than a single atom. In addition, 2D nanomaterials are intrinsically anisotropic, and therefore the precise location of the chemical addition of such 0D materials strongly depends on the experimental conditions. For instance, hybridization across the edges occurs more easily than on the 2D basal surface. Transition metal dichalcogenide (TMDC) materials are generally easier to conduct addition experiments to, as compared to graphene, due to the sulfur bonds that can form from on the surface. The atomic resolution of aberration corrected TEM means it is now possible to determine the precise location and dynamics of these chemical bonding sites. It can detect the commensuration of lattices, their orientation and dynamics on an atomic scale [89]. Whilst making these hybrid samples via this method, it is important to note that the excess solvent residues should be removed to avoid contamination during imaging, which can be achieved by

heating the sample under vacuum to drive the excess from the surface.

Chemical modification of the surface of 2D materials can also be exploited to decorate its surface with metal nanoparticles. For instance, carrying out reduction of ethylene glycol on the surface a 2D material host for introducing Pt [36], exposing graphene to aqueous chloroplatinic acid [90] or chloroplatinic acid dissolved in ethanol [91] to synthesize Pt-laden sheets, etc. A commercially viable alternative to this method is plasma jet treatment, where highly dispersed Pt nanoparticles were dispersed on the 2D surface. This affixed the particles to not only one side but both, in just a single one-step process [92]. Another chemical approach exploits the reduction properties of Pt and Pd nanoparticles (NPs) on GO. These NP/GO hybrids are reduced by the use of supercritical 2-propanol to result in Pt and Pd NPs on graphene [78]. In a similar experiment, Pt, Ru and Ni NPs were also able to be deposited on the surface of graphene oxide by using the exfoliating ability of supercritical CO_2 [93]. Graphene oxide has also shown the potential to be used as a solid reductive agent for the fabrication of reduced GO (r-GO)/metal (e.g., Cu, Ni, Co) nanoparticle hybrid composites. A simple thermal reduction method at 500 °C under flowing argon without any external reductive agents (such as CO, H_2, sodium borohydride [$NaBH_4$]) was shown to form highly dispersed NPs of these metals on the surface [94]. The development of these new synthetic methods is crucial for both environmental and economic reasons, as these chemicals are readily available in sufficient quantities for industrial applications. Interestingly, not only 0D on 2D, but 2D on 0D materials also have been successfully fabricated. Peng et al. has showed the formation and growth of graphene on top of Pt nanoparticles [95]. Pt nanoparticles were first synthesized on cubic magnesium oxide, and then used for the deposition of graphene. These growth studies of graphene on MgO-supported Pt nanoparticles were conducted via both in situ and ex situ high-resolution TEM. TEM allowed for the study of the actual growth process, and the authors concluded that graphene sheets grow from steps on the Pt nanoparticle surface. This approach opens up a new way to synthesize nanocomposites based on graphene and noble metals nanoparticles at low cost. Some of the metal-2D material composites synthesized through these chemical process include ferric (III) oxide [Fe_3O_3]-Gr [96,97], cerium (IV) oxide [CeO_2]-reduced Gr [98,99], iron phosphide [FeP]/carbon nitride [C_3N_4] [100], Fe nanoparticles [NPs]/Gr [101], palladium [Pd] NPs [102], platinum [Pt]/graphene oxide [GO] [103], Pt/Gr [104], and Pt/Gr [105] (Gr = graphene).

Despite the facile nature of preparation of these NP/graphene hybrids, some of these processes are harsh for the 2D system, particularly the ones that require the use of strong acids and can lead to rupture in the 2D material or chemical modification. Therefore, baseline studies should be carried out to make sure that the properties have not changed of the 2D material after using the chemicals. Another consideration for the chemical addition method is the proper removal of solvents or catalysts after carrying out the reaction. Therefore, heat treatment of the heterostructure is necessary after the synthesis procedure to remove the solvent molecules and adsorbed species from the surface.

3.3. Drop-casting

Drop-casting provides a facile straightforward way to introduce 0D structures to the 2D surface via solution. A solvent containing the desired material can simply be introduced to the surface of the 2D material by either a simple 'drop' or by spin-coating on top. Both these routes have their advantages, where the former ensures that there will be enough material introduced to the 2D surface whereas the latter is more capable of an even spread across the 2D region. It should be noted that spin-coating often leads to significant wastage of the raw material, and simply 'dropping' the solvent on the surface can sometimes lead to a 'coffee ring' effect, whereby the material concentrates into concentric rings on the substrate when the solvent is drying. Therefore, it is important to consider the surface tension and microflow of the solvent, and a thoughtful consideration of the 2D material in question, for the best dispersion.

The migration barrier of most NPs on the 2D material surface, such as graphene, has been reported to be low [106], and therefore the 0D structures should be mobile after drop-casting them onto the surface. However, the presence of dangling bonds at the edges and the reported amorphous carbon layer formation on the surface of the 2D materials can often lead to the binding of the 0D structures to its surface. For instance, our work on $Gd_3N@C_{80}$ on graphene showed that after the drop-casting process, $Gd_3N@C_{80}$ entities on pristine graphene surface showed both translational and rotational dynamics, but the ones near the edges or in contact with the amorphous carbon layer on top were anchored [54]. One of the important factors to consider whilst using this technique is the correct choice of solvents and the use of right density of the solution for drop-casting. Using high boiling point solvents for drop-casting can make it difficult to remove the solvents afterward, whereas high density solution can lead to coalescence of NPs on the surface instead of them being separated. For the aforementioned reasons, drop-casting is an easy way to introduce metal NPs to the surface of 2D materials [107], as they are easily available in high purity ionic solutions. Ionic liquids (ILs) have been shown to have the ability to evenly disperse CNTs, thus providing the scope to potentially disperse arrays of tubular structures on 2D materials. It has also been shown that on top of dispersing the NPs on the surface, these ILs also provide stability to the NPs during the synthesis process by forming a protective layer around it [108]. The use of ILs is an area less explored for such synthetic processes and should be explored further.

Although the drop-casting technique has a downside in that it does not provide spatial control over the formation of the hybrid, it does provide a facile route to fabricate a desired 0D/2D hybrid for studying its fundamental behavior and dynamics at the atomic scale using TEM.

3.4. Ultrasonication

Of the many methodologies being reported so far, ultrasonication best facilitates the lost-cost synthesis of the 0D-2D hybrid material as the instrument cost is lower than that of other methods, such as vacuum deposition or electrochemical synthesis. Coupling quantum dots (QDs) with 2D materials have attracted great attention recently, as they show remarkable photocatalytic efficiency [109]. Ultrasonication of QDs with the 2D material provides a platform for the efficient formation of colloidal-QD/2D-material nanocomposites [110]. Anchoring of these QDs on the surface of the 2D material can occur easily via static charge attraction between the QDs ligand anions and the vacancies in the 2D sheets, for instance S-vacancies in MoS_2. The resultant nanocomposites have been reported to consist of uniformly deposited QDs on the surface and can be easily studied by transferring them to the TEM grid via the drop-casting method. Ultrasonication is often combined with other methodologies such as solvent transfer and surface deposition method (STSD) and chemical addition, to produce thin films after the addition of 0D materials to the surface of a 2D material. Ultrasonication helps separate the sheets afterward to provide thin films of the 0D/2D hybrid. It is important to use the right power and duration to carry out ultrasonication, as high power could lead to the disintegration of 2D materials into smaller pieces, and less time utilized to carry out the process can

lead to ineffective separation of the thick layered materials into thin sheets, thus only having thick material, as it was shown by Sinha et al. when using PbI_2 on graphene substrates [111].

3.5. Electrochemical methods

In this method, the spontaneous galvanic reaction of nanoparticles to a 2D host is exploited to facilitate the formation of clean 0D/2D hybrids. Park et al. [81] demonstrated that a spontaneous galvanic reaction occurs in the sandwich structures of reductant/graphene/oxidant that leads to deposition of the metal nanoparticles on the 2D surface. The authors fabricated Au nanoparticles on graphene by placing an Au ion solution on graphene, as made on Cu foil, to form a Au ions/graphene/Cu foil structure. The use of a galvanic reaction technique to form noble metal deposition on 2D materials has the advantage of being contamination free, which is an issue for the more conventional methods that frequently require organic solvents for nanoparticle formation. Nanoparticle-graphene hybrid structures, in particular, have attracted much attention and importance due to both their fundamental physical properties and especially sensor applications [112]. The accessibility of such clean and facile procedure for nanoparticle-graphene hybrid formation would speed up the efforts put towards their applications in electronic, electrochemical and optical sensors.

Electrostatic interactions between nanoparticles and 2D materials can provide another route for synthesis of these heterostructures, especially for electronegative 2D materials such as MXenes. Ye et al. [113] designed nanostructured electrocatalysts with high activity and long-term durability by adding electropositive CoZn−Se nanoparticles to electronegative 2D MXene nanosheets. The uniform distribution of these nanoparticles on the MXenes was ensured by their self-assembly on the 2D sheets when introduced 2-methylimidazole. Electrostatic interaction is yet another method to successfully integrate 0D material with a 2D system. QDs have been shown to uniformly intersperse into the nanosheets of MoS_2 or WS_2 based on solely electrostatic interaction [114]. Centrifugation of these two materials together leads to uniform dispersion of QDs on MoS_2. Although the QDs used in this particular work were also derived from the parent 2D material, this process can be easily replicated to other QDs. Such processes also demonstrate how two different synthetic methods, such as electrochemical addition-chemical transformation or electrostatic interaction-centrifuge can lead to beautiful, uniformly distributed introduction of 0D particles on to a 2D material target.

3.6. Solvent transfer and surface deposition method

The STSD method, as reported by Chen et al. [80], permits flexible formation of 0D/2D composites. The authors solved the issue of the large solubility difference between MoS_2 and C_{60} by utilizing the solvent transfer method to slowly transfer C_{60} dissolved in toluene to MoS_2 dispersed in isopropanol, resulting in a stable and well-dispersed C_{60} deposition on the MoS_2 flakes. The resultant hybrid was investigated at room temperature and ambient atmosphere by creating an ITO/C_{60}−MoS_2/Al configuration devices where ITO and Al were used as bottom and top electrodes respectively. The results showed excellent nonvolatile memory device behavior of the hybrid configuration with repeatable 'write−read−erase−read−rewrite' cycle with an ON/OFF ratio of up to 3.8×10^3. The STSD synthetic method can be sharply contrasted with the catalyzed transport reaction methodology, where similar C_{60} molecules acted as a growth promoter for MoS_2 and thus also consequently incorporated in the MoS_2 crystal to form a nanocomposite. But the reaction itself was carried out for weeks, in high vacuum and at high temperature (>1,000 °C) [89]. These aggressive reaction conditions are not ideal for experimental analysis and for developing applications, which highlights the benefits of the milder STSD method for preparing the same nanocomposite but under more environmentally friendly and gentle conditions. Similarly, other organic compounds such as phenyl-C_{61}-butyric acid methyl ester (PCBM) have also been reported to have deposit on MoS_2 to form nanocomposites via the STSD method, by mixing the two in n-methyl-2-pyrrolidone (NMP) and isopropanol (IPA), respectively [115].

Another variant of this method is via in-situ precipitation, where a-AgSiO particles were formed on the g-C_3N_4 surface, similar to the STSD method [116]. As verified by TEM imaging, the STSD method yielded uniform deposition of the organic material on top of the 2D surface to form nanocomposites. The important consideration is to find the right combination of solvents that are miscible and can dissolve and disperse the respective organic material and the 2D material, respectively. Ultrasonication is often employed for carrying out the actual mixing of the solutions for making nanocomposites.

3.7. Green synthesis

As has been discussed in this section, different types of synthesis methods can be employed depending on the type of hybrid material to be synthesized. An important aspect of research in this area is to find new methodologies that consume fewer resources whilst providing optimum growth conditions for creating high quality materials. One such green methodology has been reported recently for the synthesis of 0D-2D hybrid materials by Xavier et al. [117] In this process, the authors reported the use of glucose and urea, which are inexpensively available and nonhazardous precursors, for the synthesis of carbon QDs and carbon nitride sheets. The hybrid was assembled through microwave irradiation, which resulted in successful integration and uniform distribution of carbon quantum dots on the surface of the carbon nitride sheets. The resultant hybrid showed a fourfold enhancement in photocatalytic activity at the 0D-2D heterojunction, compared to the pristine carbon nitride sheets. More research in this area is required to create hybrid materials that would optimize resources by efficiently using new eco-friendly methodologies.

Ball-milling is another route to fabricate 0D/2D van der Waals heterostructures and nanocomposites [118]. A significant advantage of this mechanochemical route is it is eco-friendly and can be carried out without requiring high vacuum or inert conditions. MoS_2 and C_{60} heterostructures were reported to be synthesized via this route, with the MoS_2 later mechanically exfoliated to form thin sheets [118]. Studies via TEM showed that C_{60} was successfully bound to the edges of MoS_2, and that it was the presence of C_{60} that led to a decrease in the thickness of the MoS_2 nanosheets after mechanical exfoliation. In addition, C_{60} adhesion to the surface of MoS_2 also showed excellent visible light photocatalytic H_2 production rate, showing the success of this technique. The downside of the ball-milling method is the lack of control over the quantity and spatial distribution of these 0D materials on the 2D surface. Likewise, it is also difficult to control the domain shape and size of the 2D materials, which makes the process difficult to translate into applications.

We recognize that green synthesis has only recently been picked up by researchers in 0D-2D heterostructure preparation, and much work needs to be done in this area. We hope to have provided the readers with some ideas and what first steps are being taken in this direction, but future prospects must be addressed in the context of optimizing efficient heterostructure synthesis while maintaining high yield and low cost.

4. Solar cells

There has been a significant interest in the use of 0D/2D system in perovskite and organic solar cell systems over the past decade. Recognizing the sizeable amount of literature investigating fullerene/2D materials, we have divided this section into two subsections; the first one focuses on fullerene derivates and hybrids with other 2D materials, and the second section covers the role of other 0D/2D material hybrids in photovoltaics.

4.1. Fullerene/2D material hybrid

An impressive amount of research has been carried out on fullerenes and their derivatives, especially for application in the field of perovskite and organic solar cells [122,123]. Their unique structure, electron acceptor and transfer properties, as well as the ability to encapsulate or functionalize with a variety of different molecules, has rendered them indispensable for the development of next generation solar cells. For instance, the fullerene derivate PCBM is widely recognized for its role in suppression of hysteresis in perovskite solar cells and as an electron extraction and transport material for organic photovoltaics [124,125]. In addition, the advent of thin-film solar cells has inspired the study of 2D materials like graphene and TMDCs in photovoltaics because of their enhanced charge transport and slower exciton recombination [126–129]. It has been shown that 2D materials not only lower the cost of fabrication, but also enhance the efficiency as well as minimize energy barriers for charge extraction [130]. They have been used as electrode material [131], both hole and electron transport layer, as well as in the perovskite layer (Fig. 4a). In this section, we will review the novel properties and applications of the hybridization of these two 0D-2D materials for photovoltaics and the novel properties they bring.

The investigation of fullerene-graphene hybrids can exploit the high carrier mobility of graphene and the strong electron accepting properties of fullerene derivatives [132]. It was demonstrated for the first time by Kakavelakis et al. [133] that although the utilization of PCBM functionalized r-GO initially increases the conductivity of the film by five times, leading to a higher short circuit current density, it simultaneously also reduces surface traps as well as passivates the perovskite surface. The r-GO acts like a third layer in the charge transfer of electrons from the perovskite to the PCBM layer. The authors also showed that the hybrid led to reduced series resistance and surface roughness for electron transport, which has not been achieved by a PCBM-only or 2D material-only interface. Subsequently, Bi et al. [134] demonstrated that a doped graphene-PCBM hybrid is almost three times as effective in blocking the ions and molecules, compared to a conventional electron extraction layer of the same thickness. The resultant device also maintained 98% efficiency in the prolonged 500 h 85 °C aging test.

Increase in performance of organic solar cells have also been reported recently, by exploiting the hybrid PCBM-graphene system. The ability to easily drop-cast, spin coat or vacuum deposit this fullerene derivate on top of the 2D material facilitates the facile use of this hybrid in fabricating solar cells [135]. It has also been reported that fullerene derivate PCBM can also be hybridized with graphene in the form of quantum dots [136–138]. Graphene quantum dots (GQDs) are just graphene sheets, with single or a few layer thickness, but smaller than 10 nm in diameter. These GQDs benefit from the fact that they still exhibit all the excellent electronic and mechanical properties of graphene, whilst also encompassing the distinct properties of quantum dots, such as photoluminescence, quantum confinement, etc. This portfolio of properties offered by GQDs, when combined with PCBM, has the potential to increase the performance and stability of the perovskite solar cells. Shin et al. showed that this is not only true for classic rigid substrates, but an excellent approach for also creating perovskite solar cells on flexible substrates. The resultant hybrid helps improve light absorption performance [136], as well as realize highly flexible perovskite solar cells which can maintain over 80%

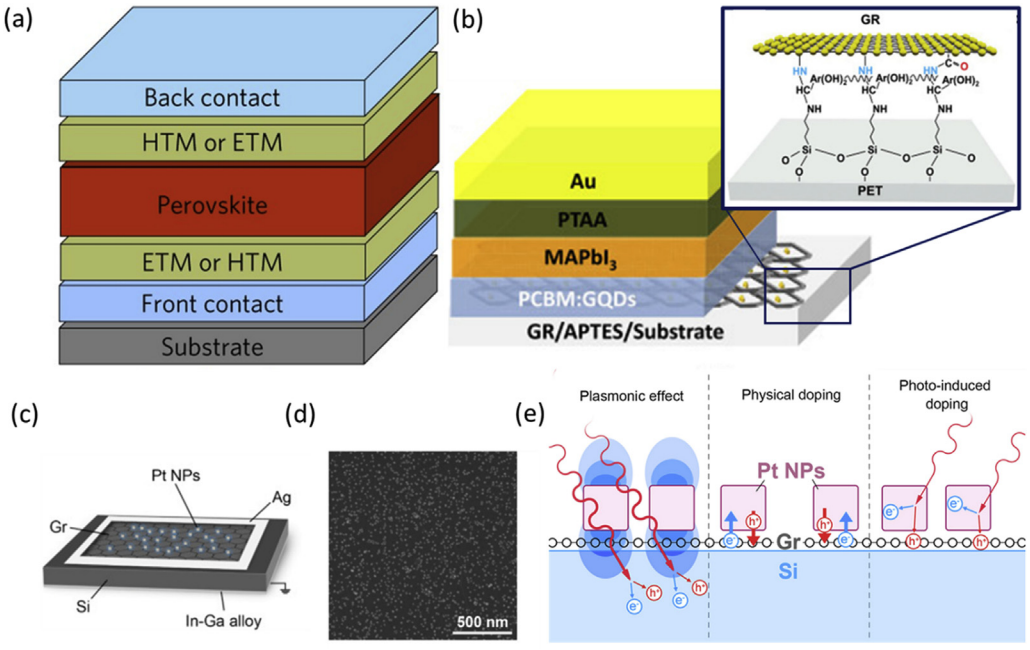

Fig. 4. (a) Schematics of a typical perovskite solar cell showing the different layers of the configuration where 0D/2D hybrid can be applied based on their type and properties. ETM and HTM refer to electron transport layer and hole transport layer respectively [139]. (b) Device structure of a solar cell utilizing graphene quantum dots. Inset shows the interaction of graphene and the substrate via an APTES layer [137,138]. (c) Schematic diagram, (d) SEM image, (e) and the three different mechanisms by which the Pt NPs can enhance the performance of Gr-Si solar cells [140].

shape of the original cell even after 3,000 bending cycles at a curvature radius of 4 mm (Fig. 4b) [137,138].

4.2. Other 0D/2D material hybrids

0D NPs functionalized on 2D materials can alter the design, efficiency and nature of photovoltaic devices. As discussed in the previous section, NPs can be easily introduced as dopants or functionalized on the surface of a 2D material via different techniques. One of the first demonstrations of a metal nanoparticle-graphene hybrid was by Wang et al., in 2014 [141]. They demonstrated improved photovoltaic performance by the use of the nanocomposite, as compared to TiO_2-only devices. Since then, many studies have been carried out on synthesizing and applying NP/graphene hybrids in photovoltaic devices, and have shown that the deposition of NPs on graphene can lead to higher efficiency of photovoltaic devices, as they can alter the work function of graphene [142,143] and reduce energy barrier formation at interfaces, owing to the p- or n-type doping (Fig. 4c–e).

Bhosale et al. [144] showed that MoO_x doped GO films do not cause trapping or delocalization of holes in the GO film, and reduced charge recombination at the interface of perovskite/GO-MoO_x, leading to better power conversion efficiency of 16.7% as well as enduring stability. In a similar experiment, Xie et al. [145] showed that even better stability and power conversion efficiency of up to 18.5% can be achieved by using MoO_x doped r-GO as a hole transport layer. The results can be attributed to not only the doping effect of the NPs to the 2D material, but also to the surface morphology, film formation of the hybrid material, as well as its surface contact angle with the perovskite material which is critical to the perovskite solar cell performance. For instance, although Au NP/GO hybrids show the highest transmittance and conductance, their role as a hole transport layer in devices showed a decrease in efficiency of 1.25% due to deterioration of the crystalline structure of the perovskite material in the presence of Au NPs. NP/graphene hybrids can also act as an electron transport layer, as shown by the ZnO-graphene hybrid - a widely studied NP/graphene hybrid material [146]. ZnO-GO nanoparticles have shown to increase conductivity, as compared to pristine ZnO, by reducing the interfacial resistance between the ZnO/GO and the perovskite layer [147]. Similar results were shown for increased conductivity in SnO_2 where incorporation of graphene quantum dots with SnO_2 led to improved conductivity as compared to pristine SnO_2 [148,149]. Another important aspect of the NP/graphene hybrid was shown by Tavakoli et al. [150], where incorporation of graphene with ZnO was shown to assist in high temperature annealing during the formation of perovskite crystal, as compared to pristine ZnO, that results in formation of bigger grains of perovskite.

Several different integration schemes, and associated improvements in device performance, have been reported for other NP/2D material hybrids, such as C/GO [151], Au/Gr [152], and MoO_3/Gr [142]. One of the many benefits of incorporating graphene-NP composites in solar cells is also that the processing can be carried out at much lower temperature than what is required for processing of conventional electron collection layer such as titanium dioxide (TiO_2) [141]. The use of these nanohybrids can thus pave the way forward for low-temperature processed high-efficiency solar cells for future.

5. Catalysts in energy applications

Many reactions necessary for future energy technologies, such as the hydrogen evolution reaction (HER) for a hydrogen energy economy, or the oxygen evolution reaction and oxygen reduction reaction (OER and ORR) for fuel cell cathodes, currently require rare and expensive noble metal catalysts to be viable. There has been significant recent research activity into harnessing the properties of low-dimensional materials to enhance catalyst activity, selectivity, and durability, and thus addressing the challenge of developing more cost-effective catalysts for these reactions [153–157]. These properties, such as electronic structure manipulation via quantum confinement or enhancing the photosensitivity through creation of surface plasmon resonances, allow for the tailored engineering of a catalyst for a particular reaction [158]. By combining low-dimensional systems in a 0D-2D heterostructure we increase the parameter space available for such catalyst design, and also facilitate the exploitation of other complementary properties, such as high surface area, good conductivity [8,159–162], or durability under adverse pH conditions [163,164]. Physically, space confinement of the catalyst between 2D sheets can assist in the selectivity and stability of the catalyst, with a tailored geometry allowing for control of the reactant adsorption behavior [165].

A recent example of a 0D-2D heterostructure catalyst is the combination of 2D graphitic carbon nitride (g-C_3N_4) (Fig. 5a) partnered with nanoparticles for the photocatalysis of water splitting and other reactions [166]. The g-C_3N_4 nanosheets exhibit good stability, decent transport properties and are economical to prepare, which along with their 2.7 eV bandgap and 2D quantum confinement make them appealing candidates for photocatalytic applications [167,168]. However, g-C_3N_4 on its own suffers from rapid carrier recombination, limiting its quantum efficiency [169]. Thus pairing it with a nanoparticle cocatalyst is appealing, with the interfaces facilitating separation of the photoinduced charges [170–173]. Partner catalysts include noble metal nanoparticles such as gold, which in addition to helping with charge separation also improve the amount of light absorbed due to their surface plasmon resonance [174–176], and semiconductor quantum dots such as cadmium sulfide (CdS), with the heterojunction aiding in charge separation and improving photocatalytic efficiency (Fig. 5b) [177–183]. The 0D and 2D component combined complement and enhance the overall activity and performance of the paired system, beyond the 2D material simply acting as a supporting scaffold for active 0D nanoparticles.

This section will explore the use of 0D-2D hybrids as catalysts for several energy applications. It will discuss how the combination of 0D and 2D components enhances the catalytic performance beyond the sum of their parts, as illustrated with the above example, in the development of catalysts for the important oxygen reduction, hydrogen evolution, and CO_2 reduction reactions. We will review example areas which have had significant research undertaken into the potential of 0D-2D composite catalyst materials, in particular catalysts for hydrogen generation, fuel cell cathodes, and CO_2 reduction.

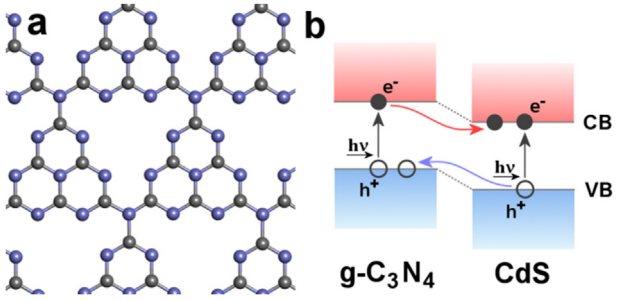

Fig. 5. Graphitic C_3N_4 as a cocatalyst in photocatalysis. (a) Atomic model of a sheet of g-C_3N_4. (b) Simple band structure sketch of a heterojunction between g-C_3N_4 and a semiconductor quantum dot, illustrating charge separation with electron accumulation to the right conduction band (CB) and hole accumulation to the left valence band (VB).

5.1. Hydrogen generation

The efficient synthesis of hydrogen will be crucial for the realization of a hydrogen economy, and so is a major target for electro- and photocatalyst research. Currently, Pt and other precious metal catalysts are considered to be the most efficient [184,185]; however, their high cost impedes their widespread use. One approach is to optimize the precious metal utility by maximizing activity and minimizing catalyst loss or deactivation with use. This can be achieved by anchoring small nanoparticles or single atoms of the precious metal on a graphene or g-C_3N_4 host [29,186–193], or to partner the precious metal with a less expensive cocatalyst [194–196]. While this method has merits, the majority of research has instead focused on an alternative approach; replacing the precious metal constituent with an alternative catalytically active material.

Leading nonprecious metal candidates include transition metal (Ni, Fe, Co, Mo) sulfide, carbide and phosphide compounds [197–205], with MoS_2 sulfur-terminated edge sites a particular area of interest due to the favorable Gibbs binding energy for H_2 [206,207]. As MoS_2 is a layered material, it presents a good partner 2D component in a 0D-2D heterostructure HER electrocatalyst, as it can act both as an effective supporting scaffold for various nanoparticle catalysts – due to its good conductivity, durability, and resilience to extremes in pH – and also contributes toward the overall HER activity [208]. Combining it with a nanoparticle cocatalyst (e.g. Pt, Au, Ni_2P) distributed on the MoS_2 sheets means that the basal plane area of the MoS_2 is effectively catalytically active as well, rather than activity limited to just the edge sites, and thus maximizing the effective active area of the electrode (Fig. 6a) [39,41–43]. However, the typically higher defect density of the MoS_2 edges vs. the basal plane tends to encourage preferential nanoparticle decoration along the MoS_2 edges, rather than the more desirable basal plane [39,42]. This can be seen in the TEM characterization of Li et al. [42], where at low loading the Pt nanoparticles are preferentially located along the MoS_2 edges (Fig. 6c).

The activity of MoS_2 (and the similar WS_2) toward the HER can be enhanced by reducing its dimensions to a quantum dot, due to the increased defect density and active sulfur terminations [211]. This reduction from 2D to 0D leads to problems with their agglomeration and detachment from the electrode. Therefore pairing the dichalcogenide quantum dot with a partner 2D material host, such as (r-) GO [114,210,212,213], g-C_3N_4 [180], MoS_2 flakes [209], or metallic VS_2 [214], is desirable for improving the stability, enhancing 0D component dispersion, and ensuring excellent electrical coupling between the 0D and 2D component. The work of Bayat et al. maximizes the number of available MoS_2 edge sites by combining MoS_2 nanoparticles with vertically oriented MoS_2 nanosheets (Fig. 6e–g), allowing for the supporting 2D component to also provide active edge sites [209]. One of the earliest works demonstrated the importance of MoS_2 nanoparticles having a large abundance of edge sites through simple in-situ formation onto reduced GO flakes (Fig. 6h–k) [210]. MoS_2 sheets have also been paired as a cocatalyst with semiconducting quantum dots (e.g. TiO_2, CdS) in photocatalytic water splitting reactions for hydrogen formation [181,215–217], where the MoS_2 helps to prevent charge recombination, generally increases the number of active sites, and improves electron transport – especially when additionally composited with graphene [218–221].

Single atomic doping of MoS_2 has shown significant promise for the hydrogen evolution reaction (HER). The addition of dopants can have the dual effect of providing active sites from the dopant orbitals, and also increasing the defectiveness of the MoS_2 basal plane, generating more S terminated edge sites that are active toward the HER [16,222–224]. Deng et al. experimentally studied Pt doping of MoS_2 toward the HER, and further extended this by exploring the effect of other dopants by modeling. The site that the metal atoms occupy is key, with direct substitution for the Mo site being inferior to a more interstitial position; the interstitial dopant configuration leaves unsaturated, and therefore catalytically active, sulfur neighbors [16]. Metal dopants like V and Cr, which prefer direct substitutions for Mo [225], are thus expected to be significantly less active than larger dopants such as Pt. The addition of certain other metal dopants can also modify the electronic structure for better energy level matching for electron transfer to the H^+, improving the thermodynamic favorability of the HER. Zn dopants are particularly effective for this [226–228].

Beyond the sulfides, other transition metal compounds that have been employed successfully for 0D-2D heterostructure HER

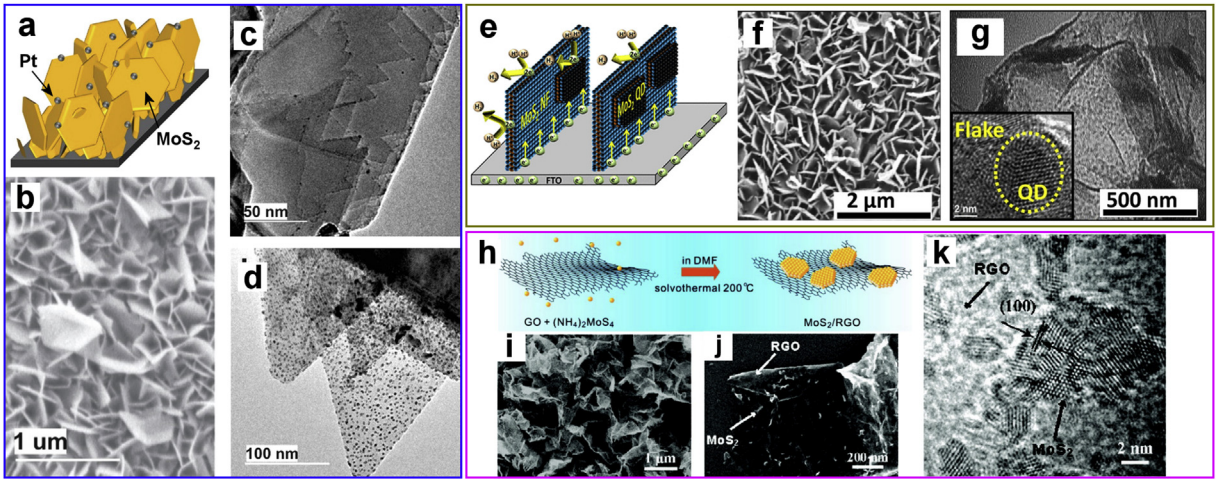

Fig. 6. 0D-2D HER catalysts based on MoS_2. (a) Schematic illustrating Pt nanoparticles on vertically grown chemical vapor deposition (CVD) MoS_2 sheets. (b) SEM image of the CVD grown MoS_2. (c) TEM image of MoS_2 flakes with low Pt (0.11% wt.) loading and (d) high Pt loading (11% wt.) [42]. (e) Graphic showing the structure of MoS_2 flakes decorated with MoS_2 nanoparticles, electrophoretically deposited vertically on a F-doped tin (IV) oxide (SnO_2) substrate. (f) SEM image of the deposited flakes. (g) TEM image of a flake, with the insert showing an attached MoS_2 nanoparticle [209]. (h) The preparation of MoS_2 decorated reduced GO sheets. (i,j) SEM images of the prepared catalyst. (k) TEM image showing MoS_2 nanoparticles attached to the reduced GO [210].

catalysts include transition metal phosphides, carbides, and oxides. Transition metal carbides, such as Mo_2C, have been shown to have good HER activity and robustness to dissolution; however, they can be challenging to synthesize in a nanoparticulate form, often oxidizing or becoming clogged with excess carbon [229]. It has been found that the in-situ preparation of the Mo_2C nanoparticles on a graphitic carbon support, such as graphene or carbon nanotubes, can minimize these problems due to the strong interaction between the Mo_2C and the graphene [230]. This strong interaction also inhibits the ripening, aggregation, and detachment of the prepared nanoparticles when catalyzing the HER, thus yielding a catalyst with excellent activity and durability [231]. Phosphides, and especially cobalt phosphide, have been intensely investigated for HER catalysis, with the balance between P and metal atom ratios along active facets being a key determinant in the catalyst effectiveness [232–234]. Many works have integrated phosphide nanoparticles into graphitic-sheet supports, either by dispersing them straight to the sheets or by encapsulating the nanoparticles in a graphene envelope, benefitting the charge transport and durability [164,203,235–240]. Nitrogen doping of the graphene support can enhance the overall catalytic activity of these hybrids by providing more active sites [241–243]. Cobalt's particularly low energy barrier for hydrogen adsorption [244] make it a popular HER catalyst candidate in its oxide and native forms as well, with similar benefits observed by pairing their nanoparticles with a (N-doped) graphene support [245–248], for instance by overcoming the low conductivity of Co_3O_4 [249], or encapsulating to minimize aggregation [250,251]. Future research could explore linking some of the aforementioned 0D metal compounds with 2D MXenes [252], yielding new hybrid catalysts [253].

Demonstrating an efficient HER with an entirely metal-free electrocatalyst is the ideal scenario, and there is potential that this may be viably achieved with suitably doped graphene. Leading dopant candidates are B, N, O, S, and P [254,255]. Jiao et al. recently conducted a systematic modeling and experimental analysis of these various doping configurations, taking care to also consider the different possible atomic configurations a dopant can occupy within the graphene lattice (edge vs. bulk sites, pyridinic vs. graphitic, etc.) [256]. These studies revealed that boron doping yielded the best activity per dopant site, and also suggested that even a theoretically ideal doped graphene catalyst would struggle to achieve the activity of a standard Pt based catalyst [256], even when pursuing a multi-element doping strategy [257]. Compositing nitrogen doped graphene with g-C_3N_4 has shown promise for promoting the activity further, with the extra active sites offered by the porous g-C_3N_4 suggested as one possible reason for the significant improvement in activity [258,259].

5.2. Catalysts for fuel cells

Fuel cells, along with batteries, are a primary energy storage candidate to support societies shift to carbon-free technology, with applications in electric cars and power grids. There are a variety of fuel cell architectures, with two of the current leading contenders being the direct methanol fuel cell (DMFC) and the proton electrolyte membrane fuel cell (PEMFC) [260–262]. As these types of fuel cell operate at or near room temperature, a catalyst is required to expedite the reactions at their electrodes. The most effective of these catalysts are noble metal nanoparticles, which while effective suffer from high cost. A major problem is their degradation with use, with the nanoparticles detaching, dissolving, ripening and agglomerating over time, necessitating high initial loading of the electrodes to offset this decay and thus increasing costs yet further [263]. As a result, research focuses on either improving the activity and resilience of the noble metal catalyst, and so reducing the amount required, or finding an alternative catalyst material that does not require expensive elements. Nanomaterial design, in particular combining 2D and 0D materials, has shown significant promise in both these areas [264–267].

A crucial reaction in a DMFC is the catalyzed oxidation of methanol at the anode, reacting with water to produce the protons and electrons for the fuel cell to operate, and that is typically the rate limiting step [268,269]. The methanol oxidation reaction (MOR) is typically catalyzed by platinum alloys (particularly Pt–Ru), minimizing the effect of surface poisoning from CO species, with research into alternative Pt-free catalyst not as developed as for the cathode reaction [270,271]. As such, much of the research has focused on reducing the size of the Pt-based nanoparticles and maximizing their activity per mass [272]. The 0D-2D application centers on applying these delicate Pt alloy nanoparticles to graphene membrane supports [273] that can maintain their ultra-fine size over many cycles (Fig. 7a–f) [34], while also providing a durable, conductive, and high surface area scaffold [274]. A variety of methods have been reported on preparing Pt and Pt alloy nanoparticles on to graphene and (r-)GO [36,275–283], leveraging graphene's excellent properties as a catalyst support, and often its important role in helping nucleate the nanoparticles during synthesis [284–286]. Recently, the encapsulation of Pt nanoparticles in multiple graphene layers has been also shown to help with the Pt stability toward electrocatalysis of the MOR [287]. Including nickel hydroxide nanoparticles with the Pt on the graphene host has been used to complement the Pt activity, by assisting with water dissociation from the electrolyte and assist the removal of deactivating CO species on the Pt [288]. Pt-based catalysts dominate for the MOR; however, some alternatives exist that have been paired with graphene in a 0D-2D heterostructure. Fe_3O_4 and Fe_3O_4–Au core-shell nanoparticles dispersed on GO have been shown to be workable, Pt free, catalysts for the MOR [289]. And $NiCo_2O_4$ catalyst nanoparticles, which lack in electrical conductivity, benefitted significantly from the high electrical performance gains from being dispersed on a r-GO support [290].

In fuel cells, and particularly PEMFCs, a major limitation is the sluggish rate of the oxygen reduction reaction (ORR) at the cathode. Currently Pt, or occasionally Pt alloy [292], nanoparticle catalysts on carbon black are used; however, their high costs and poor lifetime durability are major impeding factors in commercial scalability [293]. Finding alternative catalyst nanostructures, which either give Pt catalysts that are more efficient and durable, or to find more effective alternatives that remove the need for Pt entirely, will be essential for allowing PEMFCs to be market-viable [294]. 0D-2D hybrids offer potential research avenues in both the realization of more efficient Pt-based ORR catalysts, and the development of viable Pt-free ORR catalysts [295].

The exploration of 0D-2D composite catalysts to improve Pt utilization has often simply been a case of using graphene as a replacement for carbon black as the support [296], providing improved adhesion of the catalyst to the electrode, superior distribution and high loading of small sized nanoparticles, and being more robust to the low pH operating conditions [297,298]. This can help militate against the disadvantages of conventional Pt (or Pd) catalysts, by facilitating smaller morphologies, thus providing more active sites per weight, and reducing activity loss through detachment and etching [263,299]. Other than standard nanoparticle catalysts [92,300,301], partnering graphene supports with novel Pt/Pd morphologies, such as concave nanocubes [302], nanocages [303], or nanorings [304], are a promising route to further optimize the catalytically active surface area for a given mass. Forming bimetallic Pt alloy nanoparticles on the graphene, in particular with Co [305–308], has also been shown to be an effective strategy for minimizing Pt or Pd loading while also improving activity

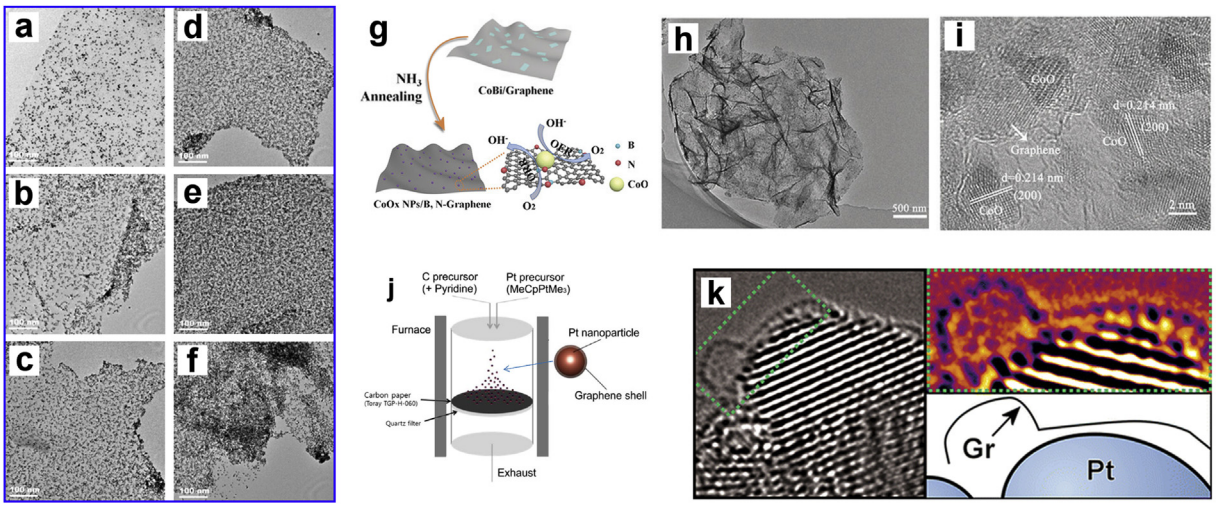

Fig. 7. 0D-2D fuel cell catalysts. (a–f) TEM of Pt nanoparticles uniformly distributed to tunable concentrations on functionalized GO for methanol oxidation. The precursor Pt weighting increases from (a) to (f) [34]. (g–i) Graphic of the preparation of Co oxide nanoparticles on to a B and N doped graphene host for coupled catalysis of the ORR [291]. (j) Schematic showing the preparation of graphene encapsulated Pt nanoparticles onto a carbon support suitable for the ORR. (k) Aberration corrected TEM of a graphene monolayer shell wrapped around a Pt nanoparticle [15].

[309–314], with the added metal reducing the binding energy of OH species, ensuring active sites remain free and available for O_2 adsorption.

Successful realization of an active and durable Pt-free ORR nanocatalyst is an alternative approach for solving the PEMFC cathode problem. Many novel catalyst candidates have been integrated with a graphene scaffold, similarly to the aforementioned Pt-based works, including transition metal oxide [315,316] and carbide nanocatalysts [317]. Co oxides and other Co compounds have been particularly successful [318–324], in particular when synergistically partnered with N doped r-GO [291,325], with the initial GO support providing a multitude of nucleation sites for nanoparticle formation (Fig. 7g–i). Graphene is an equally effective support for these nonprecious electrocatalysts. In a number of these works, it was found that the graphene's role is beyond simply being a conducting scaffold for the active 0D electrocatalyst, as doping of the graphene introduces active sites on the 2D material itself, meaning it contributes as a cocatalyst rather than just a support [297]. The importance of this synergy was demonstrated by Liang et al. [325], where they show that Co oxide nanoparticles or N-doped graphene in isolation have poor activity, and only together do they yield good performance. The dopant atom, typically N, breaks the regular sp^2 hybrid bonding of the graphene, yielding local active sites with an electronic structure dependent on the dopant. In the case of N doping of a regular graphene lattice either a pyridinic or graphitic bonding can occur to accommodate the N [297,326], with pioneering work by Guo et al. revealing that specifically the pyridinic structure appears to provide the ORR activity [327].

Other than doped graphene, there have been few reports of other 2D supporting materials exhibiting significant co-activity toward the ORR. W oxide nanosheets coupled with Pd and Pt nanoparticles have been reported, with a significant boost in activity toward ORR measured when they are paired together compared to each acting in isolation [328,329]. And a recent comprehensive modeling survey suggested that a novel two-dimensional molybdenum carbide (2D MoC_2), a 2D carbide similar to MXenes, may be an effective cocatalyst and support for a 0D catalyst partner [330]. As a conductive scaffold, and as a template for nanoparticle nucleation and growth, 2D MoS_2 has shown some promise for oxygen reduction reaction (ORR) 0D-2D catalysis, with the particular advantage over graphene of facilitating the growth of small nanoparticles or unique morphology nanocrystals [331,332], and potentially assisting with the oxygen transfer kinetics to the catalyst [333].

Recently, there has been a surge of interest in encapsulating nanoparticle catalysts in a graphene envelope, enhancing the catalyst's activity and especially its durability. Some works have explored the encapsulation of the traditional Pt nanoparticle ORR catalysts, enveloping in amorphous carbon [334,335], h-BN [336], or graphene (Fig. 7j and k) [15,337,338]. These demonstrated that encapsulation yielded significant improvements in durability, reducing the decay in catalyst activity over extended cycling. However, more recent works have focused on exploring the platinum (Pt)-free catalysts, in particular transition metal carbides and oxide nanoparticles [339–344]. Many have used N-doped graphene as the encapsulating 2D material, and while it seems to give optimal activity, there is some ambiguity over the mechanism of activity. One theory is that the N-doped graphene promotes electron transfer from the nanoparticle core, which along with the graphene surface gaining a higher electron density from the N doping yields potential active sites for the ORR [345–347]. Another explanation could be that the N-doping opens pores in the graphene envelope, allowing reactants and products to interact more easily with the nanoparticle surface [15]. Regardless of the activity mechanism, encapsulation is nearly universally observed to improve nanoparticle resilience, acting as a protective shield against dissolution, ripening, poisoning of active sites, and detachment, and thereby yielding improved activity compared to 'naked' catalysts over prolonged cycling [347,348].

This discussion of N-doped graphene, and its role in catalysis of the ORR, brings us to the application of single atom catalysts for the ORR. Metal-free catalysis via doping single sites in a graphene host [349,350], in particular with nitrogen [351–353], has been pursued as a single-atom catalyst candidate. While performance has been promising, understanding the mechanism that allows for direct one-step ORR, as opposed to other nondesired reaction paths, has proven difficult. Disentangling the role of the different types of N-doping site (pyridinic vs. graphitic direct substitution) [327,354], the potential activity of free edge sites [355–359], and the presence of other functional groups and defects [360–363], can complicate the picture. Introducing metal single atom dopants into graphene

has also been explored, allowing for ultimate dispersion of metal active sites. Dopants including Cu [364,365], Fe [366,367], Co [368], and Ru [369] have been employed successfully, although achieving high metal loading and long term durability remains a challenge due to the difficulty in securely anchoring the single metal atoms into the graphene lattice. The aforementioned references typically use defective graphene, such as graphene oxide, as the source material, allowing for metal dopant integration into the existing defect sites. However, an alternate approach is to employ g-C_3N_4 as the 2D host, with its regular array of anchor points providing a template for potential metal doping sites. This has been successfully demonstrated with Fe [370], where the g-C_3N_4 as the initial scaffold can be pyrolyzed into a more graphitic structure [371].

5.3. Catalysts for CO_2 reduction

The ability to synthesize useful fuels from an unwanted waste product, namely CO_2, is clearly desirable. Being able to perform CO_2 reduction efficiently via a photocatalytic reaction would provide a valuable source of environmentally friendly fuel [372]. However the reduction is particularly difficult [373], with many photocatalysts only achieving low conversion efficiencies [374], and conversion to compounds with two or more carbons proving particularly difficult [375]. Photocatalytic CO_2 reduction can use either water or hydrogen as the reducing agent, with the former reaction sometimes instead referred to as artificial photosynthesis. A suitable photocatalyst must achieve both good electron-hole pair separation following photoexcitation, and have a favorable surface interaction with CO_2 to make it more amenable to reduction [376–378]. As with other photocatalytic reactions, TiO_2 nanoparticles are frequently employed as the semiconducting component, often paired with a metal nanoparticle catalyst such as Cu or Ag to improve methane yield [379]. Recently, there has been significant interest in combining these nanoparticles with r-GO or g-C_3N_4, to enhance overall activity and durability [380–382].

Beyond being a robust and high surface area support, integrating graphene with semiconductor nanoparticles promotes separation of charges, with the graphene being a high mobility electron acceptor that thus helps prevent premature charge recombination [385–387]. There is also evidence that the graphene, and in particular the more defective reduced graphene oxide, can enhance the overall activity by providing binding sites for CO_2 [388,389]. Thus integrating semiconducting TiO_2 or CdS nanoparticles with r-GO has yielded promising photocatalysts for CO_2 reduction [390–392]. However, to enhance the efficiency further, and potentially allow for the production of useful higher order carbon products such as ethane [393], the addition of a metallic cocatalyst is typically desired, such as Pt or other noble metals [394,395]. Copper and copper oxide nanoparticles have also been frequently paired with graphene for CO_2 reduction, with the Cu particles offering effective hosts for multi-electron reduction reactions when paired with graphene (Fig. 8a–c) [383,396–398].

As discussed, g-C_3N_4 has attracted attention as a 2D light harvester in photocatalysts for water splitting, and there has been some work exploring its effectiveness toward CO_2 reduction [381]. Its low electrical conductivity can lead to unfavorable charge recombination rates, and so pairing with graphene or carbon dots can be an effective metal-free strategy to counteract this drawback [399–401]. Alternatively, partnering it with another semiconductor, such as Ag halides or Fe oxide nanoparticles, in order to form a heterojunction will also improve carrier lifetime and thus activity [402–405]. The deposition of Pt nanoparticle cocatalysts to g-C_3N_4 enhances activity toward CO_2 reduction, similar to reports of Pt with graphene, but also can help offset the charge recombination problem, as the Pt nanoparticles may trap the excited photoelectrons [406,407].

As an alternative to the photocatalytic method, the electrocatalytic reduction of CO_2 uses an electrolyzer with two electrodes separated by an ion conducting membrane, with the anode producing oxygen via the OER, and the cathode reducing CO_2. It remains challenging due to the poor reduction kinetics and ensuring good selectivity of the reaction product [408], yet the tailoring of two dimensional materials holds promise for overcoming these problems, such as by lowering the CO_2 adsorption energy barrier with doped graphene [409]. Metal doping of graphene sheets have been explored as potential electrocatalysts for the cathode [410,411], with most attention devoted to the integration of Ni single atom sites into nitrogen doped graphene [412–415]. These reports all integrated the single atom into the graphene host by utilizing the nitrogen dopants as anchor sites, situating the metal into an in-plane interstitial position in the graphene sheet (see Fig. 4f) [384]. These metal active sites are highly active, selective to CO_2-to-CO reduction, readily accessible to reactions on the basal plane, and with appropriate chemical engineering can be uniformly distributed across a graphene sheet [412]. Beyond graphene, Nb doping of CVD grown MoS_2 has been shown to significantly enhance the activity is MoS_2 toward CO_2 reduction to CO, with modeling suggesting this improvement was due to the Nb near the edge decreases the binding strength of CO [416].

Unfortunately, despite the above progress, few 0D-2D electrocatalysts have shown good yields of the more desirable C_{2+} or non-CO products. Some progress has recently been made in 2D material catalysts toward these more desirable products [417–419]. Future research directions could seek to improve these new 2D electrocatalysts through integrating with suitable 0D cocatalyst components, such as noble metal nanoparticles or by dopant introduction [420]. A recent example is the combination of SnO_2 particles with thin Pd nanosheets, which facilitated the electrocatalytic reduction of CO_2 to methanol [421]. The Pd and SnO_2 components have already been explored individually as CO_2 reduction electrocatalysts, with SnO_2 showing particular selectivity toward non-CO products [422,423]. But their combination in a heterostructure, with the extensive Pd–SnO_2 interfaces that the 0D-2D geometry provides, helped to preferentially suppress CO formation in favor of methanol [421].

6. Electrodes for rechargeable batteries

To support the push for greater renewable power generation, decarbonization of our transport, and more powerful portable devices, we require better rechargeable batteries. Improvements to the current incumbent technology, the lithium-ion battery, are being sought [424]. Beyond simply evolving Li-ion, the next generation of battery architectures, including Na-ion, Li-oxygen, Li-sulfur, and even multivalent chemistries, are being keenly researched [425–428]. Designing suitable electrodes that support and are robust toward these reversible chemistries is one of the core materials challenges in this research [429]. Application of resilient and conductive materials such as graphene are therefore of great interest [430,431]. Here, we will explore the role 2D materials can play in supporting and protecting a variety of anode nanoparticle candidates for Li-ion anodes, and how 0D-2D ORR catalyst heterostructures may be of use in next-generation Li-oxygen and Zn-oxygen battery cathodes.

6.1. Alloying and conversion anodes for Li-ion batteries

The anode, or negative electrode, in present Li-ion batteries use graphite, which gives an upper specific capacity limit of 372 mAh/g

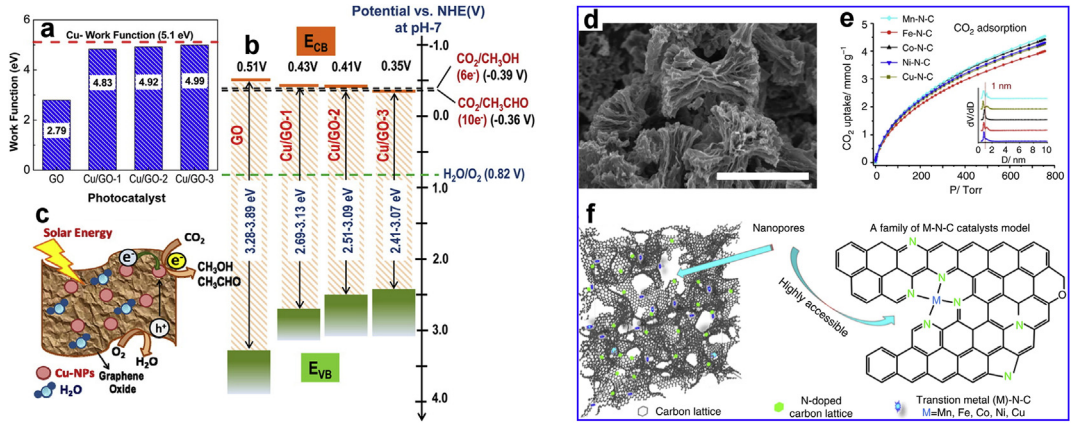

Fig. 8. 0D-2D CO_2 reduction catalysts. (a) Work function and (b) band-edges of GO with and without Cu nanoparticles. Cu/GO-1, -2, and -3 refer to increasing Cu wt. % loading, with 5, 10, and 15% respectively. (c) Schematic showing the Cu-GO system [383]. (d–f) The inclusion of various single metal atoms into nitrogen doped graphene. (d) SEM image of the graphene structure. (e) CO_2 physisorption for the respective metal dopants. Insert shows the modeled pore size distribution. (f) Schematics showing the superstructure, and the metal doping anchoring point, occupying an interstitial position and bonded exclusively to N [384].

due to accepting one Li ion per six carbons [432]. Simply replacing this anode with a pure Li metal anode would drastically increase the capacity (lithiated capacity of up to 3,860 mAh/g), however such anodes currently suffer from severe durability concerns [433]. Certain materials that can electrochemically alloy with lithium, such as Si, Sn, and Ge, are promising alternative candidate materials for the anode and are referred to as alloy anodes [434,435]. This family of anode materials suffer from debilitating structural problems over cycling, leading to material fracture and detachment from the current collector electrode.

Rather than forming alloys, an alternative approach is to utilize the reversible electrochemical reactions possible between lithium and certain transition metal compounds, forming into lithium oxides and metal particles then reverting over the course of the charge-discharge cycle. These metal oxides and chalcogenides are known as conversion anodes and promise capacities two to three times higher than that of graphite (600–1,000 mAh/g) [436]. As with the alloying anodes, there is a challenge in devising electrodes that are robust toward the large volume changes that occur during charge cycling and have issues in ensuring good electrical connectivity to the current collector due to the insulating character of the metal oxides.

While the chemical cycling mechanism of these two types of anodes is distinct, their principal drawbacks are the same; large volume changes over the course of cycling that led to pulverization of the electrode material, detachment from the current collector, and compounded by the relatively poor electrical conductivity of the electrode materials. Compositing with graphene has been shown to be a promising strategy for combatting these failure modes, in both alloy and conversion type anodes. In this section, we will illustrate the utility of 0D-2D hybrids for Li-ion anodes by exploring the alloy anode silicon, with the general concepts extending to graphene composites with Sn [437], Ge [438], metal oxide [58,439–441], and metal chalcogenide [442,443] anodes as well.

Silicon's giant theoretical delithiated capacity of 4,200 mAh/g and low electrochemical potential have made it the most attractive research candidate of the alloying anode materials. As discussed, in practice Si has severe degradation problems; the volume change silicon (Si) particles undergo during lithiation is particularly large (over 300%) [435], which leads to fragmentation of the particles and ultimately efficiency loss due to the continuous build-up of surface-electrolyte interphase (SEI) products (Fig. 9a–c). Compositing the Si nanoparticles with 2D graphene can both improve the Si resilience and the overall conductivity, with only a modest 'weight cost' associated with their inclusion. As such these 0D-2D hybrids have attracted significant interest, with the graphene able to act as a strong, flexible, and conductive scaffold for the Si particles. A frequently employed approach is to encapsulate the Si particles in a conductive layer, with initial attempts surrounding the silicon in amorphous carbon [444,445]. Extending this approach to 2D graphitic carbon has since been explored. One of the earliest reports simply dispersed Si NPs in a suspension of GO sheets and sonicated, then suction filtered to form a Si NP–GO 0D–2D composite paper, which was suitable for use as an anode following reduction. The stacks of compressed r-GO sheets sandwiched the Si NPs into the composite (Fig. 9d–f), providing good coulombic efficiency and capacity [446]. A number of further studies have used modified or alternative synthesis methods, such as CVD or introduction of NPs into Hummers' method expanded graphite, to achieve a Si NP and graphene composite electrode [447–457], as explored in detail in a recent review [458]. In-situ TEM imaging has since clearly shown the beneficial influence of containing the Si component within a graphitic shell (Fig. 9h and i), with the time-series of TEM images acquired over lithiation and delithiation showing the expansion and fragmentation of the Si NP, yet it remaining securely contained within the graphene shell (Fig. 9j and k) [459].

Some challenges with associated with this 0D-2D composite electrode include optimizing the dispersion and maximizing the utility of the Si NPs. Dispersion of the Si NPs across the graphene or r-GO has been shown to benefit from the use of an intermediate layer, such as poly-acrylic acid or phenolic resin. This helps to limit the agglomeration of the NPs, and ensures good contact is maintained between the particles and graphene support after many cycles [462–466]. And, as discussed in the previous section on catalysts, encapsulation does bring with it the risk of blocking the flow of reactants, as they are unable to easily flow through the basal graphene plane [15]. Introduction of nanoscale defects into the graphene can combat this problem, while still keeping the advantages of good electrical conductivity and structural integrity (Fig. 9g) [461,467]. However, this inclusion of defects risks making the graphene chemically active, acting as a site for undesirable electrolyte decomposition and the formation of SEI products [464].

6.2. Cathode ORR and OER catalysts for Li–O_2 and Zn–O_2 batteries

The cathode side of current Li-ion rechargeable batteries utilizes metal oxides, typically cobalt lithium dioxide ($LiCoO_2$) or lithium

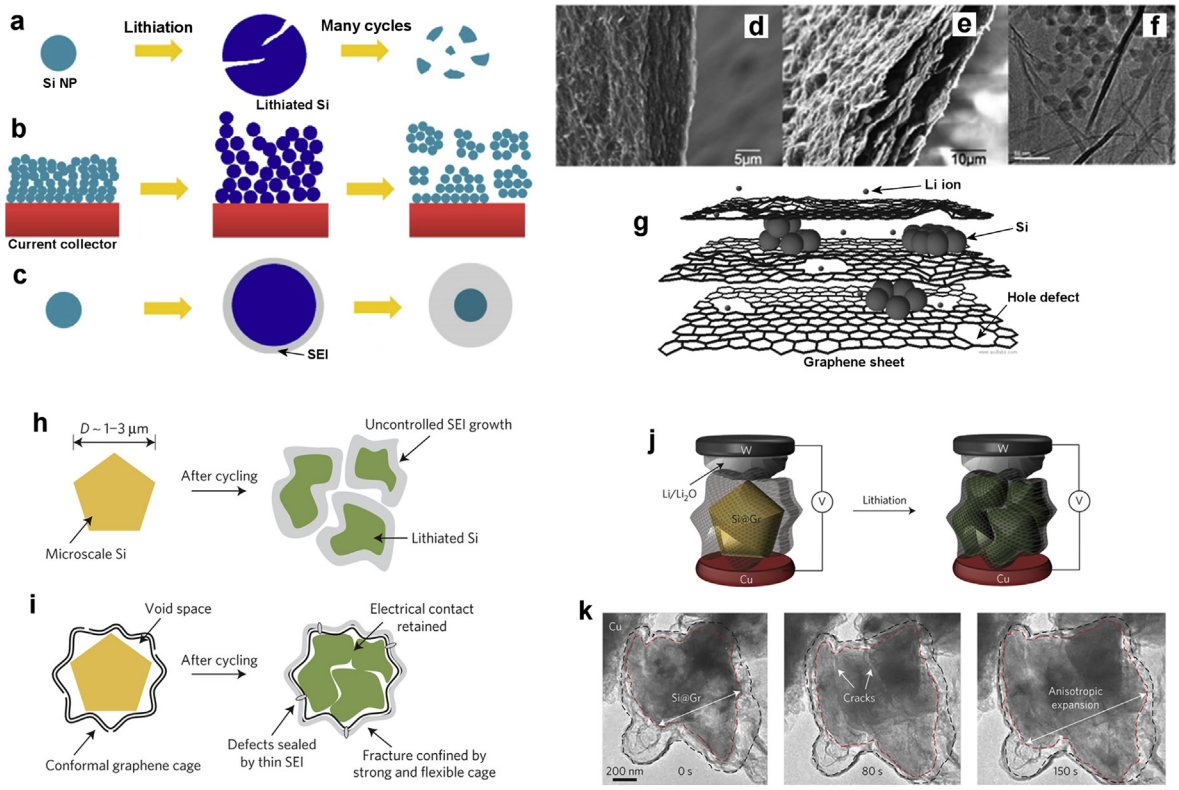

Fig. 9. 0D-2D composites for silicon anodes in Li-ion batteries. (a–c) The primary degradation mechanisms for silicon anodes [460]: (a) Pulverization due to volume change. (b) Detachment of the electrode assembly. (c) Li lost from the electrolyte due to continuous solid electrolyte interphase layer (SEI) formation, as new electrode surfaces being (re-) exposed during cycling. The thicker SEI also impedes ion conduction into the electrode. (d) Edge view SEM image of Si NP – GO composite electrode. (e) Edge view SEM image of Si NP – r-GO composite electrode. (f) TEM image of the Si NP – r-GO composite electrode [446]. (g) Sketch of a composite electrode with holey defects in the graphene, facilitating ion motion between basal layers [461]. (h,i) A cartoon illustrating the utility of an encapsulating graphene layer in preventing silicon fracture and detachment during charge cycling. (j) Diagram illustrating an apparatus for in-situ TEM imaging of lithium cycling of a Si-graphene composite. (k) Time series in-situ TEM images showing the fracture of Si while undergoing lithiation yet remaining safely confined inside the robust graphene shell [459]

manganese dioxide ($LiMnO_2$), relying on the open tetrahedral structure for the easy movement of Li ions in and out of the host crystal. A major area of current research activity is focused on developing improved oxide hosts for the cathode [468], however there is an inevitable limit to how far this can increase capacity. Fundamentally new chemistries are required, and one of the more promising is the use of an oxygen, or 'air', cathode [469,470]. These offer the promise of a high theoretical capacity of 3,861 mA h/g, which while not practically reachable, even achieving a fraction would represent a large boost over the capacities offered by layered oxide cathodes [471]. Such Li–O_2 batteries suffer from similar problems to the related PEMFC, with sluggish ORR and OER kinetics limiting the cycling rate, and overall poor durability of the cathode electrode material. Designing robust bifunctional catalysts, capable of enhancing both OER and ORR kinetics, is thus desirable to combat this [472–475].

Several works have demonstrated that the 2D materials GO, r-GO, and N-doped r-GO are themselves catalytically active to the ORR, and so show potential as Li–O_2 cathodes [476–481]. However, their activity is typically not sufficient to be practical, they aggregate during use thus reducing their active surface area, and their large overpotential is problematic. Thus compositing them with nanoparticle catalysts to supplement their activity to ORR and OER is a promising approach. Precious metal catalysts such as Pt and Ru have shown promise [482], yet due to their high cost it is critical that the nanoparticles maintain good connection with the support over sequential cycles. Graphene performs well in this regard compared to conventional carbon supports like carbon black and is a further advantage in addition to the graphene being catalytically active itself [483]. Loading the graphene, or r-GO, support with Ru or RuO_2 nanoparticles have been shown to be effective toward in catalyzing the OER and removal of the Li_2O_2 discharge products that accumulate at the cathode [484,485]. It has been suggested that this may be due to Ru promoting the formation of different Li_2O_2 morphologies during ORR that are more favorable to dissolution, rather than due to directly improving OER kinetics via catalysis [486].

The disadvantage of using Ru or Pt catalysts are their high cost, which may preclude their practical use. An alternative ORR and OER catalyst without precious metal content are metal oxide spinels, specifically those with Mn or Co transition metals [487–489], however these are only poorly conductive and so greatly benefit from compositing with materials such as graphene. 0D-2D composites of $CoMn_2O_4$ nanoparticles on GO were shown to be effective bifunctional catalysts toward the OER and ORR in aqueous solvent [490]. But the most studied oxide catalyst is Co_3O_4, whose catalytic role appears to suppress electrolyte decomposing reaction pathways [491], and has been shown to exhibit high bifunctional activity and stability toward the OER and ORR in an aqueous Li–O_2 cell [492]. As observed in related PEMFC studies, discussed earlier, a synergistic effect between the graphene and the Co_3O_4 toward catalyzing the ORR, and also the OER, highlighting the importance of graphene beyond being just a conductive support structure [493].

The rechargeable Zn–O_2 battery has similar challenges to the Li–O_2 cell, although the lower reactivity of Zn makes it more

amenable to operation with aqueous electrolytes. While the Zn−O_2 concept has been around for a number of years, the challenge of developing a cathode that can stably and efficiently catalyze both the ORR and OER remains, with electrode corrosion, high overpotentials, and leeching of metals from the catalyst being the common limits to practical use [494,495]. The advantages of 0D-2D hybrids are comparable to that case of Ln-O_2, where graphene can act as (i) a conductive and corrosion-resistant scaffold for nanoparticles [496−498], (ii) an ORR catalyst itself [499], particularly when nitrogen dopants are introduced [500,501], and (iii) encapsulation of the nanoparticles in graphene helps reduce metal leeching into the electrolyte [502].

Regardless of the nanoparticle material, designing a hierarchical, porous graphene electrode material to host the nanoparticles further promotes performance, which can be achieved by growing the graphene from a nickel foam or by linking r-GO sheets [237,503]. The pores provide volume in which the Li_2O_2 (or ZnO) particles can grow during discharge, allow for the diffusion of oxygen, and for many points of catalytic contact with the Li_2O_2 during the OER [504,505].

7. Conclusion

The combination of 0D and 2D materials presents a larger parameter space for the design of new composites with properties tailored for the desired application. As we have shown in this review, the engineering of these complementary nanomaterial combinations can yield superior solar cells, catalysts, and battery electrodes. Preparation of 0D-2D composites will require the development of synthesis techniques that are sufficiently simple to be economical, and that also preserve the properties of the parent 0D and 2D components. Future development to realize the potential of these composites will require sophisticated materials characterization to disentangle their structure-property relationship, in particular for identifying synergistic effects where the combination of the two materials yields a disproportionate improvement in performance. In other words, how do we know what makes a composite especially effective, and more than simply the sum of its parts? We must do this via characterization of the 0D-2D composite, and thus revealing the peculiar structures and interfaces that give rise to the desired properties. Developing an understanding here will allow for the intelligent design of new composites, reaching into the deep reservoir of emerging 2D materials to achieve heterostructures with the desired combination of activity, resilience, and cost.

Declaration of competing interest

The authors declare that they have no known competing financial interests or personal relationships that could have appeared to influence the work reported in this paper.

Acknowledgments

This work was supported by the Research and Development Program of Korea Institute of Energy Research (KIER/C0-2459) for SS, and (KIER/C1-2458) and National Research Foundation of Korea (NRF/2020R1A2C200831611) for HK. AWR thanks the support of the Royal Society.

References

[1] K.S. Novoselov, V.I. Fal'ko, L. Colombo, P.R. Gellert, M.G. Schwab, K. Kim, A roadmap for graphene, Nature 490 (2012) 192−200, https://doi.org/10.1038/nature11458.
[2] K.S. Novoselov, A. Mishchenko, A. Carvalho, A.H. Castro Neto, 2D materials and van der Waals heterostructures, Science (80-.) 353 (2016), aac9439, https://doi.org/10.1126/science.aac9439.
[3] M.-Y. Li, C.-H. Chen, Y. Shi, L.-J. Li, Heterostructures based on two-dimensional layered materials and their potential applications, Mater. Today 19 (2016) 322−335, https://doi.org/10.1016/j.mattod.2015.11.003.
[4] Q. Zeng, Z. Liu, Novel optoelectronic devices: transition-metal-dichalcogenide-based 2D heterostructures, Adv. Electron. Mater. 4 (2018) 1700335, https://doi.org/10.1002/aelm.201700335.
[5] J. Sun, Y. Choi, Y.J. Choi, S. Kim, J. Park, S. Lee, J.H. Cho, 2D−Organic hybrid heterostructures for optoelectronic applications, Adv. Mater. 31 (2019) 1803831, https://doi.org/10.1002/adma.201803831.
[6] Y.-T. Liu, X.-D. Zhu, L. Pan, Hybrid architectures based on 2D MXenes and low-dimensional inorganic nanostructures: methods, synergies, and energy-related applications, Small 14 (2018) 1803632, https://doi.org/10.1002/smll.201803632.
[7] P.T. Yin, S. Shah, M. Chhowalla, K.-B. Lee, Design, synthesis, and characterization of graphene−nanoparticle hybrid materials for bioapplications, Chem. Rev. 115 (2015) 2483−2531, https://doi.org/10.1021/cr500537t.
[8] B. Luo, G. Liu, L. Wang, Recent advances in 2D materials for photocatalysis, Nanoscale 8 (2016) 6904−6920, https://doi.org/10.1039/C6NR00546B.
[9] E. Morales-Narváez, L.F. Sgobbi, S.A.S. Machado, A. Merkoçi, Graphene-encapsulated materials: synthesis, applications and trends, Prog. Mater. Sci. 86 (2017) 1−24, https://doi.org/10.1016/j.pmatsci.2017.01.001.
[10] D. Thanh Tran, T. Kshetri, N. Dinh Chuong, J. Gautam, H. Van Hien, L. Huu Tuan, N.H. Kim, J.H. Lee, Emerging core-shell nanostructured catalysts of transition metal encapsulated by two-dimensional carbon materials for electrochemical applications, Nano Today 22 (2018) 100−131, https://doi.org/10.1016/j.nantod.2018.08.006.
[11] S. Low, Y.-S. Shon, Molecular interactions between pre-formed metal nanoparticles and graphene families, Adv. Nano Res. 6 (2018) 357−375.
[12] V. Georgakilas, J.N. Tiwari, K.C. Kemp, J.A. Perman, A.B. Bourlinos, K.S. Kim, R. Zboril, Noncovalent functionalization of graphene and graphene oxide for energy materials, biosensing, catalytic, and biomedical applications, Chem. Rev. 116 (2016) 5464−5519, https://doi.org/10.1021/acs.chemrev.5b00620.
[13] P. Chen, N. Zhang, S. Wang, T. Zhou, Y. Tong, C. Ao, W. Yan, L. Zhang, W. Chu, C. Wu, Y. Xie, Interfacial engineering of cobalt sulfide/graphene hybrids for highly efficient ammonia electrosynthesis, Proc. Natl. Acad. Sci. U.S.A. 116 (2019) 6635−6640, https://doi.org/10.1073/pnas.1817881116.
[14] Y. Shi, J.-K. Huang, L. Jin, Y.-T. Hsu, S.F. Yu, L.-J. Li, H.Y. Yang, Selective decoration of Au nanoparticles on monolayer MoS_2 single crystals, Sci. Rep. 3 (2013) 1839, https://doi.org/10.1038/srep01839.
[15] H. Kim, A.W. Robertson, S.O. Kim, J.M. Kim, J.H. Warner, Resilient high catalytic performance of platinum nanocatalysts with porous graphene envelope, ACS Nano 9 (2015) 5947−5957, https://doi.org/10.1021/acsnano.5b00678.
[16] J. Deng, H. Li, J. Xiao, Y. Tu, D. Deng, H. Yang, H. Tian, J. Li, P. Ren, X. Bao, Triggering the electrocatalytic hydrogen evolution activity of the inert two-dimensional MoS_2 surface via single-atom metal doping, Energy Environ. Sci. 8 (2015) 1594−1601, https://doi.org/10.1039/C5EE00751H.
[17] H. Göksu, S.F. Ho, Ö. Metin, K. Korkmaz, A. Mendoza Garcia, M.S. Gültekin, S. Sun, Tandem dehydrogenation of ammonia borane and hydrogenation of nitro/nitrile compounds catalyzed by graphene-supported NiPd alloy nanoparticles, ACS Catal. 4 (2014) 1777−1782, https://doi.org/10.1021/cs500167k.
[18] D. Luo, C. Yan, T. Wang, Interparticle forces underlying nanoparticle self--assemblies, Small 11 (2015) 5984−6008, https://doi.org/10.1002/smll.201501783.
[19] G. Lu, S. Mao, S. Park, R.S. Ruoff, J. Chen, Facile, noncovalent decoration of graphene oxide sheets with nanocrystals, Nano Res. 2 (2009) 192−200, https://doi.org/10.1007/s12274-009-9017-8.
[20] Y. Du, J. Su, W. Luo, G. Cheng, Graphene-supported nickel−platinum nanoparticles as efficient catalyst for hydrogen generation from hydrous hydrazine at room temperature, ACS Appl. Mater. Interfaces 7 (2015) 1031−1034, https://doi.org/10.1021/am5068436.
[21] A.W. Robertson, C. Ford, K. He, A.I. Kirkland, A.A.R. Watt, J.H. Warner, PbTe nanocrystal arrays on graphene and the structural influence of capping ligands, Chem. Mater. 26 (2014) 1567−1575, https://doi.org/10.1021/cm403373q.
[22] C. Gong, A.W. Robertson, K. He, C. Ford, A.A.R. Watt, J.H. Warner, Interactions of Pb and Te atoms with graphene, Dalton Trans. 43 (2014) 7442−7448, https://doi.org/10.1039/C4DT00143E.
[23] S. Mao, G. Lu, K. Yu, Z. Bo, J. Chen, Specific protein detection using thermally reduced graphene oxide sheet decorated with gold nanoparticle-antibody conjugates, Adv. Mater. 22 (2010) 3521−3526, https://doi.org/10.1002/adma.201000520.
[24] M.C. Dalfovo, G.I. Lacconi, M. Moreno, M.C. Yappert, G.U. Sumanasekera, R.C. Salvarezza, F.J. Ibañez, Synergy between graphene and Au nanoparticles (heterojunction) towards quenching, improving Raman signal, and UV light sensing, ACS Appl. Mater. Interfaces 6 (2014) 6384−6391, https://doi.org/10.1021/am405753t.
[25] A.S. Singh, S.S. Shendage, J.M. Nagarkar, Palladium supported on zinc ferrite: an efficient catalyst for ligand free C−C and C−O cross coupling reactions, Tetrahedron Lett. 54 (2013) 6319−6323, https://doi.org/10.1016/j.tetlet.2013.09.027.

[26] S. Diyarbakir, H. Can, Ö. Metin, Reduced graphene oxide-supported CuPd alloy nanoparticles as efficient catalysts for the sonogashira cross-coupling reactions, ACS Appl. Mater. Interfaces 7 (2015) 3199–3206, https://doi.org/10.1021/am507764u.
[27] L.M. Rossi, J.L. Fiorio, M.A.S. Garcia, C.P. Ferraz, The role and fate of capping ligands in colloidally prepared metal nanoparticle catalysts, Dalton Trans. 47 (2018) 5889–5915, https://doi.org/10.1039/C7DT04728B.
[28] D. Li, C. Wang, D. Tripkovic, S. Sun, N.M. Markovic, V.R. Stamenkovic, Surfactant removal for colloidal nanoparticles from solution synthesis: the effect on catalytic performance, ACS Catal. 2 (2012) 1358–1362, https://doi.org/10.1021/cs300219j.
[29] K. Guo, L.J. Rowland, L.H. Isherwood, G. Glodan, A. Baidak, Photon-induced synthesis of ultrafine metal nanoparticles on graphene as electrocatalysts: impact of functionalization and doping, J. Mater. Chem. A 8 (2020) 714–723, https://doi.org/10.1039/C9TA10518B.
[30] A. Mondal, N.R. Jana, Surfactant-free, stable noble metal–graphene nanocomposite as high performance electrocatalyst, ACS Catal. 4 (2014) 593–599, https://doi.org/10.1021/cs401032p.
[31] Y. Tao, A. Dandapat, L. Chen, Y. Huang, Y. Sasson, Z. Lin, J. Zhang, L. Guo, T. Chen, Pd-on-Au supra-nanostructures decorated graphene oxide: an advanced electrocatalyst for fuel cell application, Langmuir 32 (2016) 8557–8564, https://doi.org/10.1021/acs.langmuir.6b01382.
[32] N. Zhang, X. Yan, Y. Huang, J. Li, J. Ma, D.H.L. Ng, Electrostatically assembled magnetite nanoparticles/graphene foam as a binder-free anode for lithium ion battery, Langmuir 33 (2017) 8899–8905, https://doi.org/10.1021/acs.langmuir.7b01519.
[33] J. Yang, C. Tian, L. Wang, H. Fu, An effective strategy for small-sized and highly-dispersed palladium nanoparticles supported on graphene with excellent performance for formic acid oxidation, J. Mater. Chem. 21 (2011) 3384, https://doi.org/10.1039/c0jm03361h.
[34] J.-D. Qiu, G.-C. Wang, R.-P. Liang, X.-H. Xia, H.-W. Yu, Controllable deposition of platinum nanoparticles on graphene as an electrocatalyst for direct methanol fuel cells, J. Phys. Chem. C 115 (2011) 15639–15645, https://doi.org/10.1021/jp200580u.
[35] S. Wang, J. Li, X. Zhou, C. Zheng, J. Ning, Y. Zhong, Y. Hu, Facile preparation of 2D sandwich-like CdS nanoparticles/nitrogen-doped reduced graphene oxide hybrid nanosheets with enhanced photoelectrochemical properties, J. Mater. Chem. A 2 (2014) 19815–19821, https://doi.org/10.1039/C4TA04624B.
[36] Y. Li, W. Gao, L. Ci, C. Wang, P.M. Ajayan, Catalytic performance of Pt nanoparticles on reduced graphene oxide for methanol electro-oxidation, Carbon N.Y. 48 (2010) 1124–1130, https://doi.org/10.1016/j.carbon.2009.11.034.
[37] H. Ismaili, D. Geng, A.X. Sun, T.T. Kantzas, M.S. Workentin, Light-activated covalent formation of gold nanoparticle–graphene and gold nanoparticle–glass composites, Langmuir 27 (2011) 13261–13268, https://doi.org/10.1021/la202815g.
[38] A. Ganguly, O. Trovato, S. Duraisamy, J. Benson, Y. Han, C. Satriano, P. Papakonstantinou, Organic solvent based synthesis of gold nanoparticle-semiconducting 2H-MoS_2 hybrid nanosheets, J. Phys. Chem. C 123 (2019) 10646–10657, https://doi.org/10.1021/acs.jpcc.9b00303.
[39] J. Kim, S. Byun, A.J. Smith, J. Yu, J. Huang, Enhanced electrocatalytic properties of transition-metal dichalcogenides sheets by spontaneous gold nanoparticle decoration, J. Phys. Chem. Lett. 4 (2013) 1227–1232, https://doi.org/10.1021/jz400507t.
[40] T.S. Sreeprasad, P. Nguyen, N. Kim, V. Berry, Controlled, defect-guided, metal-nanoparticle incorporation onto MoS_2 via chemical and microwave routes: electrical, thermal, and structural properties, Nano Lett. 13 (2013) 4434–4441, https://doi.org/10.1021/nl402278y.
[41] M. Kim, M.A.R. Anjum, M. Lee, B.J. Lee, J.S. Lee, Activating MoS_2 basal plane with Ni_2P nanoparticles for Pt-like hydrogen evolution reaction in acidic media, Adv. Funct. Mater. 29 (2019) 1809151, https://doi.org/10.1002/adfm.201809151.
[42] S. Li, J.K. Lee, S. Zhou, M. Pasta, J.H. Warner, Synthesis of surface grown Pt nanoparticles on edge-enriched MoS_2 porous thin films for enhancing electrochemical performance, Chem. Mater. 31 (2019) 387–397, https://doi.org/10.1021/acs.chemmater.8b03540.
[43] J.R. Dunklin, P. Lafargue, T.M. Higgins, G.T. Forcherio, M. Benamara, N. McEvoy, D.K. Roper, J.N. Coleman, Y. Vaynzof, C. Backes, Production of monolayer-rich gold-decorated 2H–WS_2 nanosheets by defect engineering, Npj 2D Mater. Appl. 1 (2017) 43, https://doi.org/10.1038/s41699-017-0045-z.
[44] T.S. Sreeprasad, V. Berry, How do the electrical properties of graphene change with its functionalization? Small 9 (2013) 341–350, https://doi.org/10.1002/smll.201202196.
[45] L.M. Salonen, M. Ellermann, F. Diederich, Aromatic rings in chemical and biological recognition: energetics and structures, Angew. Chem. Int. Ed. 50 (2011) 4808–4842, https://doi.org/10.1002/anie.201007560.
[46] Y. Zhang, C. Liu, W. Shi, Z. Wang, L. Dai, X. Zhang, Direct measurements of the interaction between pyrene and graphite in aqueous media by single molecule force spectroscopy: understanding the π–π interactions, Langmuir 23 (2007) 7911–7915, https://doi.org/10.1021/la700876d.
[47] C.R. Martinez, B.L. Iverson, Rethinking the term "pi-stacking", Chem. Sci. 3 (2012) 2191, https://doi.org/10.1039/c2sc20045g.
[48] J. Huang, L. Zhang, B. Chen, N. Ji, F. Chen, Y. Zhang, Z. Zhang, Nanocomposites of size-controlled gold nanoparticles and graphene oxide: formation and applications in SERS and catalysis, Nanoscale 2 (2010) 2733, https://doi.org/10.1039/c0nr00473a.
[49] S. Sarkar, S. Niyogi, E. Bekyarova, R.C. Haddon, Organometallic chemistry of extended periodic π-electron systems: hexahapto-chromium complexes of graphene and single-walled carbon nanotubes, Chem. Sci. 2 (2011) 1326, https://doi.org/10.1039/c0sc00634c.
[50] S. Che, K. Jasuja, S.K. Behura, P. Nguyen, T.S. Sreeprasad, V. Berry, Retained carrier-mobility and enhanced plasmonic-photovoltaics of graphene via ring-centered η 6 functionalization and nanointerfacing, Nano Lett. 17 (2017) 4381–4389, https://doi.org/10.1021/acs.nanolett.7b01458.
[51] S. Che, S.K. Behura, V. Berry, Photo-organometallic, nanoparticle nucleation on graphene for cascaded doping, ACS Nano 13 (2019) 12929–12938, https://doi.org/10.1021/acsnano.9b05484.
[52] S. Qu, M. Li, L. Xie, X. Huang, J. Yang, N. Wang, S. Yang, Noncovalent functionalization of graphene attaching [6,6]-Phenyl-C61-butyric acid methyl ester (PCBM) and application as electron extraction layer of polymer solar cells, ACS Nano 7 (2013) 4070–4081, https://doi.org/10.1021/nn4001963.
[53] T. Gan, C. Hu, Z. Sun, S. Hu, Facile synthesis of water-soluble fullerene–graphene oxide composites for electrodeposition of phosphotungstic acid-based electrocatalysts, Electrochim. Acta 111 (2013) 738–745, https://doi.org/10.1016/j.electacta.2013.08.059.
[54] S. Sinha, Y. Sheng, I. Griffiths, N.P. Young, S. Zhou, A.I. Kirkland, K. Porfyrakis, J.H. Warner, In situ atomic-level studies of Gd atom release and migration on graphene from a metallofullerene precursor, ACS Nano 12 (2018) 10439–10451, https://doi.org/10.1021/acsnano.8b06057.
[55] A. Lavie, L. Yadgarov, L. Houben, R. Popovitz-Biro, T.-E. Shaul, A. Nagler, H. Suchowski, R. Tenne, Synthesis of core–shell single-layer MoS_2 sheathing gold nanoparticles, AuNP@1L-MoS_2, Nanotechnology 28 (2017) 24LT03, https://doi.org/10.1088/1361-6528/aa715f.
[56] W. Tang, Z. Chen, B. Tian, H.-W. Lee, X. Zhao, X. Fan, Y. Fan, K. Leng, C. Peng, M.-H. Kim, M. Li, M. Lin, J. Su, J. Chen, H.Y. Jeong, X. Yin, Q. Zhang, W. Zhou, K.P. Loh, G.W. Zheng, In situ observation and electrochemical study of encapsulated sulfur nanoparticles by MoS_2 flakes, J. Am. Chem. Soc. 139 (2017) 10133–10141, https://doi.org/10.1021/jacs.7b05371.
[57] I.H. Son, J.H. Park, S. Park, K. Park, S. Han, J. Shin, S.-G. Doo, Y. Hwang, H. Chang, J.W. Choi, Graphene balls for lithium rechargeable batteries with fast charging and high volumetric energy densities, Nat. Commun. 8 (2017) 1561, https://doi.org/10.1038/s41467-017-01823-7.
[58] C. He, S. Wu, N. Zhao, C. Shi, E. Liu, J. Li, Carbon-encapsulated Fe_3O_4 nanoparticles as a high-rate lithium ion battery anode material, ACS Nano 7 (2013) 4459–4469, https://doi.org/10.1021/nn401059h.
[59] G. Liu, A.W. Robertson, M.M.-J. Li, W.C.H. Kuo, M.T. Darby, M.H. Muhieddine, Y.-C. Lin, K. Suenaga, M. Stamatakis, J.H. Warner, S.C.E. Tsang, MoS_2 monolayer catalyst doped with isolated Co atoms for the hydrodeoxygenation reaction, Nat. Chem. 9 (2017) 810–816, https://doi.org/10.1038/nchem.2740.
[60] N. Cheng, L. Zhang, K. Doyle-Davis, X. Sun, Single-atom catalysts: from design to application, Electrochem. Energy Rev. 2 (2019) 539–573, https://doi.org/10.1007/s41918-019-00050-6.
[61] H. Zhang, G. Liu, L. Shi, J. Ye, Single-atom catalysts: emerging multifunctional materials in heterogeneous catalysis, Adv. Energy Mater. 8 (2018) 1701343, https://doi.org/10.1002/aenm.201701343.
[62] A. Wang, J. Li, T. Zhang, Heterogeneous single-atom catalysis, Nat. Rev. Chem. 2 (2018) 65–81, https://doi.org/10.1038/s41570-018-0010-1.
[63] J. Karthikeyan, H.-P. Komsa, M. Batzill, A.V. Krasheninnikov, Which transition metal atoms can Be embedded into two-dimensional molybdenum dichalcogenides and add magnetism? Nano Lett. 19 (2019) 4581–4587, https://doi.org/10.1021/acs.nanolett.9b01555.
[64] J.D. Fuhr, J.O. Sofo, A. Saúl, Coverage dependence study of the adsorption of Pd on MoS_2(100), Surf. Sci. 506 (2002) 161–171, https://doi.org/10.1016/S0039-6028(02)01153-6.
[65] A. Andersen, S.M. Kathmann, M.A. Lilga, K.O. Albrecht, R.T. Hallen, D. Mei, Adsorption of potassium on MoS_2 (100) surface: a first-principles investigation, J. Phys. Chem. C 115 (2011) 9025–9040, https://doi.org/10.1021/jp110069r.
[66] H. Sevinçli, M. Topsakal, E. Durgun, S. Ciraci, Electronic and magnetic properties of 3d transition-metal atom adsorbed graphene and graphene nanoribbons, Phys. Rev. B 77 (2008) 195434, https://doi.org/10.1103/PhysRevB.77.195434.
[67] D. Liu, A. Barbar, T. Najam, M.S. Javed, J. Shen, P. Tsiakaras, X. Cai, Single noble metal atoms doped 2D materials for catalysis, Appl. Catal. B Environ. 297 (2021) 120389, https://doi.org/10.1016/j.apcatb.2021.120389.
[68] L. Loh, Z. Zhang, M. Bosman, G. Eda, Substitutional doping in 2D transition metal dichalcogenides, Nano Res. 14 (2021) 1668–1681, https://doi.org/10.1007/s12274-020-3013-4.
[69] H. Zhu, X. Gan, A. McCreary, R. Lv, Z. Lin, M. Terrones, Heteroatom doping of two-dimensional materials: from graphene to chalcogenides, Nano Today 30 (2020) 100829, https://doi.org/10.1016/j.nantod.2019.100829.
[70] M. Chen, R. Guan, S. Yang, Hybrids of fullerenes and 2D nanomaterials, Adv. Sci. 6 (2019) 1800941, https://doi.org/10.1002/advs.201800941.
[71] D. Zhou, N. Si, Q. Tang, B. Jiang, X. Song, H. Huang, M. Zhou, Q. Ji, T. Niu, Defect generation and surface functionalization on epitaxial blue phosphorene by C60 adsorption, J. Phys. Chem. C 123 (2019) 12947–12953, https://doi.org/10.1021/acs.jpcc.9b03344.

[72] W. Auwärter, Hexagonal boron nitride monolayers on metal supports: versatile templates for atoms, molecules and nanostructures, Surf. Sci. Rep. 74 (2019) 1–95, https://doi.org/10.1016/j.surfrep.2018.10.001.
[73] A. Kumar, K. Banerjee, P. Liljeroth, Molecular assembly on two-dimensional materials, Nanotechnology 28 (2017) 82001, https://doi.org/10.1088/1361-6528/aa564f.
[74] M. Kratzer, A. Matkovic, C. Teichert, Adsorption and epitaxial growth of small organic semiconductors on hexagonal boron nitride, J. Phys. D Appl. Phys. 52 (2019) 383001, https://doi.org/10.1088/1361-6463/ab29cb.
[75] D. García, L. Rodríguez-Pérez, M.A. Herranz, D. Peña, E. Guitián, S. Bailey, Q. Al-Galiby, M. Noori, C.J. Lambert, D. Pérez, N. Martín, A C60-aryne building block: synthesis of a hybrid all-carbon nanostructure, Chem. Commun. 52 (2016) 6677–6680, https://doi.org/10.1039/C5CC10462A.
[76] S.K. Das, C.B. Kc, K. Ohkubo, Y. Yamada, S. Fukuzumi, F. D'Souza, Decorating single layer graphene oxide with electron donor and acceptor molecules for the study of photoinduced electron transfer, Chem. Commun. 49 (2013) 2013–2015, https://doi.org/10.1039/C3CC38898K.
[77] R. Mirzayev, K. Mustonen, M.R.A.A. Monazam, A. Mittelberger, T.J. Pennycook, C. Mangler, T. Susi, J. Kotakoski, J.C. Meyer, Buckyball sandwiches, Sci. Adv. 3 (2017), e1700176, https://doi.org/10.1126/sciadv.1700176.
[78] Y. Ioni, E. Buslaeva, S. Gubin, Synthesis of graphene with noble metals nanoparticles on its surface, Mater. Today Proc. 3 (2016) S209–S213, https://doi.org/10.1016/j.matpr.2016.02.035.
[79] D. Yu, K. Park, M. Durstock, L. Dai, Fullerene-grafted graphene for efficient bulk heterojunction polymer photovoltaic devices, J. Phys. Chem. Lett. 2 (2011) 1113–1118, https://doi.org/10.1021/jz200428y.
[80] R. Chen, C. Lin, H. Yu, Y. Tang, C. Song, L. Yuwen, H. Li, X. Xie, L. Wang, W. Huang, Templating C60 on MoS_2 nanosheets for 2D hybrid van der Waals p–n nanoheterojunctions, Chem. Mater. 28 (2016) 4300–4306, https://doi.org/10.1021/acs.chemmater.6b01115.
[81] Y. Park, J.Y. Koo, S. Kim, H.C. Choi, Spontaneous formation of gold nanoparticles on graphene by galvanic reaction through graphene, ACS Omega 4 (2019) 18423–18427, https://doi.org/10.1021/acsomega.9b02691.
[82] K. Kim, T. Hoon Lee, E.J.G. Santos, P. Sung Jo, A. Salleo, Y. Nishi, Z. Bao, Structural and electrical investigation of C60–graphene vertical heterostructures, ACS Nano 9 (2015) 5922–5928, https://doi.org/10.1021/acsnano.5b00581.
[83] N.N. Nguyen, H.C. Lee, M.S. Yoo, E. Lee, H. Lee, S.B. Lee, K. Cho, Charge-transfer-controlled growth of organic semiconductor crystals on graphene, Adv. Sci. 7 (2020) 1902315, https://doi.org/10.1002/advs.201902315.
[84] R. Félix, T. Breuer, P. Rotter, F. Widdascheck, B. Eckhardt, G. Witte, K. Volz, K.I. Gries, Microstructural analysis of perfluoropentacene films on graphene and graphite: interface-mediated alignment and island formation, Cryst. Growth Des. 16 (2016) 6941–6950, https://doi.org/10.1021/acs.cgd.6b01117.
[85] C. Dong, W. Zhu, S. Zhao, P. Wang, H. Wang, W. Yang, Evolution of Pt clusters on graphene induced by electron irradiation, J. Appl. Mech. 80 (2013) 40904, https://doi.org/10.1115/1.4024168.
[86] B. Chai, X. Liao, F. Song, H. Zhou, Fullerene modified C_3N_4 composites with enhanced photocatalytic activity under visible light irradiation, Dalton Trans. 43 (2014) 982–989, https://doi.org/10.1039/C3DT52454J.
[87] M. Barrejón, M. Vizuete, M.J. Gómez-Escalonilla, J.L.G. Fierro, I. Berlanga, F. Zamora, G. Abellán, P. Atienzar, J.-F. Nierengarten, H. García, F. Langa, A photoresponsive graphene oxide–C60 conjugate, Chem. Commun. 50 (2014) 9053–9055, https://doi.org/10.1039/C3CC49589B.
[88] S. Sadjadi, S. Jašo, H.R. Godini, S. Arndt, M. Wollgarten, R. Blume, O. Görke, R. Schomäcker, G. Wozny, U. Simon, Feasibility study of the Mn-Na_2WO_4/SiO_2 catalytic system for the oxidative coupling of methane in a fluidized-bed reactor, Catal. Sci. Technol. 5 (2015) 942–952, https://doi.org/10.1039/c4cy00822g.
[89] M. Remškar, A. Mrzel, A. Jesih, J. Kovač, H. Cohen, R. Sanjinés, F. Lévy, New composite MoS2–C60 crystals, Adv. Mater. 17 (2005) 911–914, https://doi.org/10.1002/adma.200400553.
[90] H.D. Jang, S.K. Kim, H. Chang, J.-W. Choi, J. Luo, J. Huang, One-step synthesis of Pt-Nanoparticles-Laden graphene crumples by aerosol spray pyrolysis and evaluation of their electrocatalytic activity, Aerosol Sci. Technol. 47 (2013) 93–98, https://doi.org/10.1080/02786826.2012.728302.
[91] E.H. Jo, H. Chang, S.K. Kim, J.-H. Choi, S.-R. Park, C.M. Lee, H.D. Jang, One-step synthesis of Pt/graphene composites from Pt acid dissolved ethanol via microwave plasma spray pyrolysis, Sci. Rep. 6 (2016) 33236, https://doi.org/10.1038/srep33236.
[92] S. Hussain, H. Erikson, N. Kongi, A. Treshchalov, M. Rähn, M. Kook, M. Merisalu, L. Matisen, V. Sammelselg, K. Tammeveski, Oxygen electroreduction on Pt nanoparticles deposited on reduced graphene oxide and N-doped reduced graphene oxide prepared by plasma-assisted synthesis in aqueous solution, ChemElectroChem 5 (2018) 2902–2911, https://doi.org/10.1002/celc.201800582.
[93] J. Morère, E. Sánchez-Miguel, M.J. Tenorio, C. Pando, A. Cabañas, Supercritical fluid preparation of Pt, Ru and Ni/graphene nanocomposites and their application as selective catalysts in the partial hydrogenation of limonene, J. Supercrit. Fluids 120 (2017) 7–17, https://doi.org/10.1016/j.supflu.2016.10.007.
[94] X. Huang, G. Zhao, X. Wang, Fabrication of reduced graphene oxide/metal (Cu, Ni, Co) nanoparticle hybrid composites via a facile thermal reduction method, RSC Adv. 5 (2015) 49973–49978, https://doi.org/10.1039/c5ra08670a.
[95] Z. Peng, F. Somodi, S. Helveg, C. Kisielowski, P. Specht, A.T. Bell, High-resolution in situ and ex situ TEM studies on graphene formation and growth on Pt nanoparticles, J. Catal. 286 (2012) 22–29, https://doi.org/10.1016/j.jcat.2011.10.008.
[96] T.T. Tung, N.V. Chien, N. Van Duy, N. Van Hieu, M.J. Nine, C.J. Coghlan, D.N.H. Tran, D. Losic, Magnetic iron oxide nanoparticles decorated graphene for chemoresistive gas sensing: the particle size effects, J. Colloid Interface Sci. 539 (2019) 315–325, https://doi.org/10.1016/j.jcis.2018.12.077.
[97] X. Liu, J. Li, J. Sun, X. Zhang, 3D Fe_3O_4 nanoparticle/graphene aerogel for NO_2 sensing at room temperature, RSC Adv. 5 (2015) 73699–73704, https://doi.org/10.1039/C5RA14857J.
[98] J. Choi, D.A. Reddy, M.J. Islam, R. Ma, T.K. Kim, Self-assembly of CeO_2 nanostructures/reduced graphene oxide composite aerogels for efficient photocatalytic degradation of organic pollutants in water, J. Alloys Compd. 688 (2016) 527–536, https://doi.org/10.1016/j.jallcom.2016.07.236.
[99] R. Rajendran, L.K. Shrestha, K. Minami, M. Subramanian, R. Jayavel, K. Ariga, Dimensionally integrated nanoarchitectonics for a novel composite from 0D {,} 1D{,} and 2D nanomaterials: RGO/CNT/CeO_2 ternary nanocomposites with electrochemical performance, J. Mater. Chem. A 2 (2014) 18480–18487, https://doi.org/10.1039/C4TA03996C.
[100] C. Zhao, H. Tang, W. Liu, C. Han, X. Yang, Q. Liu, J. Xu, Constructing 0D FeP nanodots/2D g-C_3N_4 nanosheets heterojunction for highly improved photocatalytic hydrogen evolution, ChemCatChem 11 (2019) 6310–6315, https://doi.org/10.1002/cctc.201901489.
[101] A. Mohanty, W. Baaziz, M. Lafjah, V. Da Costa, I. Janowska, Few layer graphene as a template for Fe-based 2D nanoparticles, FlatChem 9 (2018) 15–20, https://doi.org/10.1016/j.flatc.2018.04.002.
[102] X. Tang, P.-A. Haddad, N. Mager, X. Geng, N. Reckinger, S. Hermans, M. Debliquy, J.-P. Raskin, Chemically deposited palladium nanoparticles on graphene for hydrogen sensor applications, Sci. Rep. 9 (2019) 3653, https://doi.org/10.1038/s41598-019-40257-7.
[103] E. Teran-Salgado, D. Bahena-Uribe, P.A. Márquez-Aguilar, J.L. Reyes-Rodriguez, R. Cruz-Silva, O. Solorza-Feria, Platinum nanoparticles supported on electrochemically oxidized and exfoliated graphite for the oxygen reduction reaction, Electrochim. Acta 298 (2019) 172–185, https://doi.org/10.1016/j.electacta.2018.12.057.
[104] A.R. Biris, M.D. Lazar, S. Pruneanu, C. Neamtu, F. Watanabe, G.K. Kannarpady, E. Dervishi, A.S. Biris, Catalytic one-step synthesis of Pt-decorated few-layer graphenes, RSC Adv. 3 (2013) 26391, https://doi.org/10.1039/c3ra44564j.
[105] S. Pruneanu, A.R. Biris, F. Pogacean, M. Coroş, G.K. Kannarpady, F. Watanabe, A.S. Biris, The study of adenine and guanine electrochemical oxidation using electrodes modified with graphene-platinum nanoparticles composites, Electrochim. Acta 139 (2014) 386–393, https://doi.org/10.1016/j.electacta.2014.06.163.
[106] K. Nakada, A. Ishii, Migration of adatom adsorption on graphene using DFT calculation, Solid State Commun. 151 (2011) 13–16, https://doi.org/10.1016/j.ssc.2010.10.036.
[107] J.M. Yuk, M. Jeong, S.Y. Kim, H.K. Seo, J. Kim, J.Y. Lee, In situ atomic imaging of coalescence of Au nanoparticles on graphene: rotation and grain boundary migration, Chem. Commun. 49 (2013) 11479–11481, https://doi.org/10.1039/C3CC46545D.
[108] H. Naeim, F. Kheiri, M. Sirousazar, A. Afghan, Ionic liquid/reduced graphene oxide/nickel-palladium nanoparticle hybrid synthesized for non-enzymatic electrochemical glucose sensing, Electrochim. Acta 282 (2018) 137–146, https://doi.org/10.1016/j.electacta.2018.05.204.
[109] Y. Chen, Q. Dong, L. Wang, X. Guo, S. Ai, H. Ding, Graphitic-C_3N_4 quantum dots decorated {001}-faceted TiO_2 nanosheets as a 0D/2D composite with enhanced solar photocatalytic activity, Res. Chem. Intermed. 44 (2018) 7369–7389, https://doi.org/10.1007/s11164-018-3561-3.
[110] X.-Y. Liu, H. Chen, R. Wang, Y. Shang, Q. Zhang, W. Li, G. Zhang, J. Su, C.T. Dinh, F.P.G. de Arquer, J. Li, J. Jiang, Q. Mi, R. Si, X. Li, Y. Sun, Y.-T. Long, H. Tian, E.H. Sargent, Z. Ning, 0D–2D quantum dot: metal dichalcogenide nanocomposite photocatalyst achieves efficient hydrogen generation, Adv. Mater. 29 (2017) 1605646, https://doi.org/10.1002/adma.201605646.
[111] S. Sinha, T. Zhu, A. France-Lanord, Y. Sheng, J.C. Grossman, K. Porfyrakis, J.H. Warner, Atomic structure and defect dynamics of monolayer lead iodide nanodisks with epitaxial alignment on graphene, Nat. Commun. 11 (2020) 1–13, https://doi.org/10.1038/s41467-020-14481-z.
[112] P.T. Yin, T.-H. Kim, J.-W. Choi, K.-B. Lee, Prospects for graphene-nanoparticle-based hybrid sensors, Phys. Chem. Chem. Phys. 15 (2013) 12785–12799, https://doi.org/10.1039/c3cp51901e.
[113] Z. Ye, Y. Jiang, L. Li, F. Wu, R. Chen, Self-assembly of 0D–2D heterostructure electrocatalyst from MOF and MXene for boosted lithium polysulfide conversion reaction, Adv. Mater. 33 (2021) 2101204, https://doi.org/10.1002/adma.202101204.
[114] J. Zhang, T. Zhu, Y. Wang, J. Cui, J. Sun, J. Yan, Y. Qin, X. Shu, Y. Zhang, J. Wu, C.S. Tiwary, P.M. Ajayan, Y. Wu, Self-assembly of 0D/2D homostructure for enhanced hydrogen evolution, Mater. Today 36 (2020) 83–90, https://doi.org/10.1016/j.mattod.2020.02.006.
[115] W. Lv, H. Wang, L. Jia, X. Tang, C. Lin, L. Yuwen, L. Wang, W. Huang, R. Chen, Tunable nonvolatile memory behaviors of PCBM–MoS_2 2D nanocomposites through surface deposition ratio control, ACS Appl. Mater. Interfaces 10 (2018) 6552–6559, https://doi.org/10.1021/acsami.7b16878.
[116] S. Zhang, H. Gao, X. Liu, Y. Huang, X. Xu, N.S. Alharbi, T. Hayat, J. Li, Hybrid 0D–2D nanoheterostructures: in situ growth of amorphous silver silicates

dots on g-C_3N_4 nanosheets for full-spectrum photocatalysis, ACS Appl. Mater. Interfaces 8 (2016) 35138–35149, https://doi.org/10.1021/acsami.6b09260.
[117] M.M. Xavier, J. George, K.S. Divya, N.N. Adarsh, P.R. Nair, S. Mathew, Green synthesis of a metal-free 0D/2D heterojunction: a cost-effective approach, ChemistrySelect 4 (2019) 11541–11547, https://doi.org/10.1002/slct.201903314.
[118] J. Guan, J. Wu, D. Jiang, X. Zhu, R. Guan, X. Lei, P. Du, H. Zeng, S. Yang, Hybridizing MoS_2 and C_{60} via a van der Waals heterostructure toward synergistically enhanced visible light photocatalytic hydrogen production activity, Int. J. Hydrogen Energy 43 (2018) 8698–8706, https://doi.org/10.1016/j.ijhydene.2018.03.148.
[119] J. Choe, Y. Lee, J. Park, Y. Kim, C.U. Kim, K. Kim, Direct imaging of structural disordering and heterogeneous dynamics of fullerene molecular liquid, Nat. Commun. 10 (2019) 4395, https://doi.org/10.1038/s41467-019-12320-4.
[120] T. Hoon Lee, K. Kim, G. Kim, H. Ju Park, D. Scullion, L. Shaw, M.-G. Kim, X. Gu, W.-G. Bae, E.J.G. Santos, Z. Lee, H. Suk Shin, Y. Nishi, Z. Bao, Chemical vapor-deposited hexagonal boron nitride as a scalable template for high-performance organic field-effect transistors, Chem. Mater. 29 (2017) 2341–2347, https://doi.org/10.1021/acs.chemmater.6b05517.
[121] X. Chen, H. Chen, J. Guan, J. Zhen, Z. Sun, P. Du, Y. Lu, S. Yang, A facile mechanochemical route to a covalently bonded graphitic carbon nitride (g-C_3N_4) and fullerene hybrid toward enhanced visible light photocatalytic hydrogen production, Nanoscale 9 (2017) 5615–5623, https://doi.org/10.1039/C7NR01237C.
[122] S. Collavini, J.L. Delgado, Fullerenes: the stars of photovoltaics, Sustain. Energy Fuels. 2 (2018) 2480–2493, https://doi.org/10.1039/C8SE00254A.
[123] P.-W. Liang, C.-C. Chueh, S.T. Williams, A.K.-Y. Jen, Roles of fullerene-based interlayers in enhancing the performance of organometal perovskite thin-film solar cells, Adv. Energy Mater. 5 (2015) 1402321, https://doi.org/10.1002/aenm.201402321.
[124] Y. Zhong, M. Hufnagel, M. Thelakkat, C. Li, S. Huettner, Role of PCBM in the suppression of hysteresis in perovskite solar cells, Adv. Funct. Mater. (2020), https://doi.org/10.1002/adfm.201908920.
[125] S. Sun, T. Buonassisi, J.-P. Correa-Baena, State-of-the-art electron-selective contacts in perovskite solar cells, Adv. Mater. Interfaces 5 (2018) 1800408, https://doi.org/10.1002/admi.201800408.
[126] S. Das, D. Pandey, J. Thomas, T. Roy, The role of graphene and other 2D materials in solar photovoltaics, Adv. Mater. 31 (2019) 1802722, https://doi.org/10.1002/adma.201802722.
[127] P. You, G. Tang, F. Yan, Two-dimensional materials in perovskite solar cells, Mater. Today Energy 11 (2019) 128–158, https://doi.org/10.1016/j.mtener.2018.11.006.
[128] B. Wang, J. Iocozzia, M. Zhang, M. Ye, S. Yan, H. Jin, S. Wang, Z. Zou, Z. Lin, The charge carrier dynamics, efficiency and stability of two-dimensional material-based perovskite solar cells, Chem. Soc. Rev. 48 (2019) 4854–4891, https://doi.org/10.1039/C9CS00254E.
[129] A.P. Litvin, X. Zhang, K. Berwick, A.V. Fedorov, W. Zheng, A.V. Baranov, Carbon-based interlayers in perovskite solar cells, Renew. Sustain. Energy Rev. 124 (2020) 109774, https://doi.org/10.1016/j.rser.2020.109774.
[130] N. Balis, E. Stratakis, E. Kymakis, Graphene and transition metal dichalcogenide nanosheets as charge transport layers for solution processed solar cells, Mater. Today 19 (2016) 580–594, https://doi.org/10.1016/j.mattod.2016.03.018.
[131] J. Zhu, P. Li, X. Chen, D. Legut, Y. Fan, R. Zhang, Y. Lu, X. Cheng, Q. Zhang, Rational design of graphitic-inorganic Bi-layer artificial SEI for stable lithium metal anode, Energy Storage Mater. 16 (2019) 426–433, https://doi.org/10.1016/j.ensm.2018.06.023.
[132] M. Hilal, J.I. Han, Study of interface chemistry between the carrier-transporting layers and their influences on the stability and performance of organic solar cells, Appl. Nanosci. 8 (2018) 1325–1341, https://doi.org/10.1007/s13204-018-0818-5.
[133] G. Kakavelakis, T. Maksudov, D. Konios, I. Paradisanos, G. Kioseoglou, E. Stratakis, E. Kymakis, Efficient and highly air stable planar inverted perovskite solar cells with reduced graphene oxide doped PCBM electron transporting layer, Adv. Energy Mater. 7 (2017) 1602120, https://doi.org/10.1002/aenm.201602120.
[134] E. Bi, H. Chen, F. Xie, Y. Wu, W. Chen, Y. Su, A. Islam, M. Grätzel, X. Yang, L. Han, Diffusion engineering of ions and charge carriers for stable efficient perovskite solar cells, Nat. Commun. 8 (2017) 15330, https://doi.org/10.1038/ncomms15330.
[135] J. Nicasio-Collazo, J.-L. Maldonado, J. Salinas-Cruz, D. Barreiro-Argüelles, I. Caballero-Quintana, C. Vázquez-Espinosa, D. Romero-Borja, Functionalized and reduced graphene oxide as hole transport layer and for use in ternary organic solar cell, Opt. Mater. (Amst) 98 (2019) 109434, https://doi.org/10.1016/j.optmat.2019.109434.
[136] J. Zhang, T. Tong, L. Zhang, X. Li, H. Zou, J. Yu, Enhanced performance of planar perovskite solar cell by graphene quantum dot modification, ACS Sustain. Chem. Eng. 6 (2018) 8631–8640, https://doi.org/10.1021/acssuschemeng.8b00938.
[137] D.H. Shin, J.M. Kim, S.H. Shin, S.-H. Choi, Highly-flexible graphene transparent conductive electrode/perovskite solar cells with graphene quantum dots-doped PCBM electron transport layer, Dyes Pigments 170 (2019) 107630, https://doi.org/10.1016/j.dyepig.2019.107630.
[138] Z. Yang, J. Xie, V. Arivazhagan, K. Xiao, Y. Qiang, K. Huang, M. Hu, C. Cui, X. Yu, D. Yang, Efficient and highly light stable planar perovskite solar cells with graphene quantum dots doped PCBM electron transport layer, Nano Energy 40 (2017) 345–351, https://doi.org/10.1016/j.nanoen.2017.08.008.
[139] F. Fu, T. Feurer, T.P. Weiss, S. Pisoni, E. Avancini, C. Andres, S. Buecheler, A.N. Tiwari, High-efficiency inverted semi-transparent planar perovskite solar cells in substrate configuration, Nat. Energy 2 (2016) 16190, https://doi.org/10.1038/nenergy.2016.190.
[140] K. Huang, Y. Yan, X. Yu, H. Zhang, D. Yang, Graphene coupled with Pt cubic nanoparticles for high performance, air-stable graphene-silicon solar cells, Nano Energy 32 (2017) 225–231, https://doi.org/10.1016/j.nanoen.2016.12.042.
[141] J.T.-W. Wang, J.M. Ball, E.M. Barea, A. Abate, J.A. Alexander-Webber, J. Huang, M. Saliba, I. Mora-Sero, J. Bisquert, H.J. Snaith, R.J. Nicholas, Low-temperature processed electron collection layers of graphene/TiO_2 nanocomposites in thin film perovskite solar cells, Nano Lett. 14 (2014) 724–730, https://doi.org/10.1021/nl403997a.
[142] J. Meyer, P.R. Kidambi, B.C. Bayer, C. Weijtens, A. Kuhn, A. Centeno, A. Pesquera, A. Zurutuza, J. Robertson, S. Hofmann, Metal oxide induced charge transfer doping and band Alignment of graphene electrodes for efficient organic light emitting diodes, Sci. Rep. 4 (2014) 5380, https://doi.org/10.1038/srep05380.
[143] K.C. Kwon, K.S. Choi, S.Y. Kim, Increased work function in few-layer graphene sheets via metal chloride doping, Adv. Funct. Mater. 22 (2012) 4724–4731, https://doi.org/10.1002/adfm.201200997.
[144] S.S. Bhosale, E. Jokar, A. Fathi, C.-M. Tsai, C.-Y. Wang, E.W.-G. Diau, Functionalization of graphene oxide films with Au and MoOx nanoparticles as efficient p-contact electrodes for inverted planar perovskite solar cells, Adv. Funct. Mater. 28 (2018) 1803200, https://doi.org/10.1002/adfm.201803200.
[145] B. Xie, Y. Zhang, Y. Li, W. Chen, X. Hu, S. Zhang, Solution preparation of molybdenum oxide on graphene: a hole transport layer for efficient perovskite solar cells with a 1.12 V high open-circuit voltage, J. Mater. Sci. Mater. Electron. 31 (2020) 6248–6254, https://doi.org/10.1007/s10854-020-03179-z.
[146] F.-X. Liang, Y. Gao, C. Xie, X.-W. Tong, Z.-J. Li, L.-B. Luo, Recent advances in the fabrication of graphene–ZnO heterojunctions for optoelectronic device applications, J. Mater. Chem. C. 6 (2018) 3815–3833, https://doi.org/10.1039/C8TC00172C.
[147] P.S. Chandrasekhar, V.K. Komarala, Graphene/ZnO nanocomposite as an electron transport layer for perovskite solar cells; the effect of graphene concentration on photovoltaic performance, RSC Adv. 7 (2017) 28610–28615, https://doi.org/10.1039/C7RA02036H.
[148] J. Xie, K. Huang, X. Yu, Z. Yang, K. Xiao, Y. Qiang, X. Zhu, L. Xu, P. Wang, C. Cui, D. Yang, Enhanced electronic properties of SnO_2 via electron transfer from graphene quantum dots for efficient perovskite solar cells, ACS Nano 11 (2017) 9176–9182, https://doi.org/10.1021/acsnano.7b04070.
[149] J.A. Hong, E.D. Jung, J.C. Yu, D.W. Kim, Y.S. Nam, I. Oh, E. Lee, J.-W. Yoo, S. Cho, M.H. Song, Improved efficiency of perovskite solar cells using a nitrogen-doped graphene-oxide-treated tin oxide layer, ACS Appl. Mater. Interfaces 12 (2020) 2417–2423, https://doi.org/10.1021/acsami.9b17705.
[150] M.M. Tavakoli, R. Tavakoli, P. Yadav, J. Kong, A graphene/ZnO electron transfer layer together with perovskite passivation enables highly efficient and stable perovskite solar cells, J. Mater. Chem. A 7 (2019) 679–686, https://doi.org/10.1039/C8TA10857A.
[151] D. Benetti, E. Jokar, C.-H. Yu, A. Fathi, H. Zhao, A. Vomiero, E. Wei-Guang Diau, F. Rosei, Hole-extraction and photostability enhancement in highly efficient inverted perovskite solar cells through carbon dot-based hybrid material, Nano Energy 62 (2019) 781–790, https://doi.org/10.1016/j.nanoen.2019.05.084.
[152] M. Jawad, A.F. Khan, A. Waseem, A.H. Kamboh, M. Mohsin, S.A. Shahzad, S.H. Shah, S. Mathur, A.J. Shaikh, Effect of gold nanoparticles on transmittance and conductance of graphene oxide thin films and efficiency of perovskite solar cells, Appl. Nanosci. 10 (2020) 485–497, https://doi.org/10.1007/s13204-019-01134-x.
[153] T.A. Shifa, F. Wang, Y. Liu, J. He, Heterostructures based on 2D materials: a versatile platform for efficient catalysis, Adv. Mater. 31 (2019) 1804828, https://doi.org/10.1002/adma.201804828.
[154] D. Voiry, H.S. Shin, K.P. Loh, M. Chhowalla, Low-dimensional catalysts for hydrogen evolution and CO_2 reduction, Nat. Rev. Chem. 2 (2018), 0105, https://doi.org/10.1038/s41570-017-0105.
[155] B. Xia, Y. Yan, X. Wang, X.W. (David) Lou, Recent progress on graphene-based hybrid electrocatalysts, Mater. Horiz. 1 (2014) 379–399, https://doi.org/10.1039/C4MH00040D.
[156] C. Tang, M.-M. Titirici, Q. Zhang, A review of nanocarbons in energy electrocatalysis: multifunctional substrates and highly active sites, J. Energy Chem. 26 (2017) 1077–1093, https://doi.org/10.1016/j.jechem.2017.08.008.
[157] R. Wang, D. Li, S. Maurya, Y.S. Kim, Y. Wu, Y. Liu, D. Strmcnik, N.M. Markovic, V.R. Stamenkovic, Ultrafine Pt cluster and RuO_2 heterojunction anode catalysts designed for ultra-low Pt-loading anion exchange membrane fuel cells, Nanoscale Horiz. 5 (2020) 316–324, https://doi.org/10.1039/C9NH00533A.
[158] Z.W. Seh, J. Kibsgaard, C.F. Dickens, I. Chorkendorff, J.K. Nørskov, T.F. Jaramillo, Combining theory and experiment in electrocatalysis: insights into materials design, Science (80-.) 355 (2017), eaad4998, https://doi.org/10.1126/science.aad4998.

[159] G. Xie, K. Zhang, B. Guo, Q. Liu, L. Fang, J.R. Gong, Graphene-based materials for hydrogen generation from light-driven water splitting, Adv. Mater. 25 (2013) 3820–3839, https://doi.org/10.1002/adma.201301207.
[160] X. Xie, K. Kretschmer, G. Wang, Advances in graphene-based semiconductor photocatalysts for solar energy conversion: fundamentals and materials engineering, Nanoscale 7 (2015) 13278–13292, https://doi.org/10.1039/C5NR03338A.
[161] N. Zhang, M.-Q. Yang, S. Liu, Y. Sun, Y.-J. Xu, Waltzing with the versatile platform of graphene to synthesize composite photocatalysts, Chem. Rev. 115 (2015) 10307–10377, https://doi.org/10.1021/acs.chemrev.5b00267.
[162] Q. Xiang, B. Cheng, J. Yu, Graphene-based photocatalysts for solar-fuel generation, Angew. Chem. Int. Ed. 54 (2015) 11350–11366, https://doi.org/10.1002/anie.201411096.
[163] B.-J. Su, K.-W. Wang, C.-J. Tseng, C.-W. Pao, J.-L. Chen, K.-T. Lu, J.-M. Chen, High durability of Pt_3Sn/graphene electrocatalysts toward the oxygen reduction reaction studied with in situ QEXAFS, ACS Appl. Mater. Interfaces 12 (2020) 24710–24716, https://doi.org/10.1021/acsami.0c02415.
[164] K. Ojha, M. Sharma, H. Kolev, A.K. Ganguli, Reduced graphene oxide and MoP composite as highly efficient and durable electrocatalyst for hydrogen evolution in both acidic and alkaline media, Catal. Sci. Technol. 7 (2017) 668–676, https://doi.org/10.1039/C6CY02406H.
[165] T.A. Shifa, A. Vomiero, Confined catalysis: progress and prospects in energy conversion, Adv. Energy Mater. 9 (2019) 1902307, https://doi.org/10.1002/aenm.201902307.
[166] D. Huang, Z. Li, G. Zeng, C. Zhou, W. Xue, X. Gong, X. Yan, S. Chen, W. Wang, M. Cheng, Megamerger in photocatalytic field: 2D g-C_3N_4 nanosheets serve as support of 0D nanomaterials for improving photocatalytic performance, Appl. Catal. B Environ. 240 (2019) 153–173, https://doi.org/10.1016/j.apcatb.2018.08.071.
[167] P. Niu, L. Zhang, G. Liu, H.-M. Cheng, Graphene-like carbon nitride nanosheets for improved photocatalytic activities, Adv. Funct. Mater. 22 (2012) 4763–4770, https://doi.org/10.1002/adfm.201200922.
[168] X. Wang, K. Maeda, A. Thomas, K. Takanabe, G. Xin, J.M. Carlsson, K. Domen, M. Antonietti, A metal-free polymeric photocatalyst for hydrogen production from water under visible light, Nat. Mater. 8 (2009) 76–80, https://doi.org/10.1038/nmat2317.
[169] R. Acharya, K. Parida, A review on TiO_2/g-C_3N_4 visible-light- responsive photocatalysts for sustainable energy generation and environmental remediation, J. Environ. Chem. Eng. 8 (2020) 103896, https://doi.org/10.1016/j.jece.2020.103896.
[170] D. Zeng, T. Zhou, W.-J. Ong, M. Wu, X. Duan, W. Xu, Y. Chen, Y.-A. Zhu, D.-L. Peng, Sub-5 nm ultra-fine FeP nanodots as efficient Co-catalysts modified porous g-C_3N_4 for precious-metal-free photocatalytic hydrogen evolution under visible light, ACS Appl. Mater. Interfaces 11 (2019) 5651–5660, https://doi.org/10.1021/acsami.8b20958.
[171] J. Zhang, J. Sun, K. Maeda, K. Domen, P. Liu, M. Antonietti, X. Fu, X. Wang, Sulfur-mediated synthesis of carbon nitride: band-gap engineering and improved functions for photocatalysis, Energy Environ. Sci. 4 (2011) 675–678, https://doi.org/10.1039/C0EE00418A.
[172] D. Zeng, P. Wu, W.-J. Ong, B. Tang, M. Wu, H. Zheng, Y. Chen, D.-L. Peng, Construction of network-like and flower-like 2H-$MoSe_2$ nanostructures coupled with porous g-C_3N_4 for noble-metal-free photocatalytic H_2 evolution under visible light, Appl. Catal. B Environ. 233 (2018) 26–34, https://doi.org/10.1016/j.apcatb.2018.03.102.
[173] J. Wen, J. Xie, X. Chen, X. Li, A review on g-C_3N_4 -based photocatalysts, Appl. Surf. Sci. 391 (2017) 72–123, https://doi.org/10.1016/j.apsusc.2016.07.030.
[174] X. Li, J. Zhu, B. Wei, Hybrid nanostructures of metal/two-dimensional nanomaterials for plasmon-enhanced applications, Chem. Soc. Rev. 45 (2016) 3145–3187, https://doi.org/10.1039/C6CS00195E.
[175] J. Jiang, J. Yu, S. Cao, Au/PtO nanoparticle-modified g-C_3N_4 for plasmon-enhanced photocatalytic hydrogen evolution under visible light, J. Colloid Interface Sci. 461 (2016) 56–63, https://doi.org/10.1016/j.jcis.2015.08.076.
[176] X. Wei, C. Shao, X. Li, N. Lu, K. Wang, Z. Zhang, Y. Liu, Facile in situ synthesis of plasmonic nanoparticles-decorated g-C_3N_4/TiO_2 heterojunction nanofibers and comparison study of their photosynergistic effects for efficient photocatalytic H_2 evolution, Nanoscale 8 (2016) 11034–11043, https://doi.org/10.1039/C6NR01491G.
[177] S.-W. Cao, Y.-P. Yuan, J. Fang, M.M. Shahjamali, F.Y.C. Boey, J. Barber, S.C. Joachim Loo, C. Xue, In-situ growth of CdS quantum dots on g-C_3N_4 nanosheets for highly efficient photocatalytic hydrogen generation under visible light irradiation, Int. J. Hydrogen Energy 38 (2013) 1258–1266, https://doi.org/10.1016/j.ijhydene.2012.10.116.
[178] L. Ge, F. Zuo, J. Liu, Q. Ma, C. Wang, D. Sun, L. Bartels, P. Feng, Synthesis and efficient visible light photocatalytic hydrogen evolution of polymeric g-C_3N_4 coupled with CdS quantum dots, J. Phys. Chem. C 116 (2012) 13708–13714, https://doi.org/10.1021/jp3041692.
[179] S.-W. Cao, X.-F. Liu, Y.-P. Yuan, Z.-Y. Zhang, Y.-S. Liao, J. Fang, S.C.J. Loo, T.C. Sum, C. Xue, Solar-to-fuels conversion over In_2O_3/g-C_3N_4 hybrid photocatalysts, Appl. Catal. B Environ. 147 (2014) 940–946, https://doi.org/10.1016/j.apcatb.2013.10.029.
[180] Y. Hou, A.B. Laursen, J. Zhang, G. Zhang, Y. Zhu, X. Wang, S. Dahl, I. Chorkendorff, Layered nanojunctions for hydrogen-evolution catalysis, Angew. Chem. Int. Ed. 52 (2013) 3621–3625, https://doi.org/10.1002/anie.201210294.
[181] M. Wang, P. Ju, J. Li, Y. Zhao, X. Han, Z. Hao, Facile synthesis of MoS 2/g-C_3N_4/GO ternary heterojunction with enhanced photocatalytic activity for water splitting, ACS Sustain. Chem. Eng. 5 (2017) 7878–7886, https://doi.org/10.1021/acssuschemeng.7b01386.
[182] Y. Zou, J.-W. Shi, D. Ma, Z. Fan, L. Cheng, D. Sun, Z. Wang, C. Niu, WS 2/graphitic carbon nitride heterojunction nanosheets decorated with CdS quantum dots for photocatalytic hydrogen production, ChemSusChem 11 (2018) 1187–1197, https://doi.org/10.1002/cssc.201800053.
[183] J. Wen, J. Xie, H. Zhang, A. Zhang, Y. Liu, X. Chen, X. Li, Constructing multifunctional metallic Ni interface layers in the g-C_3N_4 nanosheets/amorphous NiS heterojunctions for efficient photocatalytic H_2 generation, ACS Appl. Mater. Interfaces 9 (2017) 14031–14042, https://doi.org/10.1021/acsami.7b02701.
[184] J. Mahmood, F. Li, S.-M. Jung, M.S. Okyay, I. Ahmad, S.-J. Kim, N. Park, H.Y. Jeong, J.-B. Baek, An efficient and pH-universal ruthenium-based catalyst for the hydrogen evolution reaction, Nat. Nanotechnol. 12 (2017) 441–446, https://doi.org/10.1038/nnano.2016.304.
[185] W. Sheng, H.a. Gasteiger, Y. Shao-Horn, Hydrogen oxidation and evolution reaction kinetics on platinum: acid vs alkaline electrolytes, J. Electrochem. Soc. 157 (2010) B1529, https://doi.org/10.1149/1.3483106.
[186] X. Li, W. Bi, L. Zhang, S. Tao, W. Chu, Q. Zhang, Y. Luo, C. Wu, Y. Xie, Single-atom Pt as Co-catalyst for enhanced photocatalytic H_2 evolution, Adv. Mater. 28 (2016) 2427–2431, https://doi.org/10.1002/adma.201505281.
[187] G. Darabdhara, M.A. Amin, G.A.M. Mersal, E.M. Ahmed, M.R. Das, M.B. Zakaria, V. Malgras, S.M. Alshehri, Y. Yamauchi, S. Szunerits, R. Boukherroub, Reduced graphene oxide nanosheets decorated with Au, Pd and Au–Pd bimetallic nanoparticles as highly efficient catalysts for electrochemical hydrogen generation, J. Mater. Chem. A 3 (2015) 20254–20266, https://doi.org/10.1039/C5TA05730B.
[188] G.-R. Xu, J.-J. Hui, T. Huang, Y. Chen, J.-M. Lee, Platinum nanocuboids supported on reduced graphene oxide as efficient electrocatalyst for the hydrogen evolution reaction, J. Power Sources 285 (2015) 393–399, https://doi.org/10.1016/j.jpowsour.2015.03.131.
[189] D. Yan, F. Li, Y. Xu, C. Liu, Y. Wang, Y. Tang, L. Yang, L. Wang, Three-dimensional reduced graphene oxide–Mn_3O_4 nanosheet hybrid decorated with palladium nanoparticles for highly efficient hydrogen evolution, Int. J. Hydrogen Energy 43 (2018) 3369–3377, https://doi.org/10.1016/j.ijhydene.2017.06.083.
[190] S. Ghasemi, S.R. Hosseini, S. Nabipour, P. Asen, Palladium nanoparticles supported on graphene as an efficient electrocatalyst for hydrogen evolution reaction, Int. J. Hydrogen Energy 40 (2015) 16184–16191, https://doi.org/10.1016/j.ijhydene.2015.09.114.
[191] Y. Shiraishi, Y. Kofuji, S. Kanazawa, H. Sakamoto, S. Ichikawa, S. Tanaka, T. Hirai, Platinum nanoparticles strongly associated with graphitic carbon nitride as efficient co-catalysts for photocatalytic hydrogen evolution under visible light, Chem. Commun. 50 (2014) 15255–15258, https://doi.org/10.1039/C4CC06960A.
[192] Y. Peng, B. Lu, L. Chen, N. Wang, J.E. Lu, Y. Ping, S. Chen, Hydrogen evolution reaction catalyzed by ruthenium ion-complexed graphitic carbon nitride nanosheets, J. Mater. Chem. A 5 (2017) 18261–18269, https://doi.org/10.1039/C7TA03826G.
[193] N. Cheng, S. Stambula, D. Wang, M.N. Banis, J. Liu, A. Riese, B. Xiao, R. Li, T.-K. Sham, L.-M. Liu, G.A. Botton, X. Sun, Platinum single-atom and cluster catalysis of the hydrogen evolution reaction, Nat. Commun. 7 (2016) 13638, https://doi.org/10.1038/ncomms13638.
[194] M. Zhu, X. Cai, M. Fujitsuka, J. Zhang, T. Majima, Au/$La_2Ti_2O_7$ nanostructures sensitized with black phosphorus for plasmon-enhanced photocatalytic hydrogen production in visible and near-infrared light, Angew. Chem. Int. Ed. 56 (2017) 2064–2068, https://doi.org/10.1002/anie.201612315.
[195] T. Oshima, D. Lu, O. Ishitani, K. Maeda, Intercalation of highly dispersed metal nanoclusters into a layered metal oxide for photocatalytic overall water splitting, Angew. Chem. Int. Ed. 54 (2015) 2698–2702, https://doi.org/10.1002/anie.201411494.
[196] Y. Xin, L. Wu, L. Ge, C. Han, Y. Li, S. Fang, Gold–palladium bimetallic nanoalloy decorated ultrathin 2D TiO_2 nanosheets as efficient photocatalysts with high hydrogen evolution activity, J. Mater. Chem. A 3 (2015) 8659–8666, https://doi.org/10.1039/C5TA00759C.
[197] P.C.K. Vesborg, B. Seger, I. Chorkendorff, Recent development in hydrogen evolution reaction catalysts and their practical implementation, J. Phys. Chem. Lett. 6 (2015) 951–957, https://doi.org/10.1021/acs.jpclett.5b00306.
[198] E.J. Popczun, C.G. Read, C.W. Roske, N.S. Lewis, R.E. Schaak, Highly active electrocatalysis of the hydrogen evolution reaction by cobalt phosphide nanoparticles, Angew. Chem. Int. Ed. 53 (2014) 5427–5430, https://doi.org/10.1002/anie.201402646.
[199] J. Kibsgaard, T.F. Jaramillo, Molybdenum phosphosulfide: an active, acid-stable, earth-abundant catalyst for the hydrogen evolution reaction, Angew. Chem. Int. Ed. 53 (2014) 14433–14437, https://doi.org/10.1002/anie.201408222.
[200] E.J. Popczun, J.R. McKone, C.G. Read, A.J. Biacchi, A.M. Wiltrout, N.S. Lewis, R.E. Schaak, Nanostructured nickel phosphide as an electrocatalyst for the hydrogen evolution reaction, J. Am. Chem. Soc. 135 (2013) 9267–9270, https://doi.org/10.1021/ja403440e.
[201] H. Kim, A.W. Robertson, G. Kwon, J. O, J.H. Warner, J.M. Kim, Biomass-derived nickel phosphide nanoparticles as a robust catalyst for hydrogen production

by catalytic decomposition of C_2H_2 or dry reforming of CH_4, ACS Appl. Energy Mater. 2 (2019) 8649–8658, https://doi.org/10.1021/acsaem.9b01599.
[202] J.-S. Li, J.-Y. Li, X.-R. Wang, S. Zhang, J.-Q. Sha, G.-D. Liu, Reduced graphene oxide-supported MoP@P-doped porous carbon nano-octahedrons as high-performance electrocatalysts for hydrogen evolution, ACS Sustain. Chem. Eng. 6 (2018) 10252–10259, https://doi.org/10.1021/acssuschemeng.8b01575.
[203] D.Y. Chung, S.W. Jun, G. Yoon, H. Kim, J.M. Yoo, K.-S. Lee, T. Kim, H. Shin, A.K. Sinha, S.G. Kwon, K. Kang, T. Hyeon, Y.-E. Sung, Large-scale synthesis of carbon-shell-coated FeP nanoparticles for robust hydrogen evolution reaction electrocatalyst, J. Am. Chem. Soc. 139 (2017) 6669–6674, https://doi.org/10.1021/jacs.7b01530.
[204] J.-T. Ren, L. Chen, D.-D. Yang, Z.-Y. Yuan, Molybdenum-based nanoparticles (Mo_2C, MoP and MoS_2) coupled heteroatoms-doped carbon nanosheets for efficient hydrogen evolution reaction, Appl. Catal. B Environ. 263 (2020) 118352, https://doi.org/10.1016/j.apcatb.2019.118352.
[205] S. Kan, M. Xu, W. Feng, Y. Wu, C. Du, X. Gao, Y.A. Wu, H. Liu, Tuning overall water splitting on an electrodeposited NiCoFeP films, ChemElectroChem 8 (2021) 539–546, https://doi.org/10.1002/celc.202001501.
[206] B. Hinnemann, P.G. Moses, J. Bonde, K.P. Jørgensen, J.H. Nielsen, S. Horch, I. Chorkendorff, J.K. Nørskov, Biomimetic hydrogen evolution: MoS_2 nanoparticles as catalyst for hydrogen evolution, J. Am. Chem. Soc. 127 (2005) 5308–5309, https://doi.org/10.1021/ja0504690.
[207] T.F. Jaramillo, K.P. Jørgensen, J. Bonde, J.H. Nielsen, S. Horch, I. Chorkendorff, Identification of active edge sites for electrochemical H_2 evolution from MoS_2 nanocatalysts, Science (80-.) 317 (2007) 100–102, https://doi.org/10.1126/science.1141483.
[208] Q. Fu, J. Han, X. Wang, P. Xu, T. Yao, J. Zhong, W. Zhong, S. Liu, T. Gao, Z. Zhang, L. Xu, B. Song, 2D transition metal dichalcogenides: design, modulation, and challenges in electrocatalysis, Adv. Mater. 33 (2021) 1907818, https://doi.org/10.1002/adma.201907818.
[209] A. Bayat, M. Zirak, E. Saievar-Iranizad, Vertically aligned MoS_2 quantum dots/nanoflakes heterostructure: facile deposition with excellent performance toward hydrogen evolution reaction, ACS Sustain. Chem. Eng. 6 (2018) 8374–8382, https://doi.org/10.1021/acssuschemeng.8b00441.
[210] Y. Li, H. Wang, L. Xie, Y. Liang, G. Hong, H. Dai, MoS_2 nanoparticles grown on graphene: an advanced catalyst for the hydrogen evolution reaction, J. Am. Chem. Soc. 133 (2011) 7296–7299, https://doi.org/10.1021/ja201269b.
[211] J. Benson, M. Li, S. Wang, P. Wang, P. Papakonstantinou, Electrocatalytic hydrogen evolution reaction on edges of a few layer molybdenum disulfide nanodots, ACS Appl. Mater. Interfaces 7 (2015) 14113–14122, https://doi.org/10.1021/acsami.5b03399.
[212] L. Liao, J. Zhu, X. Bian, L. Zhu, M.D. Scanlon, H.H. Girault, B. Liu, MoS_2 formed on mesoporous graphene as a highly active catalyst for hydrogen evolution, Adv. Funct. Mater. 23 (2013) 5326–5333, https://doi.org/10.1002/adfm.201300318.
[213] E. Heydari-Bafrooei, N.S. Shamszadeh, Synergetic effect of CoNPs and graphene as cocatalysts for enhanced electrocatalytic hydrogen evolution activity of MoS 2, RSC Adv. 6 (2016) 95979–95986, https://doi.org/10.1039/C6RA21610B.
[214] C. Du, D. Liang, M. Shang, J. Zhang, J. Mao, P. Liu, W. Song, In situ engineering MoS_2 NDs/VS_2 lamellar heterostructure for enhanced electrocatalytic hydrogen evolution, ACS Sustain. Chem. Eng. 6 (2018) 15471–15479, https://doi.org/10.1021/acssuschemeng.8b03929.
[215] S. Kanda, T. Akita, M. Fujishima, H. Tada, Facile synthesis and catalytic activity of MoS_2/TiO_2 by a photodeposition-based technique and its oxidized derivative MoO_3/TiO_2 with a unique photochromism, J. Colloid Interface Sci. 354 (2011) 607–610, https://doi.org/10.1016/j.jcis.2010.11.007.
[216] M. Wang, P. Ju, Y. Zhao, J. Li, X. Han, Z. Hao, In situ ion exchange synthesis of MoS 2/g-C_3N_4 heterojunctions for highly efficient hydrogen production, New J. Chem. 42 (2018) 910–917, https://doi.org/10.1039/C7NJ03483K.
[217] L. Yang, D. Zhong, J. Zhang, Z. Yan, S. Ge, P. Du, J. Jiang, D. Sun, X. Wu, Z. Fan, S.A. Dayeh, B. Xiang, Optical properties of metal–molybdenum disulfide hybrid nanosheets and their application for enhanced photocatalytic hydrogen evolution, ACS Nano 8 (2014) 6979–6985, https://doi.org/10.1021/nn501807y.
[218] Q. Xiang, J. Yu, M. Jaroniec, Synergetic effect of MoS_2 and graphene as cocatalysts for enhanced photocatalytic H_2 production activity of TiO_2 nanoparticles, J. Am. Chem. Soc. 134 (2012) 6575–6578, https://doi.org/10.1021/ja302846n.
[219] K. Chang, Z. Mei, T. Wang, Q. Kang, S. Ouyang, J. Ye, MoS 2/graphene cocatalyst for efficient photocatalytic H_2 evolution under visible light irradiation, ACS Nano 8 (2014) 7078–7087, https://doi.org/10.1021/nn5019945.
[220] Z. Guan, P. Wang, Q. Li, G. Li, J. Yang, Constructing a $ZnIn_2S_4$ nanoparticle/MoS_2-RGO nanosheet 0D/2D heterojunction for significantly enhanced visible-light photocatalytic H_2 production, Dalton Trans. 47 (2018) 6800–6807, https://doi.org/10.1039/C8DT00946E.
[221] X.-Y. Zhang, H.-P. Li, X.-L. Cui, Y. Lin, Graphene/TiO_2 nanocomposites: synthesis, characterization and application in hydrogen evolution from water photocatalytic splitting, J. Mater. Chem. 20 (2010) 2801, https://doi.org/10.1039/b917240h.
[222] J. Deng, H. Li, S. Wang, D. Ding, M. Chen, C. Liu, Z. Tian, K.S. Novoselov, C. Ma, D. Deng, X. Bao, Multiscale structural and electronic control of molybdenum disulfide foam for highly efficient hydrogen production, Nat. Commun. 8 (2017) 14430, https://doi.org/10.1038/ncomms14430.
[223] Z. Luo, Y. Ouyang, H. Zhang, M. Xiao, J. Ge, Z. Jiang, J. Wang, D. Tang, X. Cao, C. Liu, W. Xing, Chemically activating MoS_2 via spontaneous atomic palladium interfacial doping towards efficient hydrogen evolution, Nat. Commun. 9 (2018) 2120, https://doi.org/10.1038/s41467-018-04501-4.
[224] H. Li, C. Tsai, A.L. Koh, L. Cai, A.W. Contryman, A.H. Fragapane, J. Zhao, H.S. Han, H.C. Manoharan, F. Abild-Pedersen, J.K. Nørskov, X. Zheng, Activating and optimizing MoS_2 basal planes for hydrogen evolution through the formation of strained sulphur vacancies, Nat. Mater. 15 (2016) 48–53, https://doi.org/10.1038/nmat4465.
[225] A.W. Robertson, Y.-C. Lin, S. Wang, H. Sawada, C.S. Allen, Q. Chen, S. Lee, G.-D. Lee, J. Lee, S. Han, E. Yoon, A.I. Kirkland, H. Kim, K. Suenaga, J.H. Warner, Atomic structure and spectroscopy of single metal (Cr, V) substitutional dopants in monolayer MoS 2, ACS Nano 10 (2016) 10227–10236, https://doi.org/10.1021/acsnano.6b05674.
[226] J. Miao, F.-X. Xiao, H. Bin Yang, S.Y. Khoo, J. Chen, Z. Fan, Y.-Y. Hsu, H.M. Chen, H. Zhang, B. Liu, Hierarchical Ni-Mo-S nanosheets on carbon fiber cloth: a flexible electrode for efficient hydrogen generation in neutral electrolyte, Sci. Adv. 1 (2015), e1500259, https://doi.org/10.1126/sciadv.1500259.
[227] Y. Shi, Y. Zhou, D.-R. Yang, W.-X. Xu, C. Wang, F.-B. Wang, J.-J. Xu, X.-H. Xia, H.-Y. Chen, Energy level engineering of MoS_2 by transition-metal doping for accelerating hydrogen evolution reaction, J. Am. Chem. Soc. 139 (2017) 15479–15485, https://doi.org/10.1021/jacs.7b08881.
[228] P. Liu, J. Zhu, J. Zhang, K. Tao, D. Gao, P. Xi, Active basal plane catalytic activity and conductivity in Zn doped MoS_2 nanosheets for efficient hydrogen evolution, Electrochim. Acta 260 (2018) 24–30, https://doi.org/10.1016/j.electacta.2017.11.080.
[229] W.-F. Chen, J.T. Muckerman, E. Fujita, Recent developments in transition metal carbides and nitrides as hydrogen evolution electrocatalysts, Chem. Commun. 49 (2013) 8896, https://doi.org/10.1039/c3cc44076a.
[230] W.-F. Chen, C.-H. Wang, K. Sasaki, N. Marinkovic, W. Xu, J.T. Muckerman, Y. Zhu, R.R. Adzic, Highly active and durable nanostructured molybdenum carbide electrocatalysts for hydrogen production, Energy Environ. Sci. 6 (2013) 943, https://doi.org/10.1039/c2ee23891h.
[231] W. Cui, N. Cheng, Q. Liu, C. Ge, A.M. Asiri, X. Sun, Mo_2C nanoparticles decorated graphitic carbon sheets: biopolymer-derived solid-state synthesis and application as an efficient electrocatalyst for hydrogen generation, ACS Catal. 4 (2014) 2658–2661, https://doi.org/10.1021/cs5005294.
[232] Y. Shi, B. Zhang, Recent advances in transition metal phosphide nanomaterials: synthesis and applications in hydrogen evolution reaction, Chem. Soc. Rev. 45 (2016) 1529–1541, https://doi.org/10.1039/C5CS00434A.
[233] G. Zhang, G. Wang, Y. Liu, H. Liu, J. Qu, J. Li, Highly active and stable catalysts of phytic acid-derivative transition metal phosphides for full water splitting, J. Am. Chem. Soc. 138 (2016) 14686–14693, https://doi.org/10.1021/jacs.6b08491.
[234] P. Liu, J. Zhu, J. Zhang, P. Xi, K. Tao, D. Gao, D. Xue, P dopants triggered new basal plane active sites and enlarged interlayer spacing in MoS_2 nanosheets toward electrocatalytic hydrogen evolution, ACS Energy Lett. 2 (2017) 745–752, https://doi.org/10.1021/acsenergylett.7b00111.
[235] L. Li, X. Wang, Y. Guo, J. Li, Synthesis of an ultrafine CoP nanocrystal/graphene sandwiched structure for efficient overall water splitting, Langmuir 36 (2020) 1916–1922, https://doi.org/10.1021/acs.langmuir.9b03810.
[236] S. Lv, J. Chen, X. Chen, J. Chen, Y. Li, Simple 2D/0D CoP integration in a metal–organic framework-derived bifunctional electrocatalyst for efficient overall water splitting, ChemSusChem (2020), https://doi.org/10.1002/cssc.202000566 cssc.202000566.
[237] A. Han, S. Jin, H. Chen, H. Ji, Z. Sun, P. Du, A robust hydrogen evolution catalyst based on crystalline nickel phosphide nanoflakes on three-dimensional graphene/nickel foam: high performance for electrocatalytic hydrogen production from pH 0–14, J. Mater. Chem. A 3 (2015) 1941–1946, https://doi.org/10.1039/C4TA06071G.
[238] J. Li, M. Yan, X. Zhou, Z.-Q. Huang, Z. Xia, C.-R. Chang, Y. Ma, Y. Qu, Mechanistic insights on ternary Ni 2− x Co x P for hydrogen evolution and their hybrids with graphene as highly efficient and robust catalysts for overall water splitting, Adv. Funct. Mater. 26 (2016) 6785–6796, https://doi.org/10.1002/adfm.201601420.
[239] H. Huang, C. Yu, J. Yang, C. Zhao, X. Han, Z. Liu, J. Qiu, Strongly coupled architectures of cobalt phosphide nanoparticles assembled on graphene as bifunctional electrocatalysts for water splitting, ChemElectroChem 3 (2016) 719–725, https://doi.org/10.1002/celc.201600001.
[240] U.P. Suryawanshi, U.V. Ghorpade, D.M. Lee, M. He, S.W. Shin, P.V. Kumar, J.S. Jang, H.R. Jung, M.P. Suryawanshi, J.H. Kim, Colloidal Ni_2P nanocrystals encapsulated in heteroatom-doped graphene nanosheets: a synergy of 0D@2D heterostructure toward overall water splitting, Chem. Mater. 33 (2021) 234–245, https://doi.org/10.1021/acs.chemmater.0c03543.
[241] M. Zhuang, X. Ou, Y. Dou, L. Zhang, Q. Zhang, R. Wu, Y. Ding, M. Shao, Z. Luo, Polymer-embedded fabrication of Co_2P nanoparticles encapsulated in N,P-doped graphene for hydrogen generation, Nano Lett. 16 (2016) 4691–4698, https://doi.org/10.1021/acs.nanolett.6b02203.
[242] J. Ma, M. Wang, G. Lei, G. Zhang, F. Zhang, W. Peng, X. Fan, Y. Li, Polyaniline derived N-doped carbon-coated cobalt phosphide nanoparticles deposited on N-doped graphene as an efficient electrocatalyst for hydrogen evolution reaction, Small 14 (2018) 1702895, https://doi.org/10.1002/smll.201702895.
[243] Y. Pan, N. Yang, Y. Chen, Y. Lin, Y. Li, Y. Liu, C. Liu, Nickel phosphide nanoparticles-nitrogen-doped graphene hybrid as an efficient catalyst for

enhanced hydrogen evolution activity, J. Power Sources 297 (2015) 45–52, https://doi.org/10.1016/j.jpowsour.2015.07.077.
[244] Y. Zheng, Y. Jiao, M. Jaroniec, S.Z. Qiao, Advancing the electrochemistry of the hydrogen-evolution reaction through combining experiment and theory, Angew. Chem. Int. Ed. 54 (2015) 52–65, https://doi.org/10.1002/anie.201407031.
[245] X. Yan, L. Tian, M. He, X. Chen, Three-dimensional crystalline/amorphous Co/Co_3O_4 core/shell nanosheets as efficient electrocatalysts for the hydrogen evolution reaction, Nano Lett. 15 (2015), https://doi.org/10.1021/acs.nanolett.5b02205, 150825090140007.
[246] H. Fei, Y. Yang, Z. Peng, G. Ruan, Q. Zhong, L. Li, E.L.G. Samuel, J.M. Tour, Cobalt nanoparticles embedded in nitrogen-doped carbon for the hydrogen evolution reaction, ACS Appl. Mater. Interfaces 7 (2015) 8083–8087, https://doi.org/10.1021/acsami.5b00652.
[247] H. Zhang, Z. Ma, J. Duan, H. Liu, G. Liu, T. Wang, K. Chang, M. Li, L. Shi, X. Meng, K. Wu, J. Ye, Active sites implanted carbon cages in core–shell architecture: highly active and durable electrocatalyst for hydrogen evolution reaction, ACS Nano 10 (2016) 684–694, https://doi.org/10.1021/acsnano.5b05728.
[248] D. Hou, W. Zhou, K. Zhou, Y. Zhou, J. Zhong, L. Yang, J. Lu, G. Li, S. Chen, Flexible and porous catalyst electrodes constructed by Co nanoparticles@nitrogen-doped graphene films for highly efficient hydrogen evolution, J. Mater. Chem. A 3 (2015) 15962–15968, https://doi.org/10.1039/C5TA03905C.
[249] H. Jin, J. Wang, D. Su, Z. Wei, Z. Pang, Y. Wang, In situ cobalt–cobalt oxide/N-doped carbon hybrids as superior bifunctional electrocatalysts for hydrogen and oxygen evolution, J. Am. Chem. Soc. 137 (2015) 2688–2694, https://doi.org/10.1021/ja5127165.
[250] W. Zhou, J. Zhou, Y. Zhou, J. Lu, K. Zhou, L. Yang, Z. Tang, L. Li, S. Chen, N-doped carbon-wrapped cobalt nanoparticles on N-doped graphene nanosheets for high-efficiency hydrogen production, Chem. Mater. 27 (2015) 2026–2032, https://doi.org/10.1021/acs.chemmater.5b00331.
[251] J. Wang, D. Gao, G. Wang, S. Miao, H. Wu, J. Li, X. Bao, Cobalt nanoparticles encapsulated in nitrogen-doped carbon as a bifunctional catalyst for water electrolysis, J. Mater. Chem. A 2 (2014) 20067–20074, https://doi.org/10.1039/C4TA04337E.
[252] A. Bhat, S. Anwer, K.S. Bhat, M.I.H. Mohideen, K. Liao, A. Qurashi, Prospects challenges and stability of 2D MXenes for clean energy conversion and storage applications, Npj 2D Mater. Appl. 5 (2021) 61, https://doi.org/10.1038/s41699-021-00239-8.
[253] P.V. Shinde, P. Mane, B. Chakraborty, C. Sekhar Rout, Spinel $NiFe_2O_4$ nanoparticles decorated 2D Ti_3C_2 MXene sheets for efficient water splitting: experiments and theories, J. Colloid Interface Sci. 602 (2021) 232–241, https://doi.org/10.1016/j.jcis.2021.06.007.
[254] Y. Ito, W. Cong, T. Fujita, Z. Tang, M. Chen, High catalytic activity of nitrogen and sulfur Co-doped nanoporous graphene in the hydrogen evolution reaction, Angew. Chem. Int. Ed. 54 (2015) 2131–2136, https://doi.org/10.1002/anie.201410050.
[255] G. Zhao, K. Rui, S.X. Dou, W. Sun, Heterostructures for electrochemical hydrogen evolution reaction: a review, Adv. Funct. Mater. 28 (2018) 1803291, https://doi.org/10.1002/adfm.201803291.
[256] Y. Jiao, Y. Zheng, K. Davey, S.-Z. Qiao, Activity origin and catalyst design principles for electrocatalytic hydrogen evolution on heteroatom-doped graphene, Nat. Energy 1 (2016) 16130, https://doi.org/10.1038/nenergy.2016.130.
[257] Y. Zheng, Y. Jiao, L.H. Li, T. Xing, Y. Chen, M. Jaroniec, S.Z. Qiao, Toward design of synergistically active carbon-based catalysts for electrocatalytic hydrogen evolution, ACS Nano 8 (2014) 5290–5296, https://doi.org/10.1021/nn501434a.
[258] J. Duan, S. Chen, M. Jaroniec, S.Z. Qiao, Porous C_3N_4 nanolayers@N-graphene films as catalyst electrodes for highly efficient hydrogen evolution, ACS Nano 9 (2015) 931–940, https://doi.org/10.1021/nn506701x.
[259] Y. Zheng, Y. Jiao, Y. Zhu, L.H. Li, Y. Han, Y. Chen, A. Du, M. Jaroniec, S.Z. Qiao, Hydrogen evolution by a metal-free electrocatalyst, Nat. Commun. 5 (2014) 3783, https://doi.org/10.1038/ncomms4783.
[260] M. Winter, R.J. Brodd, What are batteries, fuel cells, and supercapacitors? Chem. Rev. 104 (2004) 4245–4270, https://doi.org/10.1021/cr020730k.
[261] X. Li, A. Faghri, Review and advances of direct methanol fuel cells (DMFCs) part I: design, fabrication, and testing with high concentration methanol solutions, J. Power Sources 226 (2013) 223–240, https://doi.org/10.1016/j.jpowsour.2012.10.061.
[262] M.K. Debe, Electrocatalyst approaches and challenges for automotive fuel cells, Nature 486 (2012) 43–51, https://doi.org/10.1038/nature11115.
[263] S. Zhang, X.-Z. Yuan, J.N.C. Hin, H. Wang, K.A. Friedrich, M. Schulze, A review of platinum-based catalyst layer degradation in proton exchange membrane fuel cells, J. Power Sources 194 (2009) 588–600, https://doi.org/10.1016/j.jpowsour.2009.06.073.
[264] D.Y. Chung, J.M. Yoo, Y.-E. Sung, Highly durable and active Pt-based nanoscale design for fuel-cell oxygen-reduction electrocatalysts, Adv. Mater. 30 (2018) 1704123, https://doi.org/10.1002/adma.201704123.
[265] K.S. Dhathathreyan, N. Rajalakshmi, R. Balaji, Nanomaterials for fuel cell technology, in: Nanotechnol. Energy Sustain., Wiley-VCH Verlag GmbH & Co. KGaA, Weinheim, Germany, 2017, pp. 569–596, https://doi.org/10.1002/9783527696109.ch24.
[266] L. Dai, Y. Xue, L. Qu, H.-J. Choi, J.-B. Baek, Metal-free catalysts for oxygen reduction reaction, Chem. Rev. 115 (2015) 4823–4892, https://doi.org/10.1021/cr5003563.
[267] H. Kim, G. Kwon, S.O. Han, A. Robertson, Platinum encapsulated within a bacterial nanocellulosic–graphene nanosandwich as a durable thin-film fuel cell catalyst, ACS Appl. Energy Mater. 4 (2021) 1286–1293, https://doi.org/10.1021/acsaem.0c02533.
[268] S.S. Munjewar, S.B. Thombre, R.K. Mallick, A comprehensive review on recent material development of passive direct methanol fuel cell, Ionics 23 (2017) 1–18, https://doi.org/10.1007/s11581-016-1864-1.
[269] H. Liu, C. Song, L. Zhang, J. Zhang, H. Wang, D.P. Wilkinson, A review of anode catalysis in the direct methanol fuel cell, J. Power Sources 155 (2006) 95–110, https://doi.org/10.1016/j.jpowsour.2006.01.030.
[270] L. Gong, Z. Yang, K. Li, W. Xing, C. Liu, J. Ge, Recent development of methanol electrooxidation catalysts for direct methanol fuel cell, J. Energy Chem. 27 (2018) 1618–1628, https://doi.org/10.1016/j.jechem.2018.01.029.
[271] A. Serov, C. Kwak, Review of non-platinum anode catalysts for DMFC and PEMFC application, Appl. Catal. B Environ. 90 (2009) 313–320, https://doi.org/10.1016/j.apcatb.2009.03.030.
[272] R. Serra-Maia, C. Winkler, M. Murayama, K. Tranhuu, F.M. Michel, Abundance and speciation of surface oxygen on nanosized platinum catalysts and effect on catalytic activity, ACS Appl. Energy Mater. 1 (2018) 3255–3266, https://doi.org/10.1021/acsaem.8b00474.
[273] A. Ali, P.K. Shen, Recent advances in graphene-based platinum and palladium electrocatalysts for the methanol oxidation reaction, J. Mater. Chem. A 7 (2019) 22189–22217, https://doi.org/10.1039/C9TA06088J.
[274] Z.A.C. Ramli, S.K. Kamarudin, Platinum-based catalysts on various carbon supports and conducting polymers for direct methanol fuel cell applications: a review, Nanoscale Res. Lett. 13 (2018) 410, https://doi.org/10.1186/s11671-018-2799-4.
[275] H. Huang, S. Yang, R. Vajtai, X. Wang, P.M. Ajayan, Pt-decorated 3D architectures built from graphene and graphitic carbon nitride nanosheets as efficient methanol oxidation catalysts, Adv. Mater. 26 (2014) 5160–5165, https://doi.org/10.1002/adma.201401877.
[276] K. Kakaei, M. Zhiani, A new method for manufacturing graphene and electrochemical characteristic of graphene-supported Pt nanoparticles in methanol oxidation, J. Power Sources 225 (2013) 356–363, https://doi.org/10.1016/j.jpowsour.2012.10.003.
[277] H. Huang, X. Wang, Pd nanoparticles supported on low-defect graphene sheets: for use as high-performance electrocatalysts for formic acid and methanol oxidation, J. Mater. Chem. 22 (2012) 22533, https://doi.org/10.1039/c2jm33727d.
[278] Y. Hu, H. Zhang, P. Wu, H. Zhang, B. Zhou, C. Cai, Bimetallic Pt–Au nanocatalysts electrochemically deposited on graphene and their electrocatalytic characteristics towards oxygen reduction and methanol oxidation, Phys. Chem. Chem. Phys. 13 (2011) 4083, https://doi.org/10.1039/c0cp01998d.
[279] L. Dong, R.R.S. Gari, Z. Li, M.M. Craig, S. Hou, Graphene-supported platinum and platinum–ruthenium nanoparticles with high electrocatalytic activity for methanol and ethanol oxidation, Carbon N.Y. 48 (2010) 781–787, https://doi.org/10.1016/j.carbon.2009.10.027.
[280] S. Guo, S. Dong, E. Wang, Three-dimensional Pt-on-Pd bimetallic nanodendrites supported on graphene nanosheet: facile synthesis and used as an advanced nanoelectrocatalyst for methanol oxidation, ACS Nano 4 (2010) 547–555, https://doi.org/10.1021/nn9014483.
[281] R. Ojani, J.-B. Raoof, M. Goli, R. Valiollahi, Pt–Co nanostructures electrodeposited on graphene nanosheets for methanol electrooxidation, J. Power Sources 264 (2014) 76–82, https://doi.org/10.1016/j.jpowsour.2014.03.147.
[282] Y. Hu, P. Wu, Y. Yin, H. Zhang, C. Cai, Effects of structure, composition, and carbon support properties on the electrocatalytic activity of Pt-Ni-graphene nanocatalysts for the methanol oxidation, Appl. Catal. B Environ. 111–112 (2012) 208–217, https://doi.org/10.1016/j.apcatb.2011.10.001.
[283] L. Li, M. Chen, G. Huang, N. Yang, L. Zhang, H. Wang, Y. Liu, W. Wang, J. Gao, A green method to prepare Pd–Ag nanoparticles supported on reduced graphene oxide and their electrochemical catalysis of methanol and ethanol oxidation, J. Power Sources 263 (2014) 13–21, https://doi.org/10.1016/j.jpowsour.2014.04.021.
[284] Y. Lu, Y. Jiang, W. Chen, Graphene nanosheet-tailored PtPd concave nanocubes with enhanced electrocatalytic activity and durability for methanol oxidation, Nanoscale 6 (2014) 3309–3315, https://doi.org/10.1039/C3NR06186H.
[285] B. Xiong, Y. Zhou, Y. Zhao, J. Wang, X. Chen, R. O'Hayre, Z. Shao, The use of nitrogen-doped graphene supporting Pt nanoparticles as a catalyst for methanol electrocatalytic oxidation, Carbon N.Y. 52 (2013) 181–192, https://doi.org/10.1016/j.carbon.2012.09.019.
[286] S. Sharma, A. Ganguly, P. Papakonstantinou, X. Miao, M. Li, J.L. Hutchison, M. Delichatsios, S. Ukleja, Rapid microwave synthesis of CO tolerant reduced graphene oxide-supported platinum electrocatalysts for oxidation of methanol, J. Phys. Chem. C 114 (2010) 19459–19466, https://doi.org/10.1021/jp107872z.
[287] C. Berghian-Grosan, T. Radu, A.R. Biris, M. Dan, C. Voica, F. Watanabe, A.S. Biris, A. Vulcu, Platinum nanoparticles coated by graphene layers: a low-metal loading catalyst for methanol oxidation in alkaline media, J. Energy Chem. 40 (2020) 81–88, https://doi.org/10.1016/j.jechem.2019.03.003.

[288] W. Huang, H. Wang, J. Zhou, J. Wang, P.N. Duchesne, D. Muir, P. Zhang, N. Han, F. Zhao, M. Zeng, J. Zhong, C. Jin, Y. Li, S.-T. Lee, H. Dai, Highly active and durable methanol oxidation electrocatalyst based on the synergy of platinum–nickel hydroxide–graphene, Nat. Commun. 6 (2015) 10035, https://doi.org/10.1038/ncomms10035.
[289] N. Atar, T. Eren, M.L. Yola, H. Karimi-Maleh, B. Demirdögen, Magnetic iron oxide and iron oxide@gold nanoparticle anchored nitrogen and sulfur-functionalized reduced graphene oxide electrocatalyst for methanol oxidation, RSC Adv. 5 (2015) 26402–26409, https://doi.org/10.1039/C5RA03735B.
[290] A.K. Das, R.K. Layek, N.H. Kim, D. Jung, J.H. Lee, Reduced graphene oxide (RGO)-supported $NiCo_2O_4$ nanoparticles: an electrocatalyst for methanol oxidation, Nanoscale 6 (2014) 10657, https://doi.org/10.1039/C4NR02370F.
[291] Y. Tong, P. Chen, T. Zhou, K. Xu, W. Chu, C. Wu, Y. Xie, A bifunctional hybrid electrocatalyst for oxygen reduction and evolution: cobalt oxide nanoparticles strongly coupled to B,N-decorated graphene, Angew. Chem. Int. Ed. 56 (2017) 7121–7125, https://doi.org/10.1002/anie.201702430.
[292] J. Sun, H. Ma, H. Jiang, L. Dang, Q. Lu, F. Gao, General synthesis of binary PtM and ternary PtM_1M_2 alloy nanoparticles on graphene as advanced electrocatalysts for methanol oxidation, J. Mater. Chem. A 3 (2015) 15882–15888, https://doi.org/10.1039/C5TA01613D.
[293] A. Kongkanand, M.F. Mathias, The priority and challenge of high-power performance of low-platinum proton-exchange membrane fuel cells, J. Phys. Chem. Lett. 7 (2016) 1127–1137, https://doi.org/10.1021/acs.jpclett.6b00216.
[294] Z. Chen, D. Higgins, A. Yu, L. Zhang, J. Zhang, A review on non-precious metal electrocatalysts for PEM fuel cells, Energy Environ. Sci. 4 (2011) 3167, https://doi.org/10.1039/c0ee00558d.
[295] D.K. Perivoliotis, N. Tagmatarchis, Recent advancements in metal-based hybrid electrocatalysts supported on graphene and related 2D materials for the oxygen reduction reaction, Carbon N.Y. 118 (2017) 493–510, https://doi.org/10.1016/j.carbon.2017.03.073.
[296] Y. Kameya, T. Hayashi, M. Motosuke, Stability of platinum nanoparticles supported on surface-treated carbon black, Appl. Catal. B Environ. 189 (2016) 219–225, https://doi.org/10.1016/j.apcatb.2016.02.049.
[297] P. Hu, K. Liu, C.P. Deming, S. Chen, Multifunctional graphene-based nanostructures for efficient electrocatalytic reduction of oxygen, J. Chem. Technol. Biotechnol. 90 (2015) 2132–2151, https://doi.org/10.1002/jctb.4797.
[298] S. Sharma, B.G. Pollet, Support materials for PEMFC and DMFC electrocatalysts—a review, J. Power Sources 208 (2012) 96–119, https://doi.org/10.1016/j.jpowsour.2012.02.011.
[299] L. Castanheira, W.O. Silva, F.H.B. Lima, A. Crisci, L. Dubau, F. Maillard, Carbon corrosion in proton-exchange membrane fuel cells: effect of the carbon structure, the degradation protocol, and the gas atmosphere, ACS Catal. (2015) 2184–2194, https://doi.org/10.1021/cs501973j.
[300] Y. Li, Y. Li, E. Zhu, T. McLouth, C.-Y. Chiu, X. Huang, Y. Huang, Stabilization of high-performance oxygen reduction reaction Pt electrocatalyst supported on reduced graphene oxide/carbon black composite, J. Am. Chem. Soc. 134 (2012) 12326–12329, https://doi.org/10.1021/ja3031449.
[301] Y. Zhang, H. Liu, H. Wu, Z. Sun, L. Qian, Facile synthesis of Pt nanoparticles loaded porous graphene towards oxygen reduction reaction, Mater. Des. 96 (2016) 323–328, https://doi.org/10.1016/j.matdes.2016.02.030.
[302] C. Wang, L. Ma, L. Liao, S. Bai, R. Long, M. Zuo, Y. Xiong, A unique platinum-graphene hybrid structure for high activity and durability in oxygen reduction reaction, Sci. Rep. 3 (2013) 2580, https://doi.org/10.1038/srep02580.
[303] S. Bai, C. Wang, W. Jiang, N. Du, J. Li, J. Du, R. Long, Z. Li, Y. Xiong, Etching approach to hybrid structures of PtPd nanocages and graphene for efficient oxygen reduction reaction catalysts, Nano Res. 8 (2015) 2789–2799, https://doi.org/10.1007/s12274-015-0770-6.
[304] S.-S. Li, J.-J. Lv, L.-N. Teng, A.-J. Wang, J.-R. Chen, J.-J. Feng, Facile synthesis of PdPt@Pt nanorings supported on reduced graphene oxide with enhanced electrocatalytic properties, ACS Appl. Mater. Interfaces 6 (2014) 10549–10555, https://doi.org/10.1021/am502148z.
[305] C.V. Rao, A.L.M. Reddy, Y. Ishikawa, P.M. Ajayan, Synthesis and electrocatalytic oxygen reduction activity of graphene-supported Pt_3Co and Pt_3Cr alloy nanoparticles, Carbon N.Y. 49 (2011) 931–936, https://doi.org/10.1016/j.carbon.2010.10.056.
[306] V.R. Stamenkovic, B.S. Mun, M. Arenz, K.J.J. Mayrhofer, C.A. Lucas, G. Wang, P.N. Ross, N.M. Markovic, Trends in electrocatalysis on extended and nanoscale Pt-bimetallic alloy surfaces, Nat. Mater. 6 (2007) 241–247, https://doi.org/10.1038/nmat1840.
[307] D.S. Choi, A.W. Robertson, J.H. Warner, S.O. Kim, H. Kim, Low-temperature chemical vapor deposition synthesis of Pt-Co alloyed nanoparticles with enhanced oxygen reduction reaction catalysis, Adv. Mater. 28 (2016) 7115–7122, https://doi.org/10.1002/adma.201600469.
[308] B. Patrick, H.C. Ham, Y. Shao-Horn, L.F. Allard, G.S. Hwang, P.J. Ferreira, Atomic structure and composition of "Pt_3Co" nanocatalysts in fuel cells: an aberration-corrected STEM HAADF study, Chem. Mater. 25 (2013) 530–535, https://doi.org/10.1021/cm3029164.
[309] S. Guo, S. Sun, FePt nanoparticles assembled on graphene as enhanced catalyst for oxygen reduction reaction, J. Am. Chem. Soc. 134 (2012) 2492–2495, https://doi.org/10.1021/ja2104334.
[310] Y. Zheng, S. Zhao, S. Liu, H. Yin, Y.-Y. Chen, J. Bao, M. Han, Z. Dai, Component-controlled synthesis and assembly of Cu–Pd nanocrystals on graphene for oxygen reduction reaction, ACS Appl. Mater. Interfaces 7 (2015) 5347–5357, https://doi.org/10.1021/acsami.5b01541.
[311] J.-J. Lv, S.-S. Li, A.-J. Wang, L.-P. Mei, J.-J. Feng, J.-R. Chen, Z. Chen, One-pot synthesis of monodisperse palladium–copper nanocrystals supported on reduced graphene oxide nanosheets with improved catalytic activity and methanol tolerance for oxygen reduction reaction, J. Power Sources 269 (2014) 104–110, https://doi.org/10.1016/j.jpowsour.2014.07.036.
[312] J.-J. Lv, S.-S. Li, A.-J. Wang, L.-P. Mei, J.-R. Chen, J.-J. Feng, Monodisperse Au-Pd bimetallic alloyed nanoparticles supported on reduced graphene oxide with enhanced electrocatalytic activity towards oxygen reduction reaction, Electrochim. Acta 136 (2014) 521–528, https://doi.org/10.1016/j.electacta.2014.05.138.
[313] W. Suh, P. Ganesan, B. Son, H. Kim, S. Shanmugam, Graphene supported Pt–Ni nanoparticles for oxygen reduction reaction in acidic electrolyte, Int. J. Hydrogen Energy 41 (2016) 12983–12994, https://doi.org/10.1016/j.ijhydene.2016.04.090.
[314] D.K. Perivoliotis, Y. Sato, K. Suenaga, N. Tagmatarchis, Core–shell Pd@M (M=Ni, Cu, Co) nanoparticles/graphene ensembles with high mass electrocatalytic activity toward the oxygen reduction reaction, Chem. – A Eur. J. 25 (2019) 11105–11113, https://doi.org/10.1002/chem.201901588.
[315] X.-Y. Yan, X.-L. Tong, Y.-F. Zhang, X.-D. Han, Y.-Y. Wang, G.-Q. Jin, Y. Qin, X.-Y. Guo, Cuprous oxide nanoparticles dispersed on reduced graphene oxide as an efficient electrocatalyst for oxygen reduction reaction, Chem. Commun. 48 (2012) 1892, https://doi.org/10.1039/c2cc17537a.
[316] Y. Li, Y. Zhou, C. Zhu, Y.H. Hu, S. Gao, Q. Liu, X. Cheng, L. Zhang, J. Yang, Y. Lin, Porous graphene doped with Fe/N/S and incorporating Fe_3O_4 nanoparticles for efficient oxygen reduction, Catal. Sci. Technol. 8 (2018) 5325–5333, https://doi.org/10.1039/C8CY01328D.
[317] M. Chen, J. Liu, W. Zhou, J. Lin, Z. Shen, Nitrogen-doped graphene-supported transition-metals carbide electrocatalysts for oxygen reduction reaction, Sci. Rep. 5 (2015) 10389, https://doi.org/10.1038/srep10389.
[318] H. Wang, Y. Liang, Y. Li, H. Dai, Co1−xS-Graphene hybrid: a high-performance metal chalcogenide electrocatalyst for oxygen reduction, Angew. Chem. Int. Ed. 50 (2011) 10969–10972, https://doi.org/10.1002/anie.201104004.
[319] X. Wen, X. Yang, M. Li, L. Bai, J. Guan, Co/CoOx nanoparticles inlaid onto nitrogen-doped carbon-graphene as a trifunctional electrocatalyst, Electrochim. Acta 296 (2019) 830–841, https://doi.org/10.1016/j.electacta.2018.11.129.
[320] S. Guo, S. Zhang, L. Wu, S. Sun, Co/CoO nanoparticles assembled on graphene for electrochemical reduction of oxygen, Angew. Chem. Int. Ed. 51 (2012) 11770–11773, https://doi.org/10.1002/anie.201206152.
[321] Y. Niu, X. Huang, L. Zhao, W. Hu, C.M. Li, One-Pot synthesis of $Co/CoFe_2O_4$ nanoparticles supported on N-doped graphene for efficient bifunctional oxygen electrocatalysis, ACS Sustain. Chem. Eng. 6 (2018) 3556–3564, https://doi.org/10.1021/acssuschemeng.7b03888.
[322] Y. Liang, H. Wang, J. Zhou, Y. Li, J. Wang, T. Regier, H. Dai, Covalent hybrid of spinel manganese–cobalt oxide and graphene as advanced oxygen reduction electrocatalysts, J. Am. Chem. Soc. 134 (2012) 3517–3523, https://doi.org/10.1021/ja210924t.
[323] T. Zhang, Z. Li, L. Wang, Z. Zhang, S. Wang, Spinel $CoFe_2O_4$ supported by three dimensional graphene as high-performance bi-functional electrocatalysts for oxygen reduction and evolution reaction, Int. J. Hydrogen Energy 44 (2019) 1610–1619, https://doi.org/10.1016/j.ijhydene.2018.11.120.
[324] H. Ghanbarlou, S. Rowshanzamir, B. Kazeminasab, M.J. Parnian, Non-precious metal nanoparticles supported on nitrogen-doped graphene as a promising catalyst for oxygen reduction reaction: synthesis, characterization and electrocatalytic performance, J. Power Sources 273 (2015) 981–989, https://doi.org/10.1016/j.jpowsour.2014.10.001.
[325] Y. Liang, Y. Li, H. Wang, J. Zhou, J. Wang, T. Regier, H. Dai, Co_3O_4 nanocrystals on graphene as a synergistic catalyst for oxygen reduction reaction, Nat. Mater. 10 (2011) 780–786, https://doi.org/10.1038/nmat3087.
[326] S.K. Singh, K. Takeyasu, J. Nakamura, Active sites and mechanism of oxygen reduction reaction electrocatalysis on nitrogen-doped carbon materials, Adv. Mater. 31 (2019) 1804297, https://doi.org/10.1002/adma.201804297.
[327] D. Guo, R. Shibuya, C. Akiba, S. Saji, T. Kondo, J. Nakamura, Active sites of nitrogen-doped carbon materials for oxygen reduction reaction clarified using model catalysts, Science (80-.) 351 (2016) 361–365, https://doi.org/10.1126/science.aad0832.
[328] Y. Lu, Y. Jiang, X. Gao, X. Wang, W. Chen, Strongly coupled Pd nanotetrahedron/tungsten oxide nanosheet hybrids with enhanced catalytic activity and stability as oxygen reduction electrocatalysts, J. Am. Chem. Soc. 136 (2014) 11687–11697, https://doi.org/10.1021/ja5041094.
[329] Y. Liu, S. Shrestha, W.E. Mustain, Synthesis of nanosize tungsten oxide and its evaluation as an electrocatalyst support for oxygen reduction in acid media, ACS Catal. 2 (2012) 456–463, https://doi.org/10.1021/cs200657w.
[330] Y. Yu, J. Zhou, Z. Sun, Novel 2D transition-metal carbides: ultrahigh performance electrocatalysts for overall water splitting and oxygen reduction, Adv. Funct. Mater. (2020) 2000570, https://doi.org/10.1002/adfm.202000570.
[331] L.-X. Zuo, L.-P. Jiang, J.-J. Zhu, A facile sonochemical route for the synthesis of MoS_2/Pd composites for highly efficient oxygen reduction reaction, Ultrason. Sonochem. 35 (2017) 681–688, https://doi.org/10.1016/j.ultsonch.2016.02.006.

[332] S. Ramakrishnan, M. Karuppannan, M. Vinothkannan, K. Ramachandran, O.J. Kwon, D.J. Yoo, Ultrafine Pt nanoparticles stabilized by MoS 2/N-doped reduced graphene oxide as a durable electrocatalyst for alcohol oxidation and oxygen reduction reactions, ACS Appl. Mater. Interfaces 11 (2019) 12504–12515, https://doi.org/10.1021/acsami.9b00192.
[333] E. Lee, Y.-U. Kwon, Epitaxial growth of Pd nanoparticles on molybdenum disulfide by sonochemistry and its effects on electrocatalysis, RSC Adv. 6 (2016) 47468–47473, https://doi.org/10.1039/C6RA07064G.
[334] Z. Wen, J. Liu, J. Li, Core/shell Pt/C nanoparticles embedded in mesoporous carbon as a methanol-tolerant cathode catalyst in direct methanol fuel cells, Adv. Mater. 20 (2008) 743–747, https://doi.org/10.1002/adma.200701578.
[335] W. Wu, Z. Zhang, Z. Lei, X. Wang, Y. Tan, N. Cheng, X. Sun, Encapsulating Pt nanoparticles inside a derived two-dimensional metal–organic frameworks for the enhancement of catalytic activity, ACS Appl. Mater. Interfaces 12 (2020) 10359–10368, https://doi.org/10.1021/acsami.9b20781.
[336] M. Sun, J. Dong, Y. Lv, S. Zhao, C. Meng, Y. Song, G. Wang, J. Li, Q. Fu, Z. Tian, X. Bao, Pt@h-BN core–shell fuel cell electrocatalysts with electrocatalysis confined under outer shells, Nano Res. 11 (2018) 3490–3498, https://doi.org/10.1007/s12274-018-2029-5.
[337] L. Chen, Y. Peng, J.-E. Lu, N. Wang, P. Hu, B. Lu, S. Chen, Platinum nanoparticles encapsulated in nitrogen-doped graphene quantum dots: enhanced electrocatalytic reduction of oxygen by nitrogen dopants, Int. J. Hydrogen Energy 42 (2017) 29192–29200, https://doi.org/10.1016/j.ijhydene.2017.10.078.
[338] P.Q. Phan, R. Naraprawatphong, P. Pornaroontham, J. Park, C. Chokradjaroen, N. Saito, N-Doped few-layer graphene encapsulated Pt-based bimetallic nanoparticles via solution plasma as an efficient oxygen catalyst for the oxygen reduction reaction, Mater. Adv. 2 (2021) 322–335, https://doi.org/10.1039/D0MA00718H.
[339] D. Wu, C. Zhu, Y. Shi, H. Jing, J. Hu, X. Song, D. Si, S. Liang, C. Hao, Biomass-derived multilayer-graphene-encapsulated cobalt nanoparticles as efficient electrocatalyst for versatile renewable energy applications, ACS Sustain. Chem. Eng. 7 (2019) 1137–1145, https://doi.org/10.1021/acssuschemeng.8b04797.
[340] H.-J. Niu, L. Zhang, J.-J. Feng, Q.-L. Zhang, H. Huang, A.-J. Wang, Graphene-encapsulated cobalt nanoparticles embedded in porous nitrogen-doped graphitic carbon nanosheets as efficient electrocatalysts for oxygen reduction reaction, J. Colloid Interface Sci. 552 (2019) 744–751, https://doi.org/10.1016/j.jcis.2019.05.099.
[341] E. Hu, X.-Y. Yu, F. Chen, Y. Wu, Y. Hu, X.W.D. Lou, Graphene layers-wrapped Fe/Fe_5C_2 nanoparticles supported on N-doped graphene nanosheets for highly efficient oxygen reduction, Adv. Energy Mater. 8 (2018) 1702476, https://doi.org/10.1002/aenm.201702476.
[342] J. Zhao, N. Fu, R. Liu, Graphite-wrapped Fe core–shell nanoparticles anchored on graphene as pH-universal electrocatalyst for oxygen reduction reaction, ACS Appl. Mater. Interfaces 10 (2018) 28509–28516, https://doi.org/10.1021/acsami.8b06153.
[343] N.D. Chuong, T.D. Thanh, N.H. Kim, J.H. Lee, Hierarchical heterostructures of ultrasmall Fe_2O_3-encapsulated MoS_2/N-graphene as an effective catalyst for oxygen reduction reaction, ACS Appl. Mater. Interfaces 10 (2018) 24523–24532, https://doi.org/10.1021/acsami.8b06485.
[344] J. Gautam, T.D. Thanh, K. Maiti, N.H. Kim, J.H. Lee, Highly efficient electrocatalyst of N-doped graphene-encapsulated cobalt-iron carbides towards oxygen reduction reaction, Carbon N.Y. 137 (2018) 358–367, https://doi.org/10.1016/j.carbon.2018.05.042.
[345] J. Deng, P. Ren, D. Deng, X. Bao, Enhanced electron penetration through an ultrathin graphene layer for highly efficient catalysis of the hydrogen evolution reaction, Angew. Chem. Int. Ed. 54 (2015) 2100–2104, https://doi.org/10.1002/anie.201409524.
[346] M. Huang, S. Liu, S. Gong, P. Xu, K. Yang, S. Chen, C. Wang, Q. Chen, Silver nanoparticles encapsulated in an N-doped porous carbon matrix as high-active catalysts toward oxygen reduction reaction via electron transfer to outer graphene shells, ACS Sustain. Chem. Eng. 7 (2019) 16511–16519, https://doi.org/10.1021/acssuschemeng.9b03736.
[347] M. Sharma, J.-H. Jang, D.Y. Shin, J.A. Kwon, D.-H. Lim, D. Choi, H. Sung, J. Jang, S.-Y. Lee, K.Y. Lee, H.-Y. Park, N. Jung, S.J. Yoo, Work function-tailored graphene via transition metal encapsulation as a highly active and durable catalyst for the oxygen reduction reaction, Energy Environ. Sci. 12 (2019) 2200–2211, https://doi.org/10.1039/C9EE00381A.
[348] T.D. Thanh, N.D. Chuong, H. Van Hien, N.H. Kim, J.H. Lee, CuAg@Ag core–shell nanostructure encapsulated by N-doped graphene as a high-performance catalyst for oxygen reduction reaction, ACS Appl. Mater. Interfaces 10 (2018) 4672–4681, https://doi.org/10.1021/acsami.7b16294.
[349] Y. Jiao, Y. Zheng, M. Jaroniec, S.Z. Qiao, Origin of the electrocatalytic oxygen reduction activity of graphene-based catalysts: a roadmap to achieve the best performance, J. Am. Chem. Soc. 136 (2014) 4394–4403, https://doi.org/10.1021/ja500432h.
[350] Y. Shao, Z. Jiang, Q. Zhang, J. Guan, Progress in nonmetal-doped graphene electrocatalysts for the oxygen reduction reaction, ChemSusChem 12 (2019) 2133–2146, https://doi.org/10.1002/cssc.201900060.
[351] L. Qu, Y. Liu, J.B. Baek, L. Dai, Nitrogen-doped graphene as efficient metal-free electrocatalyst for oxygen reduction in fuel cells, ACS Nano 4 (2010) 1321–1326, https://doi.org/10.1021/nn901850u.
[352] Y. Bian, H. Wang, J. Hu, B. Liu, D. Liu, L. Dai, Nitrogen-rich holey graphene for efficient oxygen reduction reaction, Carbon N.Y. 162 (2020) 66–73, https://doi.org/10.1016/j.carbon.2020.01.110.
[353] X. Gong, S. Liu, C. Ouyang, P. Strasser, R. Yang, Nitrogen- and phosphorus-doped biocarbon with enhanced electrocatalytic activity for oxygen reduction, ACS Catal. 5 (2015) 920–927, https://doi.org/10.1021/cs501632y.
[354] Y.-C. Lin, P.-Y. Teng, C.-H. Yeh, M. Koshino, P.-W. Chiu, K. Suenaga, Structural and chemical dynamics of pyridinic-nitrogen defects in graphene, Nano Lett. 15 (2015) 7408–7413, https://doi.org/10.1021/acs.nanolett.5b02831.
[355] L. Tao, Q. Wang, S. Dou, Z. Ma, J. Huo, S. Wang, L. Dai, Edge-rich and dopant-free graphene as a highly efficient metal-free electrocatalyst for the oxygen reduction reaction, Chem. Commun. 52 (2016) 2764–2767, https://doi.org/10.1039/C5CC09173J.
[356] J.S. Kim, J.H. Warner, A.W. Robertson, A.I. Kirkland, formation of Klein edge doublets from graphene monolayers, ACS Nano 9 (2015), https://doi.org/10.1021/acsnano.5b02730.
[357] K. He, G.-D. Lee, A.W. Robertson, E. Yoon, J.H. Warner, Hydrogen-free graphene edges, Nat. Commun. 5 (2014) 3040, https://doi.org/10.1038/ncomms4040.
[358] Y. Liu, X. Quan, X. Fan, H. Wang, S. Chen, High-yield electrosynthesis of hydrogen peroxide from oxygen reduction by hierarchically porous carbon, Angew. Chem. 127 (2015) 6941–6945, https://doi.org/10.1002/ange.201502396.
[359] A. Shen, Y. Zou, Q. Wang, R.A.W. Dryfe, X. Huang, S. Dou, L. Dai, S. Wang, Oxygen reduction reaction in a droplet on graphite: direct evidence that the edge is more active than the basal plane, Angew. Chem. Int. Ed. 53 (2014) 10804–10808, https://doi.org/10.1002/anie.201406695.
[360] H.W. Kim, H. Park, J.S. Roh, J.E. Shin, T.H. Lee, L. Zhang, Y.H. Cho, H.W. Yoon, V.J. Bukas, J. Guo, H.B. Park, T.H. Han, B.D. McCloskey, Carbon defect characterization of nitrogen-doped reduced graphene oxide electrocatalysts for the two-electron oxygen reduction reaction, Chem. Mater. 31 (2019) 3967–3973, https://doi.org/10.1021/acs.chemmater.9b00210.
[361] R.J. Bowling, R.T. Packard, R.L. McCreery, Activation of highly ordered pyrolytic graphite for heterogeneous electron transfer: relationship between electrochemical performance and carbon microstructure, J. Am. Chem. Soc. 111 (1989) 1217–1223, https://doi.org/10.1021/ja00186a008.
[362] Z. Lu, G. Chen, S. Siahrostami, Z. Chen, K. Liu, J. Xie, L. Liao, T. Wu, D. Lin, Y. Liu, T.F. Jaramillo, J.K. Nørskov, Y. Cui, High-efficiency oxygen reduction to hydrogen peroxide catalysed by oxidized carbon materials, Nat. Catal. 1 (2018) 156–162, https://doi.org/10.1038/s41929-017-0017-x.
[363] H.W. Kim, M.B. Ross, N. Kornienko, L. Zhang, J. Guo, P. Yang, B.D. McCloskey, Efficient hydrogen peroxide generation using reduced graphene oxide-based oxygen reduction electrocatalysts, Nat. Catal. 1 (2018) 282–290, https://doi.org/10.1038/s41929-018-0044-2.
[364] G. Han, Y. Zheng, X. Zhang, Z. Wang, Y. Gong, C. Du, M.N. Banis, Y.-M. Yiu, T.-K. Sham, L. Gu, Y. Sun, Y. Wang, J. Wang, Y. Gao, G. Yin, X. Sun, High loading single-atom Cu dispersed on graphene for efficient oxygen reduction reaction, Nano Energy 66 (2019) 104088, https://doi.org/10.1016/j.nanoen.2019.104088.
[365] H. Wu, H. Li, X. Zhao, Q. Liu, J. Wang, J. Xiao, S. Xie, R. Si, F. Yang, S. Miao, X. Guo, G. Wang, X. Bao, Highly doped and exposed Cu(<scp>i</scp>)–N active sites within graphene towards efficient oxygen reduction for zinc–air batteries, Energy Environ. Sci. 9 (2016) 3736–3745, https://doi.org/10.1039/C6EE01867J.
[366] A. Muthukrishnan, Y. Nabae, T. Okajima, T. Ohsaka, Kinetic approach to investigate the mechanistic pathways of oxygen reduction reaction on Fe-containing N-doped carbon catalysts, ACS Catal. 5 (2015) 5194–5202, https://doi.org/10.1021/acscatal.5b00397.
[367] X. Chen, L. Yu, S. Wang, D. Deng, X. Bao, Highly active and stable single iron site confined in graphene nanosheets for oxygen reduction reaction, Nano Energy 32 (2017) 353–358, https://doi.org/10.1016/j.nanoen.2016.12.056.
[368] Y. Han, Y.-G. Wang, W. Chen, R. Xu, L. Zheng, J. Zhang, J. Luo, R.-A. Shen, Y. Zhu, W.-C. Cheong, C. Chen, Q. Peng, D. Wang, Y. Li, Hollow N-doped carbon spheres with isolated cobalt single atomic sites: superior electrocatalysts for oxygen reduction, J. Am. Chem. Soc. 139 (2017) 17269–17272, https://doi.org/10.1021/jacs.7b10194.
[369] C. Zhang, J. Sha, H. Fei, M. Liu, S. Yazdi, J. Zhang, Q. Zhong, X. Zou, N. Zhao, H. Yu, Z. Jiang, E. Ringe, B.I. Yakobson, J. Dong, D. Chen, J.M. Tour, Single-atomic ruthenium catalytic sites on nitrogen-doped graphene for oxygen reduction reaction in acidic medium, ACS Nano 11 (2017) 6930–6941, https://doi.org/10.1021/acsnano.7b02148.
[370] H.R. Byon, J. Suntivich, Y. Shao-Horn, Graphene-based non-noble-metal catalysts for oxygen reduction reaction in acid, Chem. Mater. 23 (2011) 3421–3428, https://doi.org/10.1021/cm2000649.
[371] L. Yang, D. Cheng, H. Xu, X. Zeng, X. Wan, J. Shui, Z. Xiang, D. Cao, Unveiling the high-activity origin of single-atom iron catalysts for oxygen reduction reaction, Proc. Natl. Acad. Sci. U.S.A. 115 (2018) 6626–6631, https://doi.org/10.1073/pnas.1800771115.
[372] C. Du, X. Wang, W. Chen, S. Feng, J. Wen, Y.A. Wu, CO_2 transformation to multicarbon products by photocatalysis and electrocatalysis, Mater. Today Adv. 6 (2020) 100071, https://doi.org/10.1016/j.mtadv.2020.100071.
[373] E. Karamian, S. Sharifnia, On the general mechanism of photocatalytic reduction of CO_2, J. CO2 Util. 16 (2016) 194–203, https://doi.org/10.1016/j.jcou.2016.07.004.

[374] S. Sorcar, S. Yoriya, H. Lee, C.A. Grimes, S.P. Feng, A review of recent progress in gas phase CO_2 reduction and suggestions on future advancement, Mater. Today Chem. 16 (2020) 100264, https://doi.org/10.1016/j.mtchem.2020.100264.
[375] J. Albero, Y. Peng, H. García, Photocatalytic CO_2 reduction to C2+ products, ACS Catal. 10 (2020) 5734–5749, https://doi.org/10.1021/acscatal.0c00478.
[376] S. Tan, Y. Zhao, J. Zhao, Z. Wang, C. Ma, A. Zhao, B. Wang, Y. Luo, J. Yang, J. Hou, CO_2 dissociation activated through electron attachment on the reduced rutile TiO_2 (110)-1 × 1 surface, Phys. Rev. B 84 (2011) 155418, https://doi.org/10.1103/PhysRevB.84.155418.
[377] S.N. Habisreutinger, L. Schmidt-Mende, J.K. Stolarczyk, Photocatalytic reduction of CO_2 on TiO_2 and other semiconductors, Angew. Chem. Int. Ed. 52 (2013) 7372–7408, https://doi.org/10.1002/anie.201207199.
[378] Y.A. Wu, I. McNulty, C. Liu, K.C. Lau, Q. Liu, A.P. Paulikas, C.-J. Sun, Z. Cai, J.R. Guest, Y. Ren, V. Stamenkovic, L.A. Curtiss, Y. Liu, T. Rajh, Facet-dependent active sites of a single Cu_2O particle photocatalyst for CO_2 reduction to methanol, Nat. Energy 4 (2019) 957–968, https://doi.org/10.1038/s41560-019-0490-3.
[379] J. Low, B. Cheng, J. Yu, Surface modification and enhanced photocatalytic CO_2 reduction performance of TiO_2: a review, Appl. Surf. Sci. 392 (2017) 658–686, https://doi.org/10.1016/j.apsusc.2016.09.093.
[380] S. Ali, A. Razzaq, S.-I. In, Development of graphene based photocatalysts for CO_2 reduction to C_1 chemicals: a brief overview, Catal. Today 335 (2019) 39–54, https://doi.org/10.1016/j.cattod.2018.12.003.
[381] S. Ye, R. Wang, M.-Z. Wu, Y.-P. Yuan, A review on g-C_3N_4 for photocatalytic water splitting and CO_2 reduction, Appl. Surf. Sci. 358 (2015) 15–27, https://doi.org/10.1016/j.apsusc.2015.08.173.
[382] J. Low, J. Yu, W. Ho, Graphene-based photocatalysts for CO_2 reduction to solar fuel, J. Phys. Chem. Lett. 6 (2015) 4244–4251, https://doi.org/10.1021/acs.jpclett.5b01610.
[383] I. Shown, H.-C. Hsu, Y.-C. Chang, C.-H. Lin, P.K. Roy, A. Ganguly, C.-H. Wang, J.-K. Chang, C.-I. Wu, L.-C. Chen, K.-H. Chen, Highly efficient visible light photocatalytic reduction of CO_2 to hydrocarbon fuels by Cu-nanoparticle decorated graphene oxide, Nano Lett. 14 (2014) 6097–6103, https://doi.org/10.1021/nl503609v.
[384] W. Ju, A. Bagger, G.-P. Hao, A.S. Varela, I. Sinev, V. Bon, B. Roldan Cuenya, S. Kaskel, J. Rossmeisl, P. Strasser, Understanding activity and selectivity of metal-nitrogen-doped carbon catalysts for electrochemical reduction of CO_2, Nat. Commun. 8 (2017) 944, https://doi.org/10.1038/s41467-017-01035-z.
[385] M.-Q. Yang, N. Zhang, M. Pagliaro, Y.-J. Xu, Artificial photosynthesis over graphene–semiconductor composites. Are we getting better? Chem. Soc. Rev. 43 (2014) 8240–8254, https://doi.org/10.1039/C4CS00213J.
[386] Y.T. Liang, B.K. Vijayan, O. Lyandres, K.A. Gray, M.C. Hersam, Effect of dimensionality on the photocatalytic behavior of carbon–titania nanosheet composites: charge transfer at nanomaterial interfaces, J. Phys. Chem. Lett. 3 (2012) 1760–1765, https://doi.org/10.1021/jz300491s.
[387] X.-J. Lv, W.-F. Fu, C.-Y. Hu, Y. Chen, W.-B. Zhou, Photocatalytic reduction of CO_2 with H_2O over a graphene-modified NiOx–Ta_2O_5 composite photocatalyst: coupling yields of methanol and hydrogen, RSC Adv. 3 (2013) 1753, https://doi.org/10.1039/c2ra21283h.
[388] M.-Q. Yang, Y.-J. Xu, Photocatalytic conversion of CO_2 over graphene-based composites: current status and future perspective, Nanoscale Horiz. 1 (2016) 185–200, https://doi.org/10.1039/C5NH00113G.
[389] J. Yu, J. Jin, B. Cheng, M. Jaroniec, A noble metal-free reduced graphene oxide–CdS nanorod composite for the enhanced visible-light photocatalytic reduction of CO_2 to solar fuel, J. Mater. Chem. A 2 (2014) 3407, https://doi.org/10.1039/c3ta14493c.
[390] W.-J. Ong, L.-L. Tan, S.-P. Chai, S.-T. Yong, A.R. Mohamed, Self-assembly of nitrogen-doped TiO_2 with exposed {001} facets on a graphene scaffold as photo-active hybrid nanostructures for reduction of carbon dioxide to methane, Nano Res. 7 (2014) 1528–1547, https://doi.org/10.1007/s12274-014-0514-z.
[391] W. Tu, Y. Zhou, Q. Liu, S. Yan, S. Bao, X. Wang, M. Xiao, Z. Zou, An in situ simultaneous reduction-hydrolysis technique for fabrication of TiO_2 -graphene 2D sandwich-like hybrid nanosheets: graphene-promoted selectivity of photocatalytic-driven hydrogenation and coupling of CO_2 into methane and ethane, Adv. Funct. Mater. 23 (2013) 1743–1749, https://doi.org/10.1002/adfm.201202349.
[392] P. Li, Y. Zhou, H. Li, Q. Xu, X. Meng, X. Wang, M. Xiao, Z. Zou, All-solid-state Z-scheme system arrays of $Fe_2V_4O_{13}$/RGO/CdS for visible light-driving photocatalytic CO_2 reduction into renewable hydrocarbon fuel, Chem. Commun. 51 (2015) 800–803, https://doi.org/10.1039/C4CC08744E.
[393] S. Sorcar, J. Thompson, Y. Hwang, Y.H. Park, T. Majima, C.A. Grimes, J.R. Durrant, S.-I. In, High-rate solar-light photoconversion of CO_2 to fuel: controllable transformation from C_1 to C_2 products, Energy Environ. Sci. 11 (2018) 3183–3193, https://doi.org/10.1039/C8EE00983J.
[394] C. Rogers, W.S. Perkins, G. Veber, T.E. Williams, R.R. Cloke, F.R. Fischer, Synergistic enhancement of electrocatalytic CO_2 reduction with gold nanoparticles embedded in functional graphene nanoribbon composite electrodes, J. Am. Chem. Soc. 139 (2017) 4052–4061, https://doi.org/10.1021/jacs.6b12217.
[395] L.-L. Tan, W.-J. Ong, S.-P. Chai, A.R. Mohamed, Noble metal modified reduced graphene oxide/TiO_2 ternary nanostructures for efficient visible-light-driven photoreduction of carbon dioxide into methane, Appl. Catal. B Environ. 166–167 (2015) 251–259, https://doi.org/10.1016/j.apcatb.2014.11.035.
[396] A. Wang, X. Li, Y. Zhao, W. Wu, J. Chen, H. Meng, Preparation and characterizations of Cu_2O/reduced graphene oxide nanocomposites with high photo-catalytic performances, Powder Technol. 261 (2014) 42–48, https://doi.org/10.1016/j.powtec.2014.04.004.
[397] G. Yin, M. Nishikawa, Y. Nosaka, N. Srinivasan, D. Atarashi, E. Sakai, M. Miyauchi, Photocatalytic carbon dioxide reduction by copper oxide nanocluster-grafted niobate nanosheets, ACS Nano 9 (2015) 2111–2119, https://doi.org/10.1021/nn507429e.
[398] X. An, K. Li, J. Tang, Cu_2O/reduced graphene oxide composites for the photocatalytic conversion of CO_2, ChemSusChem 7 (2014) 1086–1093, https://doi.org/10.1002/cssc.201301194.
[399] W.-J. Ong, L.-L. Tan, S.-P. Chai, S.-T. Yong, Graphene oxide as a structure-directing agent for the two-dimensional interface engineering of sandwich-like graphene–g-C_3N_4 hybrid nanostructures with enhanced visible-light photoreduction of CO_2 to methane, Chem. Commun. 51 (2015) 858–861, https://doi.org/10.1039/C4CC08996K.
[400] H. Yu, R. Shi, Y. Zhao, G.I.N. Waterhouse, L.-Z. Wu, C.-H. Tung, T. Zhang, Smart utilization of carbon dots in semiconductor photocatalysis, Adv. Mater. 28 (2016) 9454–9477, https://doi.org/10.1002/adma.201602581.
[401] W.-J. Ong, L.K. Putri, Y.-C. Tan, L.-L. Tan, N. Li, Y.H. Ng, X. Wen, S.-P. Chai, Unravelling charge carrier dynamics in protonated g-C_3N_4 interfaced with carbon nanodots as co-catalysts toward enhanced photocatalytic CO_2 reduction: a combined experimental and first-principles DFT study, Nano Res. 10 (2017) 1673–1696, https://doi.org/10.1007/s12274-016-1391-4.
[402] Z. Jiang, W. Wan, H. Li, S. Yuan, H. Zhao, P.K. Wong, A hierarchical Z-scheme α-Fe_2O_3/g-C_3N_4 hybrid for enhanced photocatalytic CO_2 reduction, Adv. Mater. 30 (2018) 1706108, https://doi.org/10.1002/adma.201706108.
[403] W.-J. Ong, L.K. Putri, L.-L. Tan, S.-P. Chai, S.-T. Yong, Heterostructured AgX/g-C_3N_4 (X = Cl and Br) nanocomposites via a sonication-assisted deposition-precipitation approach: emerging role of halide ions in the synergistic photocatalytic reduction of carbon dioxide, Appl. Catal. B Environ. 180 (2016) 530–543, https://doi.org/10.1016/j.apcatb.2015.06.053.
[404] Y. He, L. Zhang, B. Teng, M. Fan, New application of Z-scheme Ag_3PO_4/g-C_3N_4 composite in converting CO_2 to fuel, Environ. Sci. Technol. 49 (2015) 649–656, https://doi.org/10.1021/es5046309.
[405] P. Murugesan, S. Narayanan, M. Manickam, P.K. Murugesan, R. Subbiah, A direct Z-scheme plasmonic AgCl@g-C_3N_4 heterojunction photocatalyst with superior visible light CO_2 reduction in aqueous medium, Appl. Surf. Sci. 450 (2018) 516–526, https://doi.org/10.1016/j.apsusc.2018.04.111.
[406] J. Yu, K. Wang, W. Xiao, B. Cheng, Photocatalytic reduction of CO_2 into hydrocarbon solar fuels over g-C_3N_4–Pt nanocomposite photocatalysts, Phys. Chem. Chem. Phys. 16 (2014) 11492, https://doi.org/10.1039/c4cp00133h.
[407] W.-J. Ong, L.-L. Tan, S.-P. Chai, S.-T. Yong, Heterojunction engineering of graphitic carbon nitride (g-C_3N_4) via Pt loading with improved daylight-induced photocatalytic reduction of carbon dioxide to methane, Dalton Trans. 44 (2015) 1249–1257, https://doi.org/10.1039/C4DT02940B.
[408] Q. Lu, F. Jiao, Electrochemical CO_2 reduction: electrocatalyst, reaction mechanism, and process engineering, Nano Energy 29 (2016) 439–456, https://doi.org/10.1016/j.nanoen.2016.04.009.
[409] Z. Sun, T. Ma, H. Tao, Q. Fan, B. Han, Fundamentals and challenges of electrochemical CO_2 reduction using two-dimensional materials, Chem 3 (2017) 560–587, https://doi.org/10.1016/j.chempr.2017.09.009.
[410] C. Zhang, S. Yang, J. Wu, M. Liu, S. Yazdi, M. Ren, J. Sha, J. Zhong, K. Nie, A.S. Jalilov, Z. Li, H. Li, B.I. Yakobson, Q. Wu, E. Ringe, H. Xu, P.M. Ajayan, J.M. Tour, Electrochemical CO_2 reduction with atomic iron-dispersed on nitrogen-doped graphene, Adv. Energy Mater. 8 (2018) 1703487, https://doi.org/10.1002/aenm.201703487.
[411] T.N. Huan, N. Ranjbar, G. Rousse, M. Sougrati, A. Zitolo, V. Mougel, F. Jaouen, M. Fontecave, Electrochemical reduction of CO_2 catalyzed by Fe-N-C materials: a structure–selectivity study, ACS Catal. 7 (2017) 1520–1525, https://doi.org/10.1021/acscatal.6b03353.
[412] X. Li, W. Bi, M. Chen, Y. Sun, H. Ju, W. Yan, J. Zhu, X. Wu, W. Chu, C. Wu, Y. Xie, Exclusive Ni–N_4 sites realize near-unity CO selectivity for electrochemical CO_2 reduction, J. Am. Chem. Soc. 139 (2017) 14889–14892, https://doi.org/10.1021/jacs.7b09074.
[413] H. Bin Yang, S.F. Hung, S. Liu, K. Yuan, S. Miao, L. Zhang, X. Huang, H.Y. Wang, W. Cai, R. Chen, J. Gao, X. Yang, W. Chen, Y. Huang, H.M. Chen, C.M. Li, T. Zhang, B. Liu, Atomically dispersed Ni(i) as the active site for electrochemical CO_2 reduction, Nat. Energy 3 (2018) 140–147, https://doi.org/10.1038/s41560-017-0078-8.
[414] K. Jiang, S. Siahrostami, T. Zheng, Y. Hu, S. Hwang, E. Stavitski, Y. Peng, J. Dynes, M. Gangisetty, D. Su, K. Attenkofer, H. Wang, Isolated Ni single atoms in graphene nanosheets for high-performance CO_2 reduction, Energy Environ. Sci. 11 (2018) 893–903, https://doi.org/10.1039/C7EE03245E.
[415] W. Bi, X. Li, R. You, M. Chen, R. Yuan, W. Huang, X. Wu, W. Chu, C. Wu, Y. Xie, Surface immobilization of transition metal ions on nitrogen-doped graphene realizing high-efficient and selective CO_2 reduction, Adv. Mater. 30 (2018) 1706617, https://doi.org/10.1002/adma.201706617.
[416] P. Abbasi, M. Asadi, C. Liu, S. Sharifi-Asl, B. Sayahpour, A. Behranginia, P. Zapol, R. Shahbazian-Yassar, L.A. Curtiss, A. Salehi-Khojin, Tailoring the edge structure of molybdenum disulfide toward electrocatalytic reduction of carbon dioxide, ACS Nano 11 (2017) 453–460, https://doi.org/10.1021/acsnano.6b06392.
[417] L. Ji, L. Chang, Y. Zhang, S. Mou, T. Wang, Y. Luo, Z. Wang, X. Sun, Electrocatalytic CO_2 reduction to alcohols with high selectivity over a two-

dimensional $Fe_2P_2S_6$ nanosheet, ACS Catal. 9 (2019) 9721–9725, https://doi.org/10.1021/acscatal.9b03180.
[418] J. Xiong, J. Di, H. Li, Atomically thin 2D multinary nanosheets for energy-related photo, electrocatalysis, Adv. Sci. 5 (2018) 1800244, https://doi.org/10.1002/advs.201800244.
[419] L. Wang, W. Chen, D. Zhang, Y. Du, R. Amal, S. Qiao, J. Wu, Z. Yin, Surface strategies for catalytic CO_2 reduction: from two-dimensional materials to nanoclusters to single atoms, Chem. Soc. Rev. 48 (2019) 5310–5349, https://doi.org/10.1039/C9CS00163H.
[420] W. Bi, C. Wu, Y. Xie, Atomically thin two-dimensional solids: an emerging platform for CO_2 electroreduction, ACS Energy Lett. 3 (2018) 624–633, https://doi.org/10.1021/acsenergylett.7b01343.
[421] W. Zhang, Q. Qin, L. Dai, R. Qin, X. Zhao, X. Chen, D. Ou, J. Chen, T.T. Chuong, B. Wu, N. Zheng, Electrochemical reduction of carbon dioxide to methanol on hierarchical Pd/SnO_2 nanosheets with abundant Pd-O-Sn interfaces, Angew. Chem. Int. Ed. 57 (2018) 9475–9479, https://doi.org/10.1002/anie.201804142.
[422] Y. Chen, M.W. Kanan, Tin oxide dependence of the CO_2 reduction efficiency on tin electrodes and enhanced activity for tin/tin oxide thin-film catalysts, J. Am. Chem. Soc. 134 (2012) 1986–1989, https://doi.org/10.1021/ja2108799.
[423] F. Li, L. Chen, G.P. Knowles, D.R. MacFarlane, J. Zhang, Hierarchical mesoporous SnO_2 nanosheets on carbon cloth: a robust and flexible electrocatalyst for CO_2 reduction with high efficiency and selectivity, Angew. Chem. Int. Ed. 56 (2017) 505–509, https://doi.org/10.1002/anie.201608279.
[424] J.B. Goodenough, Y. Kim, Challenges for rechargeable Li batteries, Chem. Mater. 22 (2010) 587–603, https://doi.org/10.1021/cm901452z.
[425] S. Roberts, E. Kendrick, The re-emergence of sodium ion batteries: testing, processing, and manufacturability, Nanotechnol. Sci. Appl. 11 (2018) 23–33, https://doi.org/10.2147/NSA.S146365.
[426] R. Chen, T. Zhao, F. Wu, From a historic review to horizons beyond: lithium-sulphur batteries run on the wheels, Chem. Commun. 51 (2015) 18–33, https://doi.org/10.1039/C4CC05109B.
[427] P.G. Bruce, L.J. Hardwick, K.M. Abraham, Lithium-air and lithium-sulfur batteries, MRS Bull. 36 (2011) 506–512, https://doi.org/10.1557/mrs.2011.157.
[428] J.W. Choi, D. Aurbach, Promise and reality of post-lithium-ion batteries with high energy densities, Nat. Rev. Mater. 1 (2016) 16013, https://doi.org/10.1038/natrevmats.2016.13.
[429] J.P. Pender, G. Jha, D.H. Youn, J.M. Ziegler, I. Andoni, E.J. Choi, A. Heller, B.S. Dunn, P.S. Weiss, R.M. Penner, C.B. Mullins, Electrode degradation in lithium-ion batteries, ACS Nano 14 (2020) 1243–1295, https://doi.org/10.1021/acsnano.9b04365.
[430] S. Hossain, A.M. Abdalla, S.B.H. Suhaili, I. Kamal, S.P.S. Shaikh, M.K. Dawood, A.K. Azad, Nanostructured graphene materials utilization in fuel cells and batteries: a review, J. Energy Storage 29 (2020) 101386, https://doi.org/10.1016/j.est.2020.101386.
[431] D. Wang, D. Choi, J. Li, Z. Yang, Z. Nie, R. Kou, D. Hu, C. Wang, L.V. Saraf, J. Zhang, I.A. Aksay, J. Liu, Self-assembled TiO_2 –graphene hybrid nanostructures for enhanced Li-ion insertion, ACS Nano 3 (2009) 907–914, https://doi.org/10.1021/nn900150y.
[432] S. Goriparti, E. Miele, F. De Angelis, E. Di Fabrizio, R. Proietti Zaccaria, C. Capiglia, Review on recent progress of nanostructured anode materials for Li-ion batteries, J. Power Sources 257 (2014) 421–443, https://doi.org/10.1016/j.jpowsour.2013.11.103.
[433] W. Xu, J. Wang, F. Ding, X. Chen, E. Nasybulin, Y. Zhang, J.-G. Zhang, Lithium metal anodes for rechargeable batteries, Energy Environ. Sci. 7 (2014) 513, https://doi.org/10.1039/c3ee40795k.
[434] B. Wang, B. Luo, X. Li, L. Zhi, The dimensionality of Sn anodes in Li-ion batteries, Mater. Today 15 (2012) 544–552, https://doi.org/10.1016/S1369-7021(13)70012-9.
[435] X. Su, Q. Wu, J. Li, X. Xiao, A. Lott, W. Lu, B.W. Sheldon, J. Wu, Silicon-based nanomaterials for lithium-ion batteries: a review, Adv. Energy Mater. 4 (2014) 1300882, https://doi.org/10.1002/aenm.201300882.
[436] P. Poizot, S. Laruelle, S. Grugeon, L. Dupont, J.-M. Tarascon, Nano-sized transition-metal oxides as negative-electrode materials for lithium-ion batteries, Nature 407 (2000) 496–499, https://doi.org/10.1038/35035045.
[437] Y. Zhao, X. Li, B. Yan, D. Li, S. Lawes, X. Sun, Significant impact of 2D graphene nanosheets on large volume change tin-based anodes in lithium-ion batteries: a review, J. Power Sources 274 (2015) 869–884, https://doi.org/10.1016/j.jpowsour.2014.10.008.
[438] R. Mo, D. Rooney, K. Sun, H.Y. Yang, 3D nitrogen-doped graphene foam with encapsulated germanium/nitrogen-doped graphene yolk-shell nanoarchitecture for high-performance flexible Li-ion battery, Nat. Commun. 8 (2017) 13949, https://doi.org/10.1038/ncomms13949.
[439] S. Yang, X. Feng, S. Ivanovici, K. Müllen, Fabrication of graphene-encapsulated oxide nanoparticles: towards high-performance anode materials for lithium storage, Angew. Chem. Int. Ed. 49 (2010) 8408–8411, https://doi.org/10.1002/anie.201003485.
[440] D.S. Choi, C. Kim, J. Lim, S.-H. Cho, G.Y. Lee, H.J. Lee, J.W. Choi, H. Kim, I.-D. Kim, S.O. Kim, Ultrastable graphene-encapsulated 3 nm nanoparticles by in situ chemical vapor deposition, Adv. Mater. 30 (2018) 1805023, https://doi.org/10.1002/adma.201805023.
[441] L. Zhao, M. Gao, W. Yue, Y. Jiang, Y. Wang, Y. Ren, F. Hu, Sandwich-structured graphene-Fe_3O_4 @carbon nanocomposites for high-performance lithium-ion batteries, ACS Appl. Mater. Interfaces 7 (2015) 9709–9715, https://doi.org/10.1021/acsami.5b01503.
[442] G. Huang, T. Chen, Z. Wang, K. Chang, W. Chen, Synthesis and electrochemical performances of cobalt sulfides/graphene nanocomposite as anode material of Li-ion battery, J. Power Sources 235 (2013) 122–128, https://doi.org/10.1016/j.jpowsour.2013.01.093.
[443] H. Sun, J. Wang, W. Li, F. Yuan, Q. Wang, D. Zhang, B. Wang, Y.A. Wu, Spanish-dagger shaped CoP blooms decorated N-doped carbon branch anode for high-performance lithium and sodium storage, Electrochim. Acta 388 (2021) 138628, https://doi.org/10.1016/j.electacta.2021.138628.
[444] N. Dimov, S. Kugino, M. Yoshio, Carbon-coated silicon as anode material for lithium ion batteries: advantages and limitations, Electrochim. Acta 48 (2003) 1579–1587, https://doi.org/10.1016/S0013-4686(03)00030-6.
[445] J.-K. Lee, M.C. Kung, L. Trahey, M.N. Missaghi, H.H. Kung, Nanocomposites derived from phenol-functionalized Si nanoparticles for high performance lithium ion battery anodes, Chem. Mater. 21 (2009) 6–8, https://doi.org/10.1021/cm8022314.
[446] J.K. Lee, K.B. Smith, C.M. Hayner, H.H. Kung, Silicon nanoparticles–graphene paper composites for Li ion battery anodes, Chem. Commun. 46 (2010) 2025, https://doi.org/10.1039/b919738a.
[447] H. Xiang, K. Zhang, G. Ji, J.Y. Lee, C. Zou, X. Chen, J. Wu, Graphene/nanosized silicon composites for lithium battery anodes with improved cycling stability, Carbon N.Y. 49 (2011) 1787–1796, https://doi.org/10.1016/j.carbon.2011.01.002.
[448] S.-L. Chou, J.-Z. Wang, M. Choucair, H.-K. Liu, J.A. Stride, S.-X. Dou, Enhanced reversible lithium storage in a nanosize silicon/graphene composite, Electrochem. Commun. 12 (2010) 303–306, https://doi.org/10.1016/j.elecom.2009.12.024.
[449] Z. She, M. Gad, Z. Ma, Y. Li, M.A. Pope, Enhanced cycle stability of crumpled graphene-encapsulated silicon anodes via polydopamine sealing, ACS Omega 6 (2021) 12293–12305, https://doi.org/10.1021/acsomega.1c01227.
[450] J.-G. Ren, Q.-H. Wu, G. Hong, W.-J. Zhang, H. Wu, K. Amine, J. Yang, S.-T. Lee, Silicon-graphene composite anodes for high-energy lithium batteries, Energy Technol. 1 (2013) 77–84, https://doi.org/10.1002/ente.201200038.
[451] X. Zhou, Y.-X. Yin, L.-J. Wan, Y.-G. Guo, Facile synthesis of silicon nanoparticles inserted into graphene sheets as improved anode materials for lithium-ion batteries, Chem. Commun. 48 (2012) 2198, https://doi.org/10.1039/c2cc17061b.
[452] R. Hu, W. Sun, Y. Chen, M. Zeng, M. Zhu, Silicon/graphene based nanocomposite anode: large-scale production and stable high capacity for lithium ion batteries, J. Mater. Chem. A 2 (2014) 9118–9125, https://doi.org/10.1039/C4TA01013B.
[453] N. Li, S. Jin, Q. Liao, H. Cui, C.X. Wang, Encapsulated within graphene shell silicon nanoparticles anchored on vertically aligned graphene trees as lithium ion battery anodes, Nano Energy 5 (2014) 105–115, https://doi.org/10.1016/j.nanoen.2014.02.011.
[454] S.K. Kim, H. Chang, C.M. Kim, H. Yoo, H. Kim, H.D. Jang, Fabrication of ternary silicon-carbon nanotubes-graphene composites by Co-assembly in evaporating droplets for enhanced electrochemical energy storage, J. Alloys Compd. 751 (2018) 43–48, https://doi.org/10.1016/j.jallcom.2018.04.071.
[455] H. Tao, L. Xiong, S. Zhu, L. Zhang, X. Yang, Porous Si/C/reduced graphene oxide microspheres by spray drying as anode for Li-ion batteries, J. Electroanal. Chem. 797 (2017) 16–22, https://doi.org/10.1016/j.jelechem.2017.05.010.
[456] C. Zhang, T.-H. Kang, J.-S. Yu, Three-dimensional spongy nanographene-functionalized silicon anodes for lithium ion batteries with superior cycling stability, Nano Res. 11 (2018) 233–245, https://doi.org/10.1007/s12274-017-1624-1.
[457] J. Luo, X. Zhao, J. Wu, H.D. Jang, H.H. Kung, J. Huang, Crumpled graphene-encapsulated Si nanoparticles for lithium ion battery anodes, J. Phys. Chem. Lett. 3 (2012) 1824–1829, https://doi.org/10.1021/jz3006892.
[458] W. Jiang, H. Wang, Z. Xu, N. Li, C. Chen, C. Li, J. Li, H. Lv, L. Kuang, X. Tian, A review on manifold synthetic and reprocessing methods of 3D porous graphene-based architecture for Li-ion anode, Chem. Eng. J. 335 (2018) 954–969, https://doi.org/10.1016/j.cej.2017.11.020.
[459] Y. Li, K. Yan, H.-W. Lee, Z. Lu, N. Liu, Y. Cui, Growth of conformal graphene cages on micrometre-sized silicon particles as stable battery anodes, Nat. Energy 1 (2016) 15029, https://doi.org/10.1038/nenergy.2015.29.
[460] K.M. Abraham, Prospects and limits of energy storage in batteries, J. Phys. Chem. Lett. 6 (2015) 830–844, https://doi.org/10.1021/jz5026273.
[461] X. Zhao, C.M. Hayner, M.C. Kung, H.H. Kung, In-plane vacancy-enabled high-power Si-graphene composite electrode for lithium-ion batteries, Adv. Energy Mater. 1 (2011) 1079–1084, https://doi.org/10.1002/aenm.201100426.
[462] F. Maroni, R. Raccichini, A. Birrozzi, G. Carbonari, R. Tossici, F. Croce, R. Marassi, F. Nobili, Graphene/silicon nanocomposite anode with enhanced electrochemical stability for lithium-ion battery applications, J. Power Sources 269 (2014) 873–882, https://doi.org/10.1016/j.jpowsour.2014.07.064.
[463] F. Zhang, X. Yang, Y. Xie, N. Yi, Y. Huang, Y. Chen, Pyrolytic carbon-coated Si nanoparticles on elastic graphene framework as anode materials for high-performance lithium-ion batteries, Carbon N.Y. 82 (2015) 161–167, https://doi.org/10.1016/j.carbon.2014.10.046.
[464] W. Liu, H. Li, J. Jin, Y. Wang, Z. Zhang, Z. Chen, Q. Wang, Y. Chen, E. Paek, D. Mitlin, Synergy of epoxy chemical tethers and defect-free graphene in

enabling stable lithium cycling of silicon nanoparticles, Angew. Chem. 131 (2019) 16743–16753, https://doi.org/10.1002/ange.201906612.
[465] S. Palumbo, L. Silvestri, A. Ansaldo, R. Brescia, F. Bonaccorso, V. Pellegrini, Silicon few-layer graphene nanocomposite as high-capacity and high-rate anode in lithium-ion batteries, ACS Appl. Energy Mater. 2 (2019) 1793–1802, https://doi.org/10.1021/acsaem.8b01927.
[466] H. Huang, P. Rao, W.M. Choi, Carbon-coated silicon/crumpled graphene composite as anode material for lithium-ion batteries, Curr. Appl. Phys. 19 (2019) 1349–1354, https://doi.org/10.1016/j.cap.2019.08.024.
[467] H. Tang, J. Zhang, Y.J. Zhang, Q.Q. Xiong, Y.Y. Tong, Y. Li, X.L. Wang, C.D. Gu, J. P. Tu, Porous reduced graphene oxide sheet wrapped silicon composite fabricated by steam etching for lithium-ion battery application, J. Power Sources 286 (2015) 431–437, https://doi.org/10.1016/j.jpowsour.2015.03.185.
[468] R.A. House, G.J. Rees, M.A. Pérez-Osorio, J.-J. Marie, E. Boivin, A.W. Robertson, A. Nag, M. Garcia-Fernandez, K.-J. Zhou, P.G. Bruce, First-cycle voltage hysteresis in Li-rich 3d cathodes associated with molecular O_2 trapped in the bulk, Nat. Energy 5 (2020) 777–785, https://doi.org/10.1038/s41560-020-00697-2.
[469] Z. Peng, S.A. Freunberger, Y. Chen, P.G. Bruce, A reversible and higher-rate Li-O_2 battery, Science (80-.) 337 (2012) 563–566, https://doi.org/10.1126/science.1223985.
[470] M. Balaish, A. Kraytsberg, Y. Ein-Eli, A critical review on lithium-air battery electrolytes, Phys. Chem. Chem. Phys. 16 (2014) 2801–2822, https://doi.org/10.1039/c3cp54165g.
[471] N. Nitta, F. Wu, J.T. Lee, G. Yushin, Li-ion battery materials: present and future, Mater. Today 18 (2015) 252–264, https://doi.org/10.1016/j.mattod.2014.10.040.
[472] A. Débart, J. Bao, G. Armstrong, P.G. Bruce, An O_2 cathode for rechargeable lithium batteries: the effect of a catalyst, J. Power Sources 174 (2007) 1177–1182, https://doi.org/10.1016/j.jpowsour.2007.06.180.
[473] Y.C. Lu, Z. Xu, H.a. Gasteiger, S. Chen, K. Hamad-Schifferli, Y. Shao-Horn, Platinum-gold nanoparticles: a highly active bifunctional electrocatalyst for rechargeable lithium-air batteries, J. Am. Chem. Soc. 132 (2010) 12170–12171, https://doi.org/10.1021/ja1036572.
[474] J. Pan, X.L. Tian, S. Zaman, Z. Dong, H. Liu, H.S. Park, B.Y. Xia, Recent progress on transition metal oxides as bifunctional catalysts for lithium-air and zinc-air batteries, Batteries Supercaps 2 (2019) 336–347, https://doi.org/10.1002/batt.201800082.
[475] Y.-C. Lu, H.A. Gasteiger, M.C. Parent, V. Chiloyan, Y. Shao-Horn, The influence of catalysts on discharge and charge voltages of rechargeable Li–oxygen batteries, Electrochem. Solid State Lett. 13 (2010) A69, https://doi.org/10.1149/1.3363047.
[476] Y. Lin, B. Moitoso, C. Martinez-Martinez, E.D. Walsh, S.D. Lacey, J.-W. Kim, L. Dai, L. Hu, J.W. Connell, Ultrahigh-capacity lithium–oxygen batteries enabled by dry-pressed holey graphene air cathodes, Nano Lett. 17 (2017) 3252–3260, https://doi.org/10.1021/acs.nanolett.7b00872.
[477] J. Wu, Z. Pan, Y. Zhang, B. Wang, H. Peng, The recent progress of nitrogen-doped carbon nanomaterials for electrochemical batteries, J. Mater. Chem. A 6 (2018) 12932–12944, https://doi.org/10.1039/C8TA03968B.
[478] X. Zhong, B. Papandrea, Y. Xu, Z. Lin, H. Zhang, Y. Liu, Y. Huang, X. Duan, Three-dimensional graphene membrane cathode for high energy density rechargeable lithium-air batteries in ambient conditions, Nano Res. 10 (2017) 472–482, https://doi.org/10.1007/s12274-016-1306-4.
[479] J. Han, G. Huang, Y. Ito, X. Guo, T. Fujita, P. Liu, A. Hirata, M. Chen, Full performance nanoporous graphene based Li-O_2 batteries through solution phase oxygen reduction and redox-additive mediated Li_2O_2 oxidation, Adv. Energy Mater. 7 (2017) 1601933, https://doi.org/10.1002/aenm.201601933.
[480] B. Sun, B. Wang, D. Su, L. Xiao, H. Ahn, G. Wang, Graphene nanosheets as cathode catalysts for lithium-air batteries with an enhanced electrochemical performance, Carbon N.Y. 50 (2012) 727–733, https://doi.org/10.1016/j.carbon.2011.09.040.
[481] H. Liu, X. Huang, Z. Lu, T. Wang, Y. Zhu, J. Cheng, Y. Wang, D. Wu, Z. Sun, A.W. Robertson, X. Chen, Trace metals dramatically boost oxygen electrocatalysis of N-doped coal-derived carbon for zinc–air batteries, Nanoscale 12 (2020) 9628–9639, https://doi.org/10.1039/C9NR10800A.
[482] X. Lin, Y. Cao, S. Cai, J. Fan, Y. Li, Q.-H. Wu, M. Zheng, Q. Dong, Ruthenium@mesoporous graphene-like carbon: a novel three-dimensional cathode catalyst for lithium–oxygen batteries, J. Mater. Chem. A 4 (2016) 7788–7794, https://doi.org/10.1039/C6TA01008C.
[483] E. Yoo, T. Okata, T. Akita, M. Kohyama, J. Nakamura, I. Honma, Enhanced electrocatalytic activity of Pt subnanoclusters on graphene nanosheet surface, Nano Lett. 9 (2009) 2255–2259, https://doi.org/10.1021/nl900397t.
[484] H.-G. Jung, Y.S. Jeong, J.-B. Park, Y.-K. Sun, B. Scrosati, Y.J. Lee, Ruthenium-based electrocatalysts supported on reduced graphene oxide for lithium-air batteries, ACS Nano 7 (2013) 3532–3539, https://doi.org/10.1021/nn400477d.
[485] P. Xu, C. Chen, J. Zhu, J. Xie, P. Zhao, M. Wang, RuO_2-particle-decorated graphene-nanoribbon cathodes for long-cycle Li–O_2 batteries, J. Electroanal. Chem. 842 (2019) 98–106, https://doi.org/10.1016/j.jelechem.2019.04.055.
[486] Y.S. Jeong, J.-B. Park, H.-G. Jung, J. Kim, X. Luo, J. Lu, L. Curtiss, K. Amine, Y.-K. Sun, B. Scrosati, Y.J. Lee, Study on the catalytic activity of noble metal nanoparticles on reduced graphene oxide for oxygen evolution reactions in lithium–air batteries, Nano Lett. 15 (2015) 4261–4268, https://doi.org/10.1021/nl504425h.
[487] Y. Wang, H. Zhou, A lithium-air battery with a potential to continuously reduce O_2 from air for delivering energy, J. Power Sources 195 (2010) 358–361, https://doi.org/10.1016/j.jpowsour.2009.06.109.
[488] G. Wu, N. Li, D.-R. Zhou, K. Mitsuo, B.-Q. Xu, Anodically electrodeposited Co+Ni mixed oxide electrode: preparation and electrocatalytic activity for oxygen evolution in alkaline media, J. Solid State Chem. 177 (2004) 3682–3692, https://doi.org/10.1016/j.jssc.2004.06.027.
[489] F. Cheng, J. Shen, B. Peng, Y. Pan, Z. Tao, J. Chen, Rapid room-temperature synthesis of nanocrystalline spinels as oxygen reduction and evolution electrocatalysts, Nat. Chem. 3 (2011) 79–84, https://doi.org/10.1038/nchem.931.
[490] L. Wang, X. Zhao, Y. Lu, M. Xu, D. Zhang, R.S. Ruoff, K.J. Stevenson, J.B. Goodenough, $CoMn_2O_4$ spinel nanoparticles grown on graphene as bifunctional catalyst for lithium-air batteries, J. Electrochem. Soc. 158 (2011) A1379, https://doi.org/10.1149/2.068112jes.
[491] H.-D. Lim, H. Gwon, H. Kim, S.-W. Kim, T. Yoon, J.W. Choi, S.M. Oh, K. Kang, Mechanism of Co_3O_4/graphene catalytic activity in Li–O_2 batteries using carbonate based electrolytes, Electrochim. Acta 90 (2013) 63–70, https://doi.org/10.1016/j.electacta.2012.12.020.
[492] S.-H. Peng, T.-H. Chen, C.-H. Lee, H.-C. Lu, S.J. Lue, Optimal cobalt oxide (Co_3O_4): graphene (GR) ratio in Co_3O_4/GR as air cathode catalyst for air-breathing hybrid electrolyte lithium-air battery, J. Power Sources 471 (2020) 228373, https://doi.org/10.1016/j.jpowsour.2020.228373.
[493] C. Sun, F. Li, C. Ma, Y. Wang, Y. Ren, W. Yang, Z. Ma, J. Li, Y. Chen, Y. Kim, L. Chen, Graphene–Co_3O_4 nanocomposite as an efficient bifunctional catalyst for lithium–air batteries, J. Mater. Chem. A 2 (2014) 7188–7196, https://doi.org/10.1039/C4TA00802B.
[494] J. Zhang, Q. Zhou, Y. Tang, L. Zhang, Y. Li, Zinc–air batteries: are they ready for prime time? Chem. Sci. 10 (2019) 8924–8929, https://doi.org/10.1039/C9SC04221K.
[495] M.-I. Jamesh, P. Moni, A.S. Prakash, M. Harb, ORR/OER activity and zinc-air battery performance of various kinds of graphene-based air catalysts, Mater. Sci. Energy Technol. 4 (2021) 1–22, https://doi.org/10.1016/j.mset.2020.12.001.
[496] Q. Jin, B. Ren, J. Chen, H. Cui, C. Wang, A facile method to conduct 3D self-supporting Co-FeCo/N-doped graphene-like carbon bifunctional electrocatalysts for flexible solid-state zinc air battery, Appl. Catal. B Environ. 256 (2019) 117887, https://doi.org/10.1016/j.apcatb.2019.117887.
[497] Q. Wang, Y. Lei, Z. Chen, N. Wu, Y. Wang, B. Wang, Y. Wang, Fe/Fe_3C@C nanoparticles encapsulated in N-doped graphene–CNTs framework as an efficient bifunctional oxygen electrocatalyst for robust rechargeable Zn–air batteries, J. Mater. Chem. A 6 (2018) 516–526, https://doi.org/10.1039/C7TA08423D.
[498] S. Ramakrishnan, J. Balamurugan, M. Vinothkannan, A.R. Kim, S. Sengodan, D.J. Yoo, Nitrogen-doped graphene encapsulated FeCoMoS nanoparticles as advanced trifunctional catalyst for water splitting devices and zinc–air batteries, Appl. Catal. B Environ. 279 (2020) 119381, https://doi.org/10.1016/j.apcatb.2020.119381.
[499] D.U. Lee, H.W. Park, D. Higgins, L. Nazar, Z. Chen, Highly active graphene nanosheets prepared via extremely rapid heating as efficient zinc-air battery electrode material, J. Electrochem. Soc. 160 (2013) F910–F915, https://doi.org/10.1149/2.016309jes.
[500] M. Prabu, P. Ramakrishnan, H. Nara, T. Momma, T. Osaka, S. Shanmugam, Zinc–air battery: understanding the structure and morphology changes of graphene-supported $CoMn_2O_4$ bifunctional catalysts under practical rechargeable conditions, ACS Appl. Mater. Interfaces 6 (2014) 16545–16555, https://doi.org/10.1021/am5047476.
[501] M. Zeng, Y. Liu, F. Zhao, K. Nie, N. Han, X. Wang, W. Huang, X. Song, J. Zhong, Y. Li, Metallic cobalt nanoparticles encapsulated in nitrogen-enriched graphene shells: its bifunctional electrocatalysis and application in zinc-air batteries, Adv. Funct. Mater. 26 (2016) 4397–4404, https://doi.org/10.1002/adfm.201600636.
[502] J. Zhu, M. Xiao, Y. Zhang, Z. Jin, Z. Peng, C. Liu, S. Chen, J. Ge, W. Xing, Metal–organic framework-induced synthesis of ultrasmall encased NiFe nanoparticles coupling with graphene as an efficient oxygen electrode for a rechargeable Zn–air battery, ACS Catal. 6 (2016) 6335–6342, https://doi.org/10.1021/acscatal.6b01503.
[503] T.O.M. Samuels, A.W. Robertson, H. Kim, M. Pasta, J.H. Warner, Three dimensional hybrid multi-layered graphene–CNT catalyst supports via rapid thermal annealing of nickel acetate, J. Mater. Chem. A 5 (2017) 10457–10469, https://doi.org/10.1039/C7TA01852E.
[504] D. Su, D. Han Seo, Y. Ju, Z. Han, K. Ostrikov, S. Dou, H.-J. Ahn, Z. Peng, G. Wang, Ruthenium nanocrystal decorated vertical graphene nanosheets@Ni foam as highly efficient cathode catalysts for lithium-oxygen batteries, NPG Asia Mater. 8 (2016), https://doi.org/10.1038/am.2016.91 e286–e286.
[505] M. Liu, K. Sun, Q. Zhang, T. Tang, L. Huang, X. Li, X. Zeng, J. Hu, S. Liao, Rationally designed three-dimensional N-doped graphene architecture mounted with Ru nanoclusters as a high-performance air cathode for lithium–oxygen batteries, ACS Sustain. Chem. Eng. 8 (2020) 6109–6117, https://doi.org/10.1021/acssuschemeng.0c01237.